DETERMINATION OF CONTACT ANGLES OF POWDERS BY CAPILLARIC DEWATERING OF FILTER CAKES

A THESIS SUBMITTED TO
THE GRADUATE SCHOOL OF NATURAL AND APPLIED SCIENCES
OF
MIDDLE EAST TECHNICAL UNIVERSITY

BY
ÖZLEM DENİZ ERATAK

IN PARTIAL FULFILLMENT OF THE REQUIREMENTS
FOR
THE DEGREE OF MASTER OF SCIENCE
IN
DEPARTMENT OF MINING ENGINEERING

JANUARY 2005

I hereby declare that all information in this document has been obtained and presented in accordance with academic rules and ethical conduct. I also declare that, as required by these rules and conduct, I have fully cited and referenced all material and results that are not original to this work.

Name, Last name :

Signature :

ABSTRACT

DETERMINATION OF CONTACT ANGLES OF POWDERS BY CAPILLARIC DEWATERING OF FILTER CAKES

Eratak, Özlem Deniz
M. Sc., Department of Mining Engineering
Supervisor: Prof. Dr. Çetin Hoşten

January 2005, 140 pages

Solid-liquid contact angle is an important parameter in many particulate processes of the mineral, ceramic and chemical industries. In particular, modification of the contact angle through surface active agents plays a crucial role in froth flotation of minerals. In the case of flat solid surfaces, direct measurement of the contact angle is possible. However, such flat surfaces can not be obtained with finely divided solids typically encountered in flotation applications. Then, indirect methods based on powder beds as thin layers of powders deposited on glass plates or packed columns are used for the determination of apparent contact angles.

This thesis presents an alternative novel method based on the capillaric dewatering of filter cakes for the measurement of the receding contact angle and correlates the contact angles measured as such with column wicking and micro-flotation test results of zircon and rutile mineral particles. The experimental procedure is simple and fast. The results have proven that the proposed method is reliable and give a good measure of the contact angle in the absence and presence of surface active non-wetting agents.

Keywords: Contact Angle, Cake Dewatering, Column Wicking, Microflotation

ÖZ

FİLTRE KEKLERİNİN SUSUZLANDIRILMASI ÖZELLİKLERİNDEN YARARLANARAK KATI TANECİKLERİNİN SIVILARLA TEMAS AÇILARININ BELİRLENMESİ

Eratak, Özlem Deniz
Yüksek Lisans, Maden Mühendisliği Bölümü
Tez Yöneticisi: Prof. Dr. Çetin Hoşten

Ocak 2005, 140 sayfa

Katı-sıvı temas açısı, bir çok mineral,seramik ve kimya endüstrilerinin katı tanecikli işlemlerinde önemli bir parametredir. Özellikle de, yüzey aktif reaktiflerin ilavesi ile değişen temas açısı, minerallerin köpüklü flotasyonunda çok önemli bir rol oynar. Katı yüzeyi düz olduğu takdirde, temas açısının doğrudan ölçümü mümkündür. Ancak, bu tür düz yüzeylere, flotasyon uygulamalarında toz haline gelmis katılarda rastlamak mümkün değildir. Bu durumda, temas açıları ince tane yataklarına veya kolonlarına dayanan yöntemlerle dolaylı olarak belirlenir.

Bu tezde, temas açısı ölçümü için filtre keklerinin kapiler susuzlandırılmasına dayanan yeni bir yöntem önerilmekte ve sonuçları kolona emme ve mikro flotasyon yöntemleri ile karşılaştırılmaktadır. Deneysel yöntem basit ve hızlı olup elde edilen sonuçlar, yüzey aktif maddelerin yokluğunda veya varlığında güvenilir temas açısı değerleri verdiğini göstermiştir.

Anahtar Kelimaler: Temas Açısı, Filtre Keki Susuzlandırma, Kolona Emme, Mikro Flotasyon

To My Grandparents

ACKNOWLEDGEMENTS

I wish to express my deepest gratitude to my supervisor Prof. Dr. Çetin Hoşten for his valuable advice and guidance of this work. I wish also to express my special thanks and gratitude to Prof. Dr. Ali İhsan Arol, Prof. Dr. Cahit Hiçyılmaz, Prof. Dr. Gülhan Özbayoğlu and Prof. Dr. Ümit Atalay for their suggestions and comments.

I want to express my appreciation to my friend Ayşe Yasemin Yeşilay for sharing her ideas with me, helping me for this thesis and her great friendship and I wish also to express my thanks to research assistants for their help.

I wish to thank to technical staff of Department of Mining Engineering, especially Tahsin Işıksal, Tuncer Gençtan, Mehmet Çakır, Aytekin Arslan and İsmail Kaya.

I would like to sincerely thank to my family for their support and help throughout this job.

Especially, I would like to give my special thanks to Hidayet Doğan for his support, patience, partnership and understanding

The grant provided by the research fund of the Middle East Technical University through the project BAP-2002-03-05-01 is gratefully acknowledged.

TABLE OF CONTENTS

LIST OF TABLES

LIST OF FIGURES

CHAPTER 1

INTRODUCTION

The solid-liquid contact angle is used as a measure of wettability and the surface free energy of solids in many diverse fields such as mineral and coal benefication, petroleum engineering, and the manufacture of pharmaceutical powders, cosmetics, pigments, paints and paper. Therefore, contact angle measurements are fundamental to many processes. Contact angle measurements on finely divided solids are much more difficult than those on moderately large, uniform solid surfaces, but the former is often more desired and more important since many industrial applications involve processing of particulate solids. For example, the froth flotation separation of minerals is controlled to a large extent by the relative wettabilities of finely divided mineral particles in an aqueous suspension, which generally requires the use of surface active agents (surfactants) to selectively modify the wettability or the contact angle of highly irregular mineral particles.

Two general methods exist for determining powder contact angles [Adamson, 1967]: (i) the Washburn equation (or dynamic) method which is based on the rate of liquid flow into a packed bed or porous plug of particulate solids; (ii) the Bartell (or static) method which is based on equilibrium measurements of the capillary pressure increment required to prevent liquid from penetrating the packed bed. The principles of the measurement methods are simple but they both suffer some experimental and fundamental difficulties. One experimental difficulty is that both methods in their simplest form require visual observation of the wetting liquid from inside the porous bed, which may be skewed in the case of irregulary shaped polydisperse particles or its exact position may not be clearly visible due to wall effects of the enclosing glassware. A fundamental limitation with measurements in packed beds is the assumption that the packing density will not change with nature of the penetrating (or receding) liquid, as the methods require an additional calibrating liquid, perfectly wetting the solids, to determine the effective pore radius in the bed. This limitation is of more concern in systems where surfactants are present in the penetrating liquid. Flocculation or dispersion produced by surfactant solutions can change the packing density. Furthermore, the depletion of surfactant molecules from the liquid phase by adsorption on the powder surface area in the region of liquid front can seriously affect the contact angle and the liquid surface tension in rate-measuring methods.

Modified versions to circumvent difficulties of the two general measurement methods have been reported in the literature. Good R.J. et al (1993) developed the thin layer wicking method to measure the rate of advance of wetting liquids through a thin layer of solid particles deposited onto a glass slide. This method uses the Washburn equation to determine the cosine of the contact angle and requires calibration tests with a perfectly wetting liquid to calculate the effective interstitial pore radius of the thin layer. Chibowski and Perea-Carpio (2001) developed a technique involving the measurement of the weight of liquid penetrating into a powder bed, instead of monitoring the movement of the liquid front, for the determination of the solid surface free-energy components, but did not propose to derive the contact angle from such data. The powder contact angle device of Dunstan and White (1986) and that of Diggins et al. (1990) both used the Bartell concept; however, rather than applying an external pressure difference to prevent capillary rise, the penetrating liquid was allowed to rise causing a gradual increase in the pressure of air enclosed above the wetting front. The capillary pressure was calculated by measuring the air pressure to stop the rise of liquid up the packed bed and subtracting any hydrostatic head, if present.

Capillary pressure determinations in packed beds are equilibrium measurements with incremental changes in the applied air pressure and generally require long equilibrium times. Furthermore, most of the practical wetting or dewetting processes are of nonequilibrium nature. For example, the act of particle-air bubble attachment in froth flotation and filter cake dewatering upon rapid application of a certain pressure difference is governed by nonequilibrium receding contact angles. Therefore, a simple, fast method combining the dynamic and the static methods of the contact angle measurement may be of practical value for determining apparent contact angles.

The motivation for the current study was to determine apparent receding contact angles of particulate solids from irreducible (or residual) moisture contents of filter cakes dewatered at different instantaneous vacuum levels. A filter cake fully saturated with liquid is said to be in the capillary state. Upon instantaneous application of vacuum greater than the negative capillary pressure at the air-liquid interface, liquid displacement and air fingering of the cake begins. However, for a given vacuum level, a certain portion of the liquid will not drain out of the cake irrespective of drainage time. At this irreducible saturation level, liquid and air may have two distinct configurations within the cake. At relatively low applied pressure differences, the funicular state is reached in which a continuous network of liquid exists in equilibrium with air above the jagged liquid front. At higher pressure differences, further drainage of liquid occurs until there is insufficient liquid to form a continous liquid phase. Air breaks through the cake and the filter medium, if the pores of the latter are not small enough to cause very high capillary pressures. Eventually the pendular state is reached in which small lenses of liquid exist at points of particle contact. The range of the applied pressure differences corresponding to the funicular state will depend on the particle size and its distribution and the solid-liquid contact angle. As the size distribution becomes wider, there will also be a wider variation of pore radii in the filter cake, consequently, the funicular state will extend over a wider pressure range.

1.1 Objective of Thesis

The aim of the present work was to develop a simple, fast technique for the determination of apparent contact angles of particulate solids from nonequilibrium filter cake drainage tests. The residual saturation of filter cakes in the funicular state of cake drainage was correlated with the applied vacuum to determine the contact angle of particulate solids constituting the filter cake.

CHAPTER 2

THEORETICAL BACKGROUND

2.1 General

The contact angle is a very important property of solid-liquid-gas or solid–liquid–liquid interfaces. Contact angle plays a major role in technological, biological, mineral, ceramic, chemical, pharmaceutical and environmental processes and can define the surface tension of the solid on which it is formed. Powder contact angle measurement is also an important parameter in processes as diverse as flotation, wet grinding and the manufacture of pigments, paints and cosmetics [Iveson, Holt and Biggs, 2000].

Direct measurement of contact angle of powders is impossible. The very simple direct measurement of contact angles of a liquid drop on a flat and smooth solid is not applicable to small powder particles [Siebold et al, 2000]. Thus, scientists are working on indirect methods to determine the contact angle of powders so as to characterize the wettability of solids.

2.2 Contact Angle and Wetting

Angle which is formed between liquid-vapor interface and liquid-solid interface at the solid-liquid-vapor three-phase contact line is defined as the contact angle.

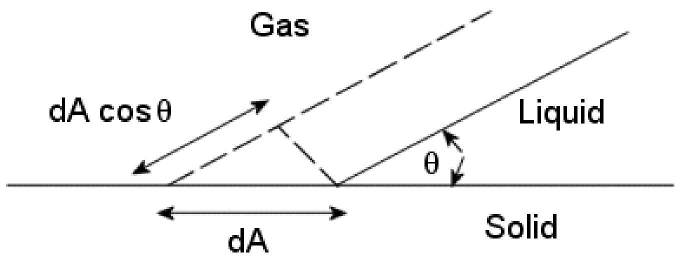

Figure 2.1. The contact angle formed by solid, liquid and gas.

The Laplace equation and the Young equation are the two fundamental equations that describe the capillarity phenomenon and the contact angle, respectively:

$$\Delta P = \gamma_{LV} \left(1/R_1 + 1/R_2\right) \qquad [1]$$

$$\gamma_{LV} \cos\theta = \gamma_{SV} - \gamma_{SL} \qquad [2]$$

where

γ_{LV} is the liquid-vapor surface tension,

γ_{SV} is the solid-vapor surface tension,

γ_{SL} is the solid-liquid surface tension,

R_1 and R_2 are the radii of the curvature,

θ is the equilibrium contact angle.

From Young's equation [Finch, Smith, 1979]:

If $\gamma_{LV} > \gamma_{SV} - \gamma_{SL}$ a three- phase contact is established.

If $\gamma_{LV} < \gamma_{SV} - \gamma_{SL}$ no vapor-solid contact is established.

The solid-liquid interfacial tension and liquid-vapor interfacial tension must be high and solid-vapor interfacial tension must be low for good flotation.

The surface free energy of solids appears a very important parameter determining the interfacial properties in solid-liquid and solid-gas interfaces [Biliński, Holysz, 1999]. Today, there are also some problems in determining the surface free energy of solids, and scientists made assumptions to formulate the value of the surface free energy. The first assumption is that the surface free energy is the sum of the dispersion (γ_s^d) and the polar (γ_s^p) interactions, and the other new formulation was proposed in the late 80's by van Oss et al. on the surface free energy, as well as a determination of the energy components from contact angles. The authors for the first time gave an expression for Lewis acid-base interactions (AB), i.e., electron donor and electron acceptor interactions, which in most systems are due to the hydrogen bonding [Chibowski, Carpio, 2001]. According to these formulations, the surface energy of the solid is given by

$$\gamma_S = \gamma_S^{LW} + \gamma_S^{AB} = \gamma_S^{LW} + 2\sqrt{(\gamma_S^{+}\gamma_S^{-})} \qquad [3]$$

where

γ_S^{LW} is the apolar Lifshitz-van der Waals

γ_S^{+} is the electron acceptor interactions

γ_S^{-} is the electron donor interactions

The solid liquid interaction is given by the following equation :

$$\gamma_{SL} = \gamma_S + \gamma_L - 2\left[\sqrt{(\gamma_S^{LW}\gamma_L^{LW})} + \sqrt{(\gamma_S^{+}\gamma_S^{-})} + \sqrt{(\gamma_S^{-}\gamma_S^{+})}\right] \qquad [4]$$

when combined with the Young equation

$$\gamma_S = \gamma_L.\cos\theta_a + \gamma_{SL} \qquad [5]$$

and

$$\gamma_{SL} = \gamma_S^{+}\gamma_L^{-}W_a \qquad [6]$$

where θ_a is the advancing contact angle and,
W_a is the work of adhesion

$$W_a = \gamma_L(1+\cos\theta_a) = 2\left[\sqrt{(\gamma_S^{LW}\gamma_L^{LW})} + \sqrt{(\gamma_S^{+}\gamma_L^{-})} + \sqrt{(\gamma_S^{-}\gamma_L^{+})}\right] \qquad [7]$$

These equations help to determine the surface properties and the surface free energy components.

2.3.1 Adhesion, cohesion and spreading

When generating 2 new interfaces of unit area the free energy is

$$\Delta G = 2\gamma_A = W_{AA} \qquad [8]$$

W_{AA} is the work of cohesion and it measures the attraction between the molecules of the liquid. The free energy change between two liquids is given by

$$\Delta G = W_{AB} = \gamma_A + \gamma_B - \gamma_{AB} \qquad [9]$$

Where W_{AB} is the work of adhesion and measures the attraction between two different phases.

The difference between the work of adhesion and cohesion of two substances is the spreading coefficient of B on A

$$S_{B/A} = W_{AB} - W_{BB} \qquad [10]$$

If $S_{B/A}$ is positive, substance A spreads and if $S_{B/A}$ is negative, it retreats. If the vapor phase replaced by another phase like oil the equation will be

$$\gamma_{ow} \cos\theta = \gamma_{so} - \gamma_{sw} \qquad [11]$$

2.3.2 Critical surface tension of wetting

When $\cos\theta = 1$, the liquid completely wets the solid. The value of the γ_{LV} is the critical surface tension of the solid and γ_c represents this value.

For Liquids:

If $\gamma_{LV} > \gamma_c$ there will be a contact angle,

If $\gamma_{lv} < \gamma_c$ the liquid will wet the solid, and the $\cos\theta_e$ is related to γ_{lv} by

$$\cos\theta_e = 1 - b\,(\gamma_{lv} - \gamma_c) \qquad [12]$$

where b is the constant, and the $\cos\theta$ versus γ_{lv} plot is the Zisman plot and the equation is the Zisman equation.

2.3. Contact Angle Measurements

2.3.1 Direct measurements of contact angle

It is observed that in most instances a liquid placed on a solid will not wet but it remains as a drop having a definite angle of contact between the liquid and solid phases [Adamson, 1967]. The direct measurement of the contact angles can be applicable for large sample of solids. The tilting plate method has given the most reproducible and probably the most accurate contact angle values. A several centimeter wide plate of the solid dips into the liquid, and its position is altered by means of an adjustable mount until the angle such that the liquid surface appears to remain perfectly flat right up to the surface of the solid [Adamson, 1967].

The other technique for measuring the contact angles directly is the sessile drop method. Sessile drop technique is a widely used for measuring the direct contact angle. For this measurement the surface of the solid must be smooth and clean then the solid dips into the liquid and on the surface a bubble is formed, the angle between sessile drop and solid can be read from goniometer.

2.3.2 Column wicking method

The contact angle of fine particles can be measured by column wicking method. This method is based on the penetration of liquid into the porous structure measuring the change of surface energy. In this technique powdered solids packed into a capillary tube and it is immersed in a liquid of known surface tension. Then, the rise of liquid into the powdered solids is observed. The contact angle can be found from the height of the liquid as a function of penetration time. Column wicking method is based on Poiseuille's law:

$$v = \frac{dh}{dt} = \frac{R_D^2}{8\eta} \frac{\Delta P}{h} \qquad [13]$$

where

v = rate of liquid penetration

h = height reached by the liquid

t = penetration time

R_D = hydrodynamic radius of pores

η = viscosity of the liquid

ΔP = the difference of pressure

After integration of the equation, the Washburn equation can form:

$$h^2 = \frac{r\gamma_L \cos\theta}{2\eta} t \qquad [14]$$

There are some modifications of the column wicking method which are based on the equation

$$W = 2\pi r\gamma\cos\theta \qquad [15]$$

When the contact angle is zero:

$$W = mg = 2\pi r\gamma \qquad [16]$$

Where m is the mass of the liquid and g is the gravitational acceleration.

If there is a contact angle liquid enters the capillary at dynamic advancing contact angle, the equation will be:

$$m_a g = 2\pi r\gamma\cos\theta_a = 2r\pi\Delta G_a \qquad [17]$$

where ΔG_a the specific free energy change. For the receding contact angle, the above equation takes the form

$$m_r g = 2\pi r\gamma\cos\theta_r = 2r\pi\Delta G_r \qquad [18]$$

2.3.3 Thin layer wicking method

Thin layer technique is based on the phenomena of a liquid penetration (wicking) into a solid porous layer deposited on a glass plate, e.g. microscope slide. The surface free energy components are then calculated from the proper form of the Washburn equation [Teixeira, et al, 1998].

In the thin layer technique, the powdered solid deposited on a microscopic slide in the form of aqueous slurry then the sample is dried and one side of the slide is immersed in a liquid in the vertical position and the liquid penetrates into the solid slowly.

Thin layer wicking method also uses the Washburn equation. The only problem in these experiments is the calculation of r value. r value can be determined from the low energy liquids such as hexane, benzene, methanol, formamide.

The methods which are based on Washburn equation give only advancing contact angles rather than equilibrium contact angles.

Contact angle can be measured directly by compressing the powders into pellets but this method is not recommended. The surface properties such as surface roughness, liquid adsorption and porosity can change in the pressing phase so the measurement of contact angle using pellets is only an assumption.

2.3.4 Hysteresis in contact angle

From the contact angle studies, it is observed that the receding and advancing contact angles can be different. The past experiments show that θ_A (Advancing Contact Angle) should be bigger than θ_R (Receding Contact Angle) and the difference between θ_A and θ_R called contact angle hysteresis. The effect can be quite large, for water on surfaces of minerals the advancing contact angle may be as much as 50° larger than the receding one [Adamson, 1967].

There are some causes of contact angle hysteresis. One of them is the liquid or solid contamination. The scientists studied with graphite and they found that cleaning can prevent the hysteresis [Fowkes 1964, Harkins, 1922].

Surface roughness is another effect of hysteresis. Johnson and Dettre studied surface roughness for water on a polytetrafluoroethylene wax and from their experiments they found the given equation [Finch, Smith, 1979].

$$\cos\theta_r = r.\cos\theta_e \qquad [19]$$

where θ_r is the contact angle observed on a surface roughness r, θ_e is the equilibrium contact angle, and r is the ratio of real surface area to the area assuming a smooth surface.

There are some scientists who studied the roughness effect on the contact angle. Oliver and Mason studied microspreading on rough surfaces by scanning electron microscopy, Cox also made equilibrium configurations during liquid spreading over periodic and randomly surfaces [Osipow, 1962].

Surface heterogeneity is the other effect for hysteresis . Cassie and Baxter studied for the effect of surface heterogeneity and they found an equation which was obtained from Wenzel equation:

$$\cos\theta_h = f_1\cos\theta_1 + f_2\cos\theta_2 \qquad [20]$$

where

θ_h is the thermodynamic equivalent of θ for a heterogeneous surface.

f_1 and f_2 are the respective fractional surface area of region 1 and 2.

θ_1 is the contact angle in region 1.

θ_2 is the contact angle in region 2.

The local contact angle will depend on the surface energy of the region with which liquid is in contact [Finch, Smith, 1979].

2.4 The theory of the proposed method of contact angle measurement

The pressure required to prevent a liquid from penetrating a single capillary tube of radius r, or that required to drain the capillary , is given by the Laplace equation:

$$\Delta P = \frac{2\gamma_{LA}\cos\theta}{r} \qquad [21]$$

where γ_{LA} is the liquid surface tension, and θ is the solid-liquid contact angle. Using the Laplace equation for packed particle beds requires a properly chosen equivalent radius. Kozeny assumed that the pore space of packed beds could be regarded as equivalent to a bundle of parallel capillaries with a common equivalent radius, and with a cross-sectional shape representative of the average shape of the pore cross section. The equivalent radius, r_e, for a packed bed was formulated as [Allen, 1977]:

$$r_e = 2 \times \frac{\text{volume of voids}}{\text{surface area of solids}} = 2\times \frac{e}{(1-e)S_V} \qquad [22]$$

where e is the packed ped porosity (volume fraction of voids), and S_V is the volume specific surface area of solids, which may be related to an equivalent diameter, d_p, or irregularly shaped particles of the particle bed by the equation

$$S_V = \frac{\alpha_{SV}}{d_p} \qquad [23]$$

where α_{SV} is the ratio of surface to volume shape factor of particles and is specific to definition of the equivalent diameter (sieve diameter, surface diameter, volume diameter, etc). Furthermore, one has to allow for random orientation of capillaries in a packed bed by introducing a correction factor c [Heertjes and Kossen, 1967]. The Laplace equation for the capillary pressure of a packed bed then takes the form.

$$\Delta P = k\,\frac{(1-e)}{e.d_P}\;\gamma_{LA}\cos\theta \qquad [24]$$

where the entry pressure coefficient k is $2\alpha_{SV}$ /c. This form of the Laplace equation has been used as means of studying the moisture-retention characteristics of porous masses. For example, attemps have been made to correlate the lowest pressure drop, or the so-called entry pressure, required to dewater an initially saturated filter cake [Wakeman, 1976; Puttock et al.,1986; Hosten and Sastry, 1989; Condie et al.,1996; Besra et al.,200; Hosten and San, 2002]

For a filter cake of unknown entry pressure coefficient k, it is appropriate to correlate the residual saturation of the cake in its funicular drainage state against the group of terms on the left side of the following rearranged form of Eq (24).

$$\frac{e.d_P \Delta P}{(1-e)\gamma_{LA}} = k.\cos\theta \qquad [25]$$

Plots of residual cake saturation versus the adjusted pressure on the left-hand side of the above equation yield straight lines for residual saturations between 1.0 and 0.60 of vacuum-dewatered filter cakes [Hosten and Sastry, 1989; Hosten and San, 2002]. This cake saturation range corresponds to the funicular state of the filter cake in which the liquid front recedes to its equilibrium capillary drain height without any air breakthrough. By definition of the entry pressure in Eq (24), the value of the adjusted pressure corresponding to the intercept of the linear portion of the plots with the full saturation line should yield the coefficient k for the cake, provided that a perfectly wetting probe liquid ($\cos\theta = 1$) is used. Having determined the value of k, cake drainage tests may be repeated with partially wetting liquids or surfactant solutions of interest on equivalent powders to determine apparent contact angles by comparing full-saturation intercepts of the linear plots.

CHAPTER 3

EXPERIMENTAL MATERIAL AND METHODS

3.1 Preparation of Samples

The samples of zircon ($ZrSiO_4$) and rutile (TiO_2) which were used in this research were obtained from DuPont Starke, Florida Operations. The zircon sample contained 67.22 % ZrO_2 , 31.11 % SiO_2, 0.11 % TiO_2. The rutile sample contained 96.66 % TiO_2, 0.48 % SiO_2, 0.39 % ZrO_2 and 0.32 % Fe_2O_3.

Zircon and rutile samples were prepared for experiments by reducing the size in a porcelain mortar to avoid iron contamination. After reducing the sizes, zircon and rutile samples dry screened to yield 150x200 mesh for capillaric dewatering, column wicking and microflotation experiments.

Zircon and rutile samples were purified with dry magnetic separator to eliminate the iron impurities. After purifying with magnetic separator, the samples cleaned by rinsing in warm HNO_3. Nitric acid ensured to remove the other powders and cleaned the rutile, zircon samples. The rutile, zircon samples which were treated with warm nitric acid were washed with distilled water several times until the samples were completely purified from HNO_3. Samples were dried in an oven with 50° C temperature after cleaning procedure. The zircon and rutile samples are known to have iso-electric points at pH 4.4 and pH 3.5, respectively.

All the materials (crucible, rod, glasses, etc.) which were used for experiments were cleaned with hot chromic acid, then washed with distilled water until the green colour of chromic acid disappeared.

3.2 Reagents

Dodecyl amine ($CH_3(CH_2)_{11}NH_2$), sodium dodecyl sulfate ($C_{12}H_{25}SO_4Na$), methanol and distilled water were used in capillaric dewatering, column wicking and microflotation experiments. HCl and NaOH were used as pH regulators.

Dodecyl amine was used as a non-wetting agent in the experiments. An amount of dodecyl amine which would be used for stock solution was taken and heated in a pH 4.5-5 solution (distilled water and HCl) to dissolve dodecyl amine and make the solution homogeneous, then 10^{-1} M stock solution was prepared. The required concentrations were prepared from the stock solution.

Sodium dodecyl sulfate was used as another non-wetting chemical in the experiments. 10^{-1} M stock solution was prepared from dry powder of the chemical and the required concentrations were prepared from the stock solutions.

3.3 Experimental Procedure and Methods

3.3.1 Dewatering of filter cakes

Dewatering experiments were conducted in a glass filter crucible of 50 ml capacity, the bottom of which consisted of a sintered disc of 40-mm diameter and a porosity index No. 4. Following the cleaning procedure, 50 g of dry particulate sample was put in the crucible and the crucible was filled with liquid until the level of the liquid was enough to mix the sample with liquid. The sample was mixed with liquid (water, surfactant solution or methanol) by the help of a glass, stirring rod to form a slurry. The crucible was then securely fitted to a vacuum flask by means of a rubber stopper and the thoroughly mixed slurry was allowed to drain by gravity, or by applying a slight vacuum, forming a fully saturated filter cake on the sintered disc (Figure 3.1). At this moment, the crucible was removed from the flask and quickly weighed on an electronic balance without disturbing the filter cake. Any excess liquid remaining on the bottom of the crucible or the porous disc was wiped off before the weighing process. Immediately after the weighing the crucible was placed back on the vacuum flask and a small vacuum (0.5 in Hg) was applied to dewater the filter cake to its residual saturation level, which generally took around two minutes of dewatering time. The vacuum was then shut off, the crucible was removed and quickly weighed, and placed back on the vacuum system. The vacuum level was incremented by another 0.5 in Hg and the cake was again dewatered to it new residual saturation level and then weighed. This procedure was repeated several times to obtain residual saturation data at various vacuum levels within the capillaric (or funicular) dewatering regime.

3.3.2 Column Wicking

Column wicking experiments were conducted in a clear plastic tube of 10 cm height and 2 mm width, the bottom of which was closed with a fritted disc. The dried powder was packed into the tube by tapping. The tube was then placed vertically so that the bottom of the tube was just in contact with the liquid. The rise of the liquid up the packed bed of particles was measured as a function of time.

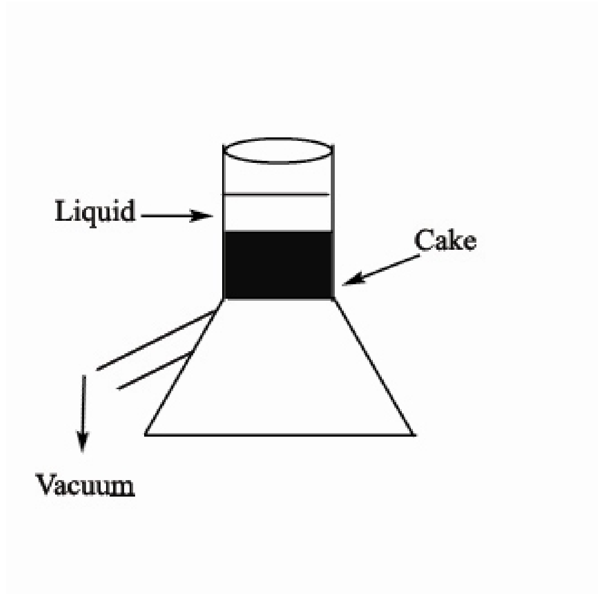

Figure 3.1. The illustration of capillaric dewatering experiments

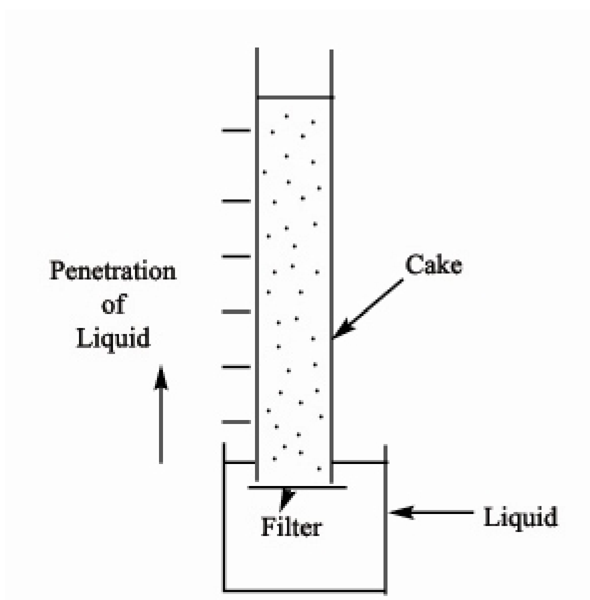

Figure 3.2. The illustration of column wicking experiments

3.3.3 Microflotation Experiments

The microflotation experiments were performed with a Hallimond tube using nitrogen gas. One gram of dry powder sample was used in each test. The powder in the tube was conditioned for 10 minutes with the prepared solutions by mixing with a magnetic stirrer. After conditioning, nitrogen gas was allowed to flow through the fritted disc at the bottom of the tube to generate air bubbles. After 5 minutes of flotation time, the nitrogen switch was turned off, and the particles in the float and sink fractions were collected separately and dried in an oven at 60°C to calculate the weight recovery of the floated particles. A schematic drawing of the microflotation system is given in Figure 3.3.

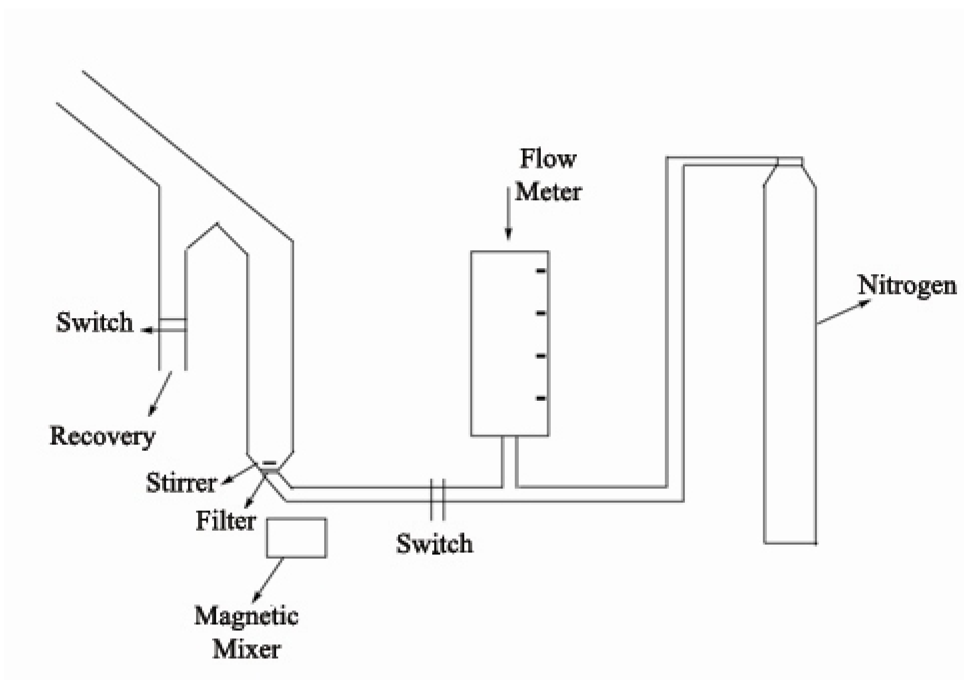

Figure 3.3 The illustration of Hallimond tube.[Muratoğlu, 2000]

CHAPTER 4

EXPERIMENTAL RESULTS AND DISCUSSION

In this chapter the results of capillaric dewatering experiments, column wicking experiments and microflotation experiments are given and compared by the help of figures.

4.1 Capillaric dewatering experiments

First the capillaric dewatering experiments were performed with methanol (the completely wetting liquid), water and water-methanol mixtures for zircon and rutile samples.

4.1.1 Experiments with zircon

It is shown in Figure 4.1 that, from the capillaric dewatering experiments by using methanol, we can find the value of $k.\cos\theta = 8.00$. It is known that methanol is a completely wetting liquid and therefore $\theta = 0$. Hence,

$$k.\cos\theta = 8.00, \quad \theta = 0 \quad \Rightarrow \; k = 8.00$$

This k value for the zircon sample will be used in all calculations in the rest of the thesis. The contact angle of zircon with water can then be found from the equation

$$k.\cos\theta = 6.02 \quad \Rightarrow \quad 8.00.\cos\theta = 6.02 \quad \Rightarrow \quad \theta = 41.19° \text{ for water}$$

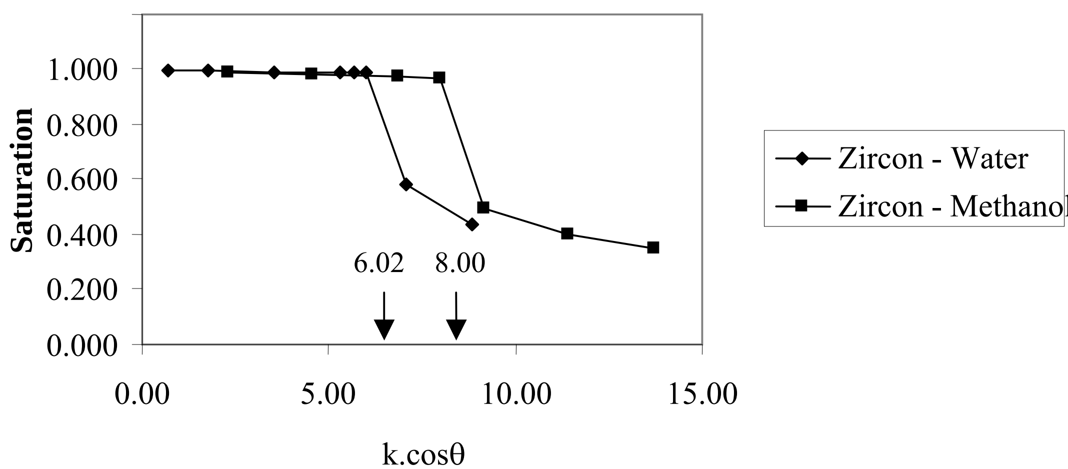

Figure 4.1 Residual cake saturation versus k.cosθ plots for -150 + 200 mesh zircon when water or methanol was used as the liquid.

Figures 4.2 through 4.7 show the experimental results obtained with the cake dewatering of zircon samples when various mixtures of water and methanol were used as the medium liquid. The purpose of these experiments was to find critical (k.cosθ) values from which the contact angle values could be obtained for the liquids of varying surface tension.

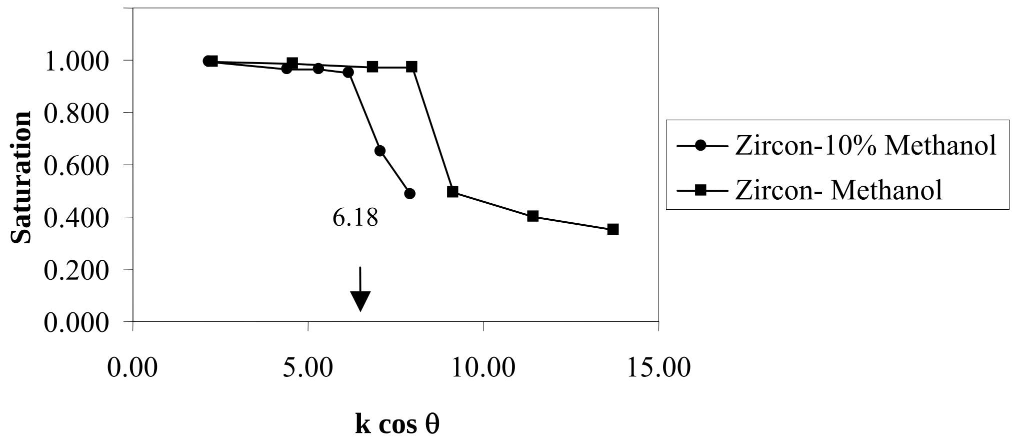

Figure 4.2 Residual cake saturation versus k.cosθ plots for -150 + 200 mesh zircon when methanol or a water-methanol mixture was used as the liquid.

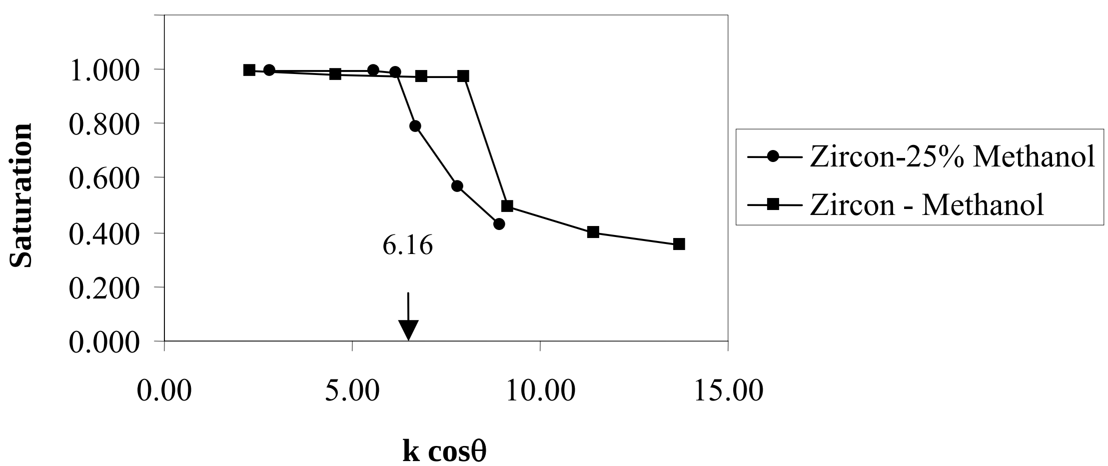

Figure 4.3 Residual cake saturation versus k.cosθ plots for -150 + 200 mesh zircon when methanol or a water-methanol mixture was used as the liquid.

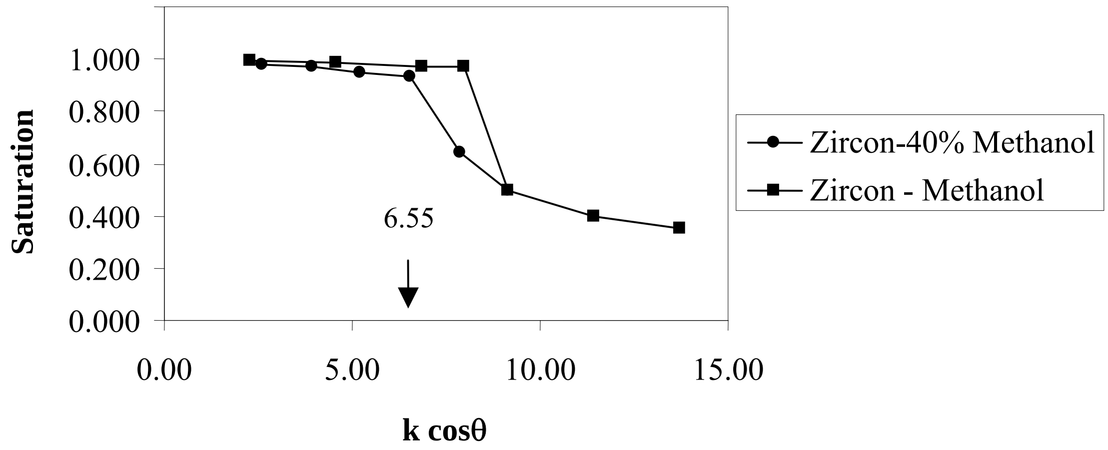

Figure 4.4 Residual cake saturation versus k.cosθ plots for -150 + 200 mesh zircon when methanol or a water-methanol mixture was used as the liquid.

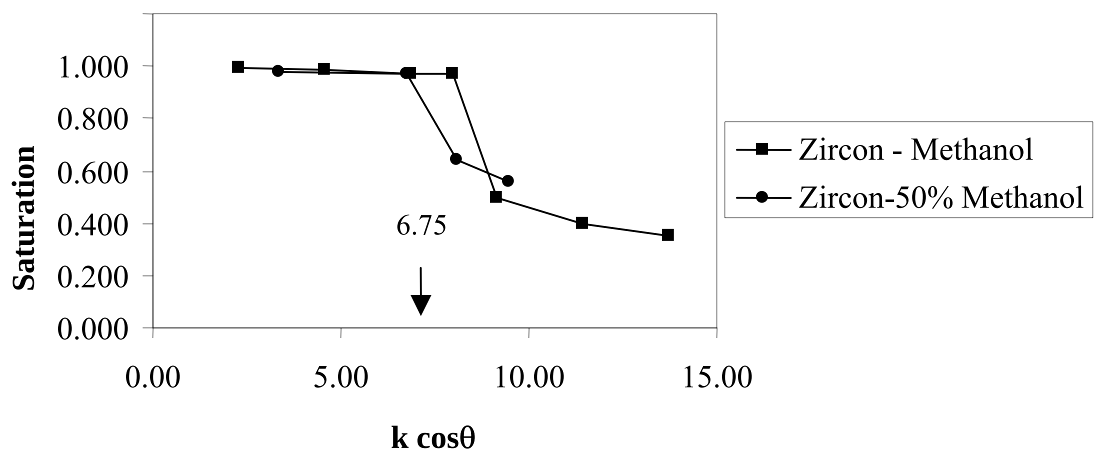

Figure 4.5 Residual cake saturation versus k.cosθ plots for -150 + 200 mesh zircon when methanol or a water-methanol mixture was used as the liquid.

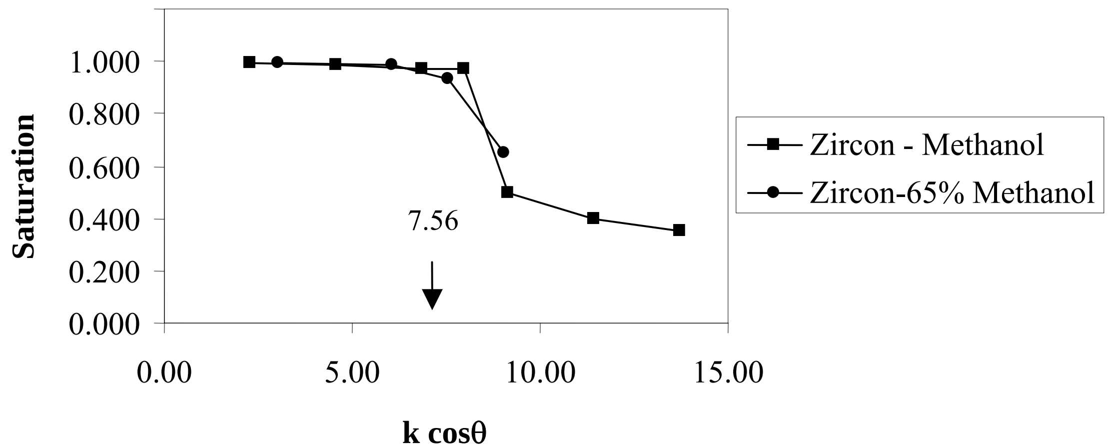

Figure 4.6 Residual cake saturation versus k.cosθ plots for -150 + 200 mesh zircon when methanol or a water-methanol mixture was used as the liquid.

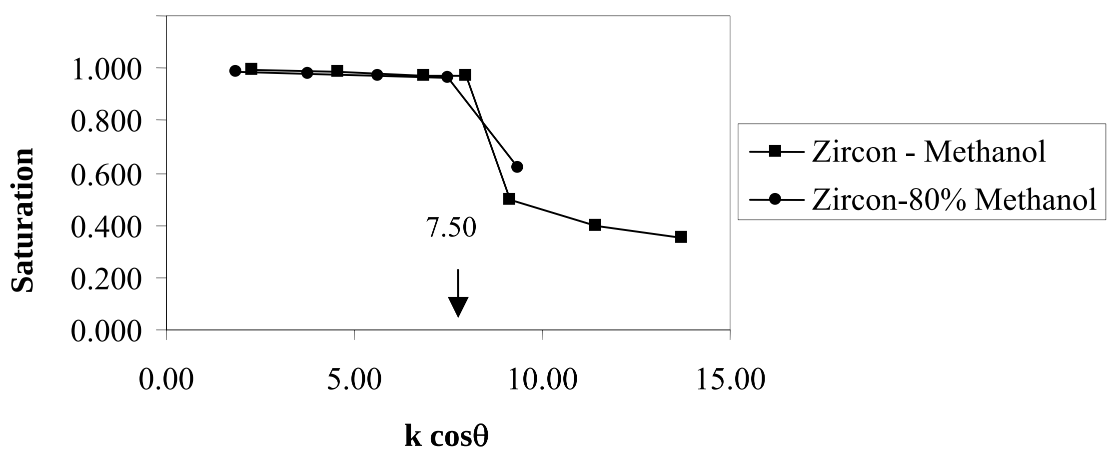

Figure 4.7 Residual cake saturation versus k.cosθ plots for -150 + 200 mesh zircon when methanol or a water-methanol mixture was used as the liquid.

Knowing the previously found k = 8.0 value for the zircon filter cakes, we can calculate the contact angle values from the k.cosθ values obtained from the figures for the cases where we have different liquid surface tensions resulting from using varying amounts of methanol in mixture with water. Table 4.1 and Figure 4.8 present the contact angle values found by this procedure.

Table 4.1 The contact angle and k.cosθ values for the zircon sample as obtained from cake dewatering tests using water-methanol mixtures.

Methanol % in water	100	80	65	50	40	25	10	0
k.cosθ	8.00	7.50	7.56	6.75	6.55	6.16	6.18	6.02
Contact angle, °	0	20.36	19.09	32.46	35.04	39.64	39.42	41.19

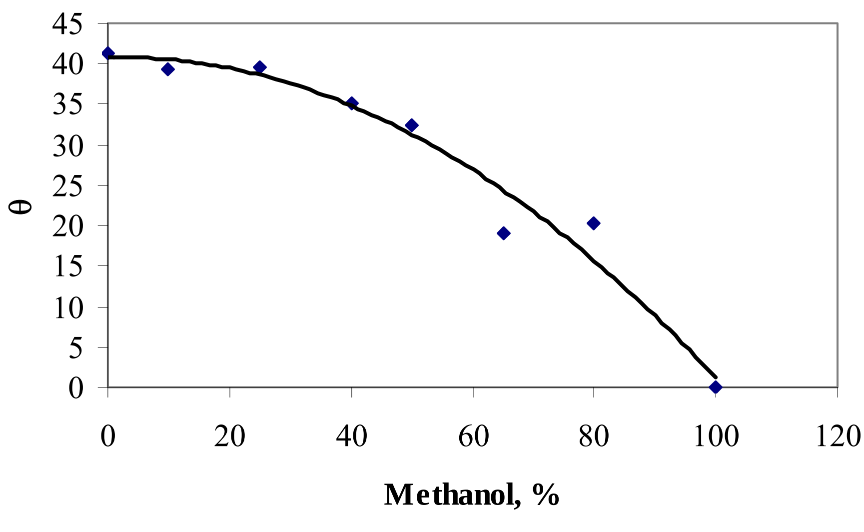

Figure 4.8 Contact angle values obtained with zircon by using methanol-water mixtures.

These results give us an idea that the capillaric dewatering method can be an applicable method for contact angle measurements because we know that methanol is a completely wetting liquid and always gives zero contact angle with all minerals. When the proportion of methanol in the mixture increases, the surface tension of the contacting liquid decreases, and, therefore, the contact angle of the methanol-water mixture on the zircon particle surfaces decreases.

Having proven the applicability of the new method with methanol, similar tests were conducted with a surfactant, dodecyl amine (DA), which is a common flotation collector. Figures 4.9 and 4.10 show the contact angles of zircon, as a function of pH when 10^{-5} M dodecylamine solutions were used as the liquid in cake dewatering tests. The k.cosθ values obtained from the point where the sharp decrease of saturation occurred and the known value of k = 8.0 for the zircon filter cakes were again used to calculate the contact angle values. Table 4.2 and Figure 4.10 summarize the results obtained as such.

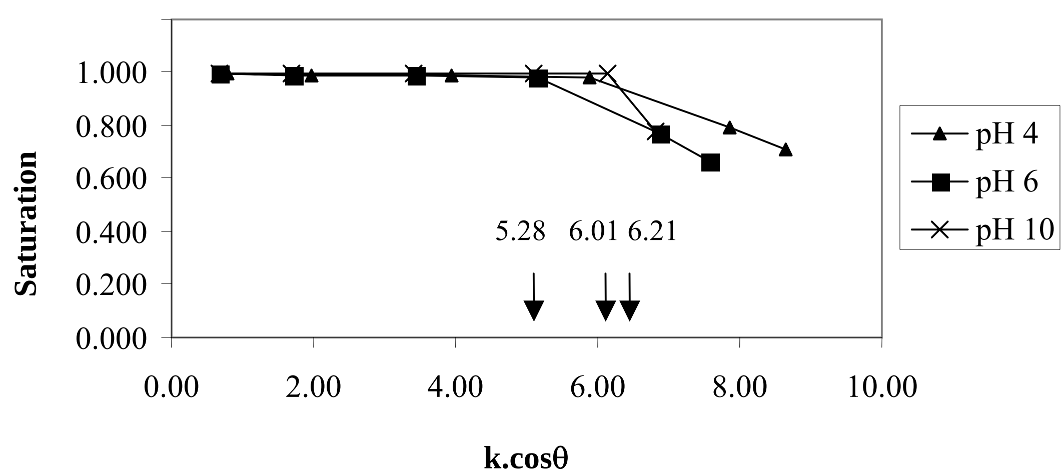

Figure 4.9 Residual cake saturation versus k.cosθ plots for -150 + 200 mesh zircon when 10^{-5}M dodecylamine solution was used as the liquid.

Table 4.2. The contact angle and k.cosθ values from the cake dewatering experiments with -150+200 mesh zircon by using 10^{-5} M dodecylamine at various pH values of the solution.

pH	4	6	8	10
Contact angle, θ°	41.30	48.70	49.74	39.8
k.cosθ	6.01	5.28	5.17	6.21

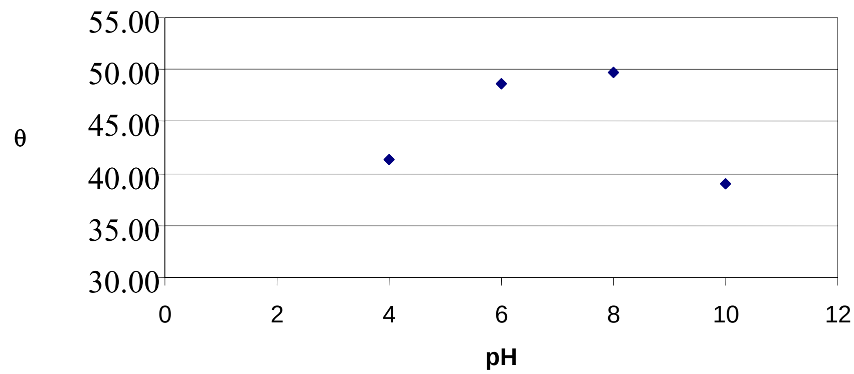

Figure 4.10 The contact angle values for the -150+200 mesh zircon sample in contact with 10^{-5}M dodecylamine solutions at various pH values.

It is obvious from the contact angle values that the highest hydrophobicity was obtained in a pH range 6 to 8. This must be the range where maximum adsorption of cationic dodecylamine ions occurred on negatively charged zircon surfaces, the iso-electric point of which was known to be pH 4.4.

Similar dewatering experiments were also performed with zircon by using 5.10^{-5} M dodecylamine solutions at different pH values, and the results obtained were almost identical with those obtained by using 10^{-5} M dodecyl amine. Therefore, figures and the contact angle values pertinent to the experiments with 10^{-5} M dodecyl amine solutions were not included here in the text to avoid repetition, but the data can be found in the appendix. The contact angle measurements could not performed with 10^{-4} M dodecylamine because of particle aggregation problems at such a high concentration of the surfactant.

Another common surfactant, but of anionic type, namely, sodium dodecyl sulfate (SDS), was also tested for generating zircon surfaces with different degrees of hydrophobicity. Figure 4.11 presents the experimental results from the dewatering of filter cakes of zircon particles treated with sodium dodecyl sulfate at various pH values. This surfactant is known to adsorb on the silicate or oxide mineral surfaces dominantly by electrostatic interaction; therefore, no effect on the contact angle was observed at pH values of 4, 6, and 8 as the zircon particle surfaces are either neutral or negatively charged at these pH values (i.e.p. is around pH4.4). On the other hand, the surfaces are positively charged at pH 2, and the anionic SDS can adsorb on the surfaces and make them more hydrophobic. The measured contact angles with SDS at pH 2 were 49.6°, 52°, and 53.2° for 10^{-5} M, 5×10^{-5} M, and 10^{-4} M solutions, respectively. It is obvious that an order of magnitude increase in SDS concentration beyond 10^{-5}M can cause only a slight increase in the contact angle.

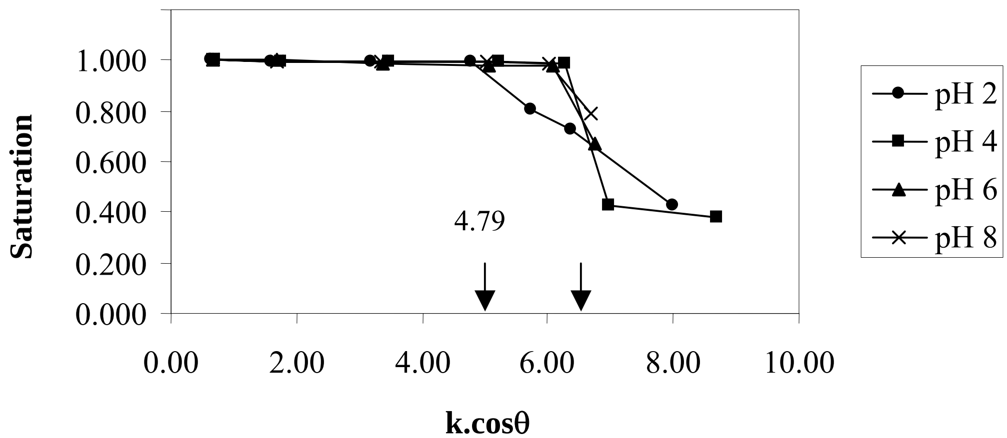

Figure 4.11 Residual cake saturation versus k.cosθ plots for -150 + 200 mesh zircon when 10^{-4} M sodium dodecyl sulfate solution was used as the liquid.

4.1.2 Experiments with Rutile

It is shown in Figure 4.12 that, from the capillaric dewatering experiments by using the completely wetting (θ = 0°) liquid methanol, we can find the value of k as 8.64. This value is again a fixed reference for all the other experiments preformed with the rutile sample. Referring the k.cosθ = 7.26 value and knowing the k value, we can calculate that the contact angle between rutile and water is 32.83° which is almost 10° lower than that found for zircon.

Figures 4-13 through 4.18 present the residual cake saturation versus k.cosθ plots for the rutile sample treated with water-methanol mixtures of varying methanol proportions to change the surface tension of the mixture liquid. Figure 4-19 shows the surface tension of the water-methanol mixtures.

Table 4.3 summarizes the information derived from the figures. Again, the contact angle increases with the increase in the liquid surface tension, or with the decrease in the proportion of methanol in the mixture. It is obvious that water is a partially-wetting liquid for rutile as well as zircon, because we observe finite contact angles with the use of water as the liquid in dewatering experiments.

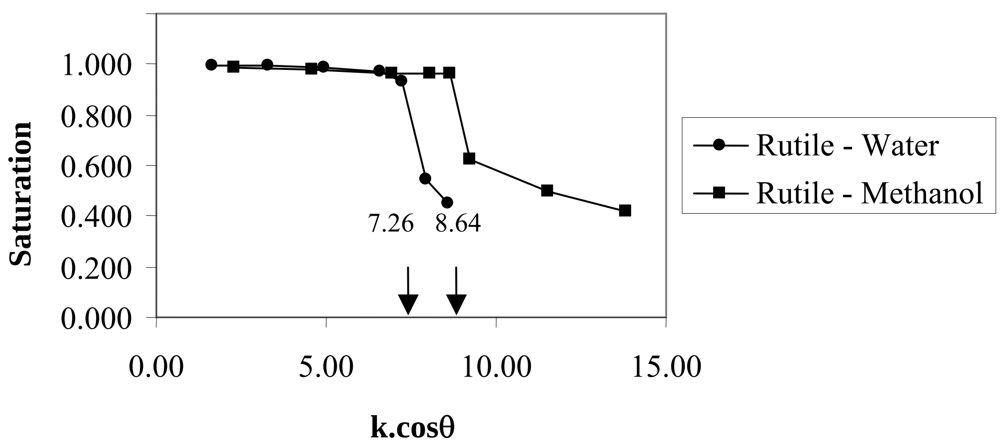

Figure 4.12 Residual cake saturation versus k.cosθ plots for -150 + 200 mesh rutile when water or methanol was used as the liquid.

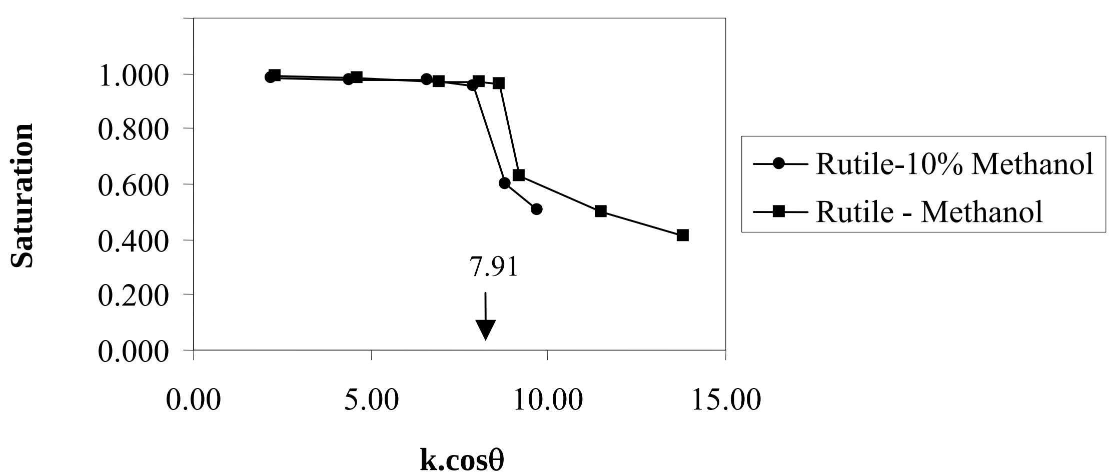

Figure 4.13 Residual cake saturation versus k.cosθ plots for -150 + 200 mesh rutile when methanol or a water-methanol mixture was used as the liquid.

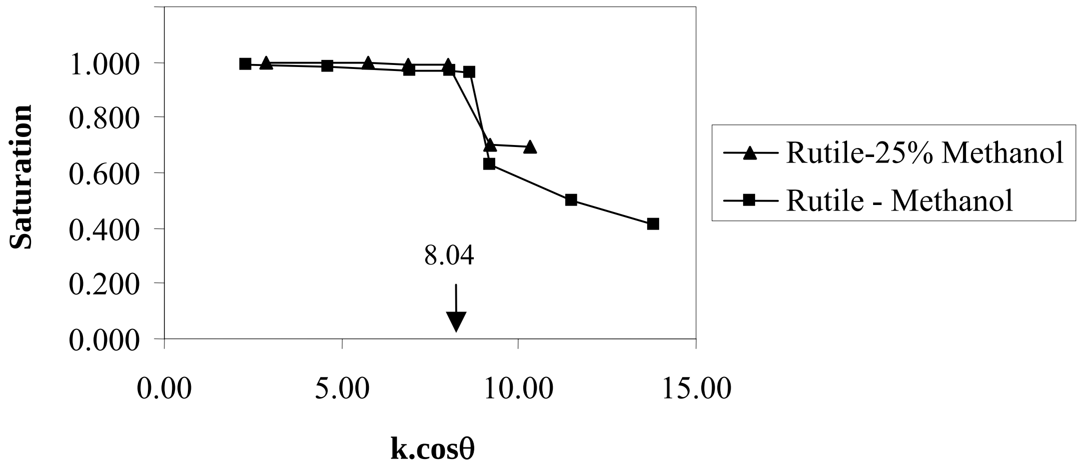

Figure 4.14 Residual cake saturation versus k.cosθ plots for -150 + 200 mesh rutile when methanol or a water-methanol mixture was used as the liquid.

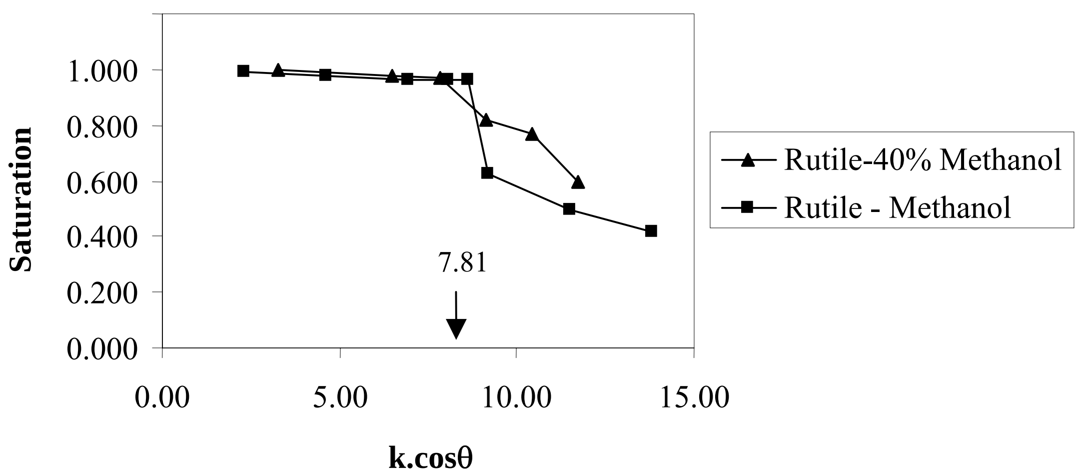

Figure 4.15 Residual cake saturation versus k.cosθ plots for -150 + 200 mesh rutile when methanol or a water-methanol mixture was used as the liquid.

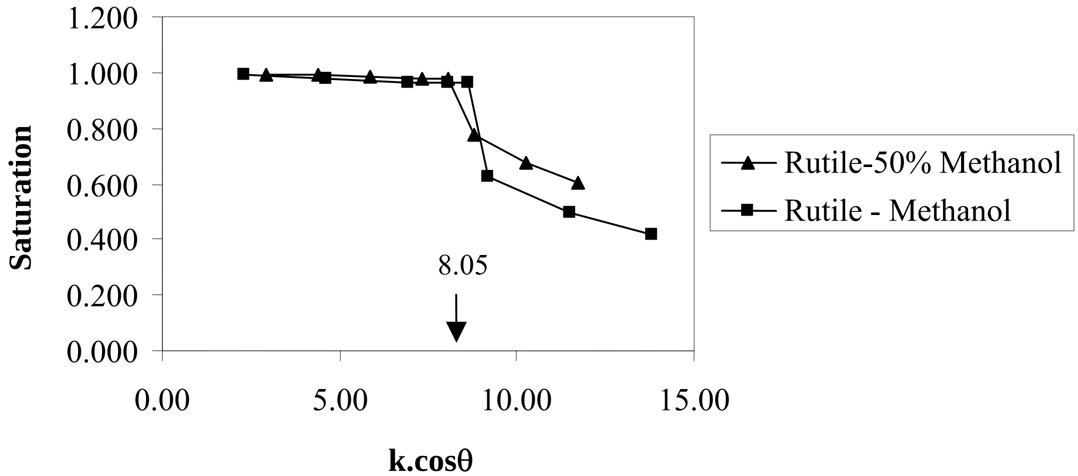

Figure 4.16 Residual cake saturation versus k.cosθ plots for -150 + 200 mesh rutile when methanol or a water-methanol mixture was used as the liquid.

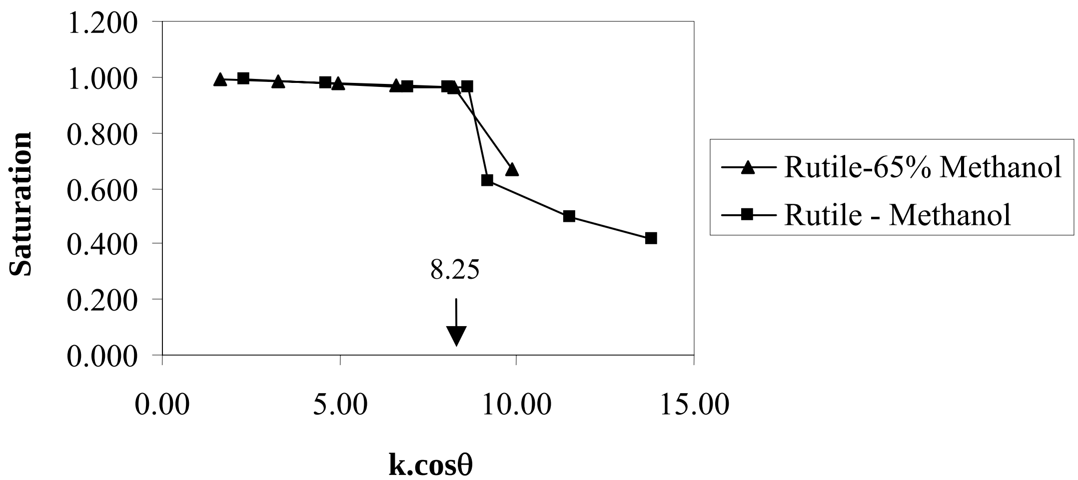

Figure 4.17 Residual cake saturation versus k.cosθ plots for -150 + 200 mesh rutile when methanol or a water-methanol mixture was used as the liquid.

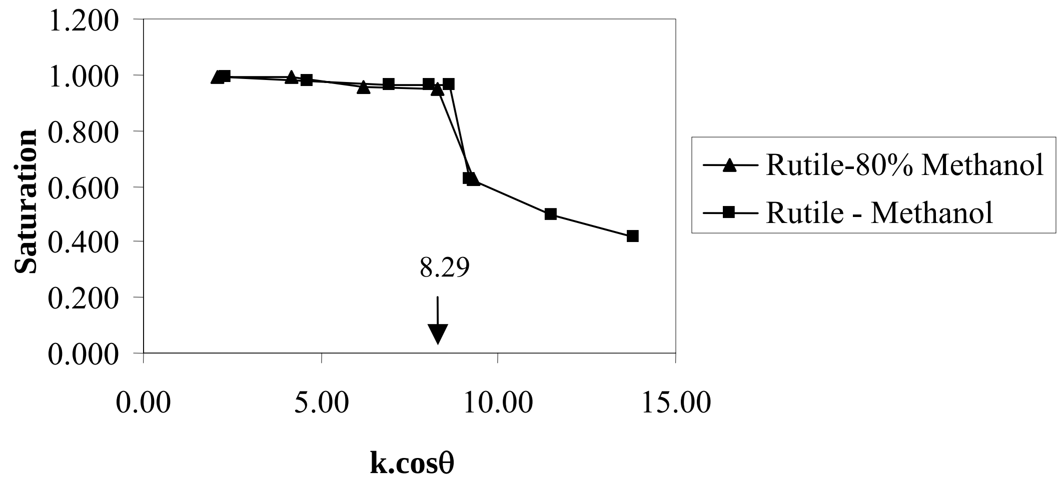

Figure 4.18 Residual cake saturation versus k.cosθ plots for -150 + 200 mesh rutile when methanol or a water-methanol mixture was used as the liquid.

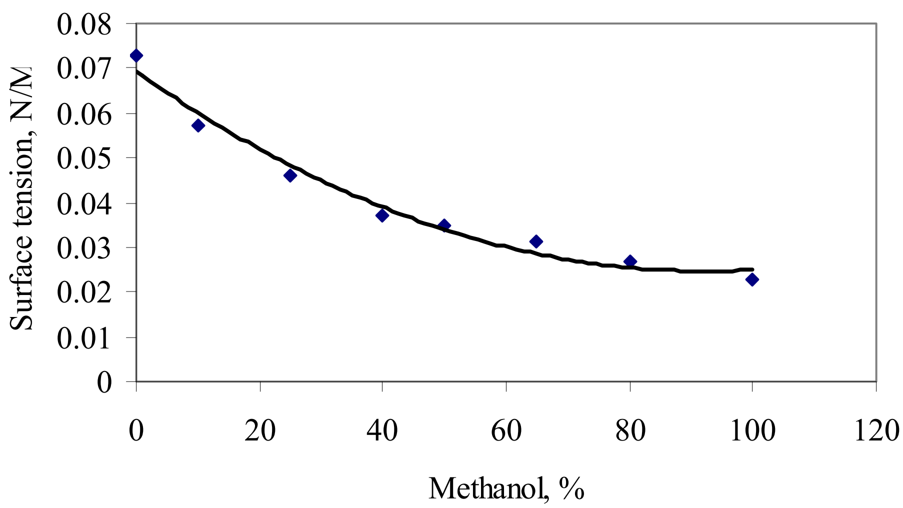

Figure 4.19 Surface tension values of methanol mixtures.

Table 4.3 The contact angle and k.cosθ values for the rutile sample as obtained from cake dewatering tests using water-methanol mixtures.

Methanol %	Contact Angle θ	k.cosθ
100	0	8.64
80	16.36	8.29
65	17.28	8.25
50	21.29	8.05
40	25.31	7.81
25	21.47	8.04
10	23.72	7.91
0	32.83	7.26

Cake dewatering experiments using dodecyl amine and sodium dodecyl sulfate solutions at various pH values were also conducted with the rutile sample. The data obtained were again plotted as saturation-versus-k.cosθ graphs, critical points on the plots were found, and the contact angles were calculated. Table 4.4 summarizes the results.

Dodecyl amine is again most effective at around pH 6 in increasing the contact angle, but the angle is almost 10° smaller than the maximum angle obtained in the case of zircon-dodecyl amine system. Sodium dodecyl sulfate was again effective only at pH 2 where the rutile surface is positively charged and led to more or less the same contact angles (54°) as the zircon-sodium dodecyl sulfate system at the optimal addition of the surfactant (10^{-4}M).

Table 4.4 Contact angles for rutile obtained from dewatering experiments using dodecyl amine and sodium dodecyl sulfate solutions at various pH values.

Concentration	pH	Contact Angle
10^{-5} M DA	4	35.31
	6	37.22
	8	35.66
	10	33.19
5.10^{-5} M DA	4	35.43
	6	38.41
	8	35.99
	10	32.71
10^{-4} M DA	4	39.04
	6	40.91
	8	41.71
	10	33.79
10^{-4} M SDS	2	54.96
5.10^{-5} M SDS	2	53.32
10^{-5} M SDS	2	40.19
Distilled Water	5.5	32.83

4.2 Column Wicking Experiments

Column wicking experiments were performed to compare the contact angle values obtained from capillaric dewatering experiments. However, one must keep in mind that the column wicking method measures the advancing contact angle and the new method proposed in this thesis measures the receding contact angle. As we have already pointed out that the advancing contact angle may be as much as 50° larger than the receding contact angle.

Figure 4.20 shows the plots obtained from the column wicking experiments with the zircon sample when methanol, hexane, formamide, and water are individually used as the liquid. Coinciding plots of methanol, hexane, and formamide justify that the methanol is, in fact, a completely-wetting liquid since it is known from the pertinent literature that hexane has been used as a completely-wetting liquid. The quantity A in the vertical axis of the figure is given by

$$A = \left(\frac{2.h^2.\eta}{\gamma_L} \right) \qquad [26]$$

so that the slope of the linear plot is equal to R.cosθ, where R is the effective interstitial pore radius between the packed particles in the column. Since cosθ = 1 for a completely-wetting liquid, the value of R for a certain packed bed of particles can be directly calculated from the slope of the plot of the completely-wetting liquid. Knowing the value of R, the contact angle for a partially-wetting liquid may be found agin by the slope of its linear plot. For example, from the column wicking plot of methanol-zircon system R = 0.02405, and for the water-zircon system

$$R.\cos\theta = 0.00826$$

$$0.02405.\ \cos\theta = 0.00687 \quad \Rightarrow \quad \theta = 69.91°$$

This is the advancing contact angle for water-zircon system and, as expected, it is greater than the receding contact angle (41.19°) obtained by the cake dewatering method by almost a difference of 29°.

A similar set of column wicking plots are given for rutile in Figure 4.21, from which it can be calculated that the advancing contact angle for water-rutile system is 63.55° which is approximately 30° greater than the receding contact angle found by the dewatering method. The resemblence with the zircon-water system is quite striking.

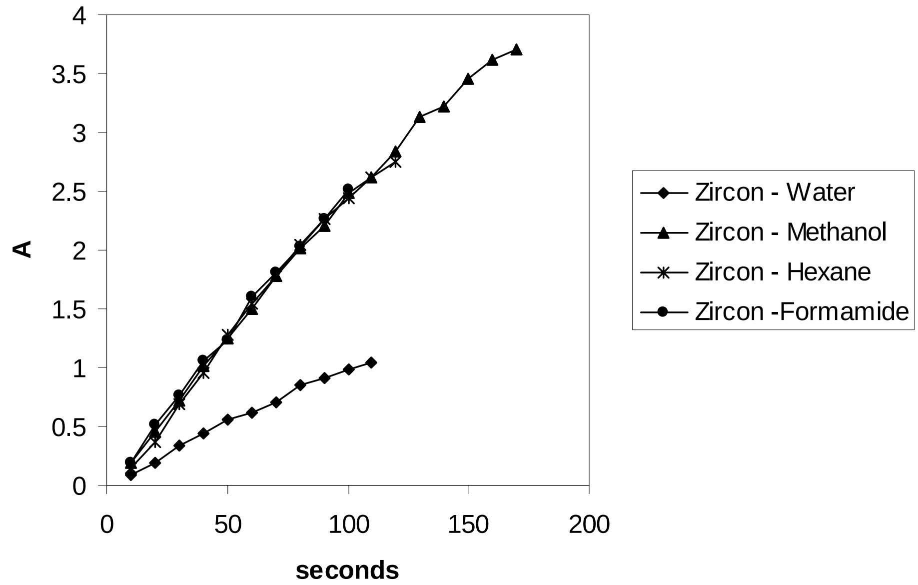

Figure 4.20 Column wicking plots for -150+200 mesh zircon particles with completely-wetting organic liquids and partially-wetting liquid water.

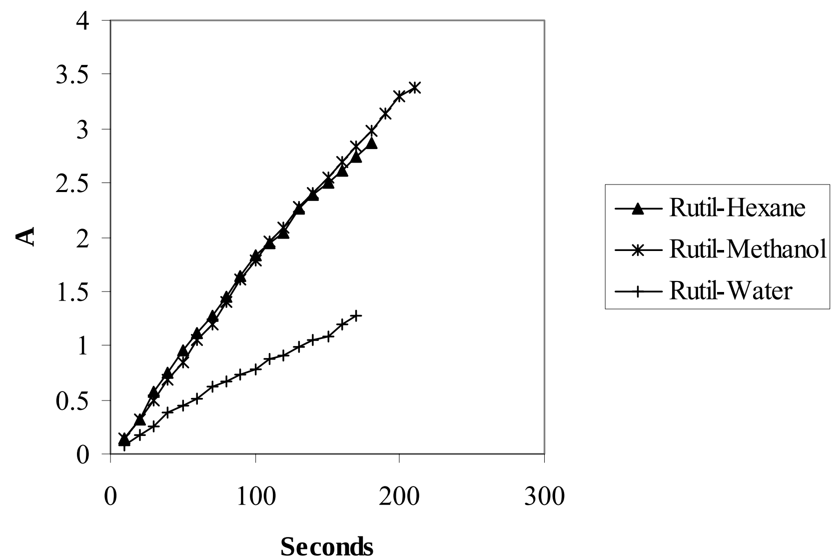

Figure 4.21 Column wicking plots for -150+200 mesh rutile particles with completely-wetting organic liquids and partially-wetting liquid water.

Figures 4.22 and 4.23 show the column wicking plots for zircon and rutile, respectively, with the use of water-methanol mixtures. The receding contact angles derived from these figures are presented in Table 4.5 and Table 4.6.

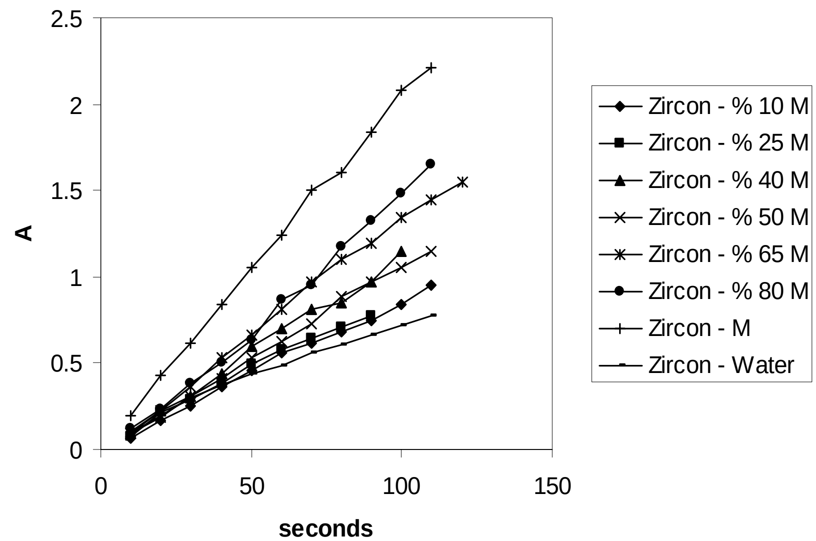

Figure 4.22 Column wicking plots for -150+200 mesh zircon particles with water-methanol mixtures.

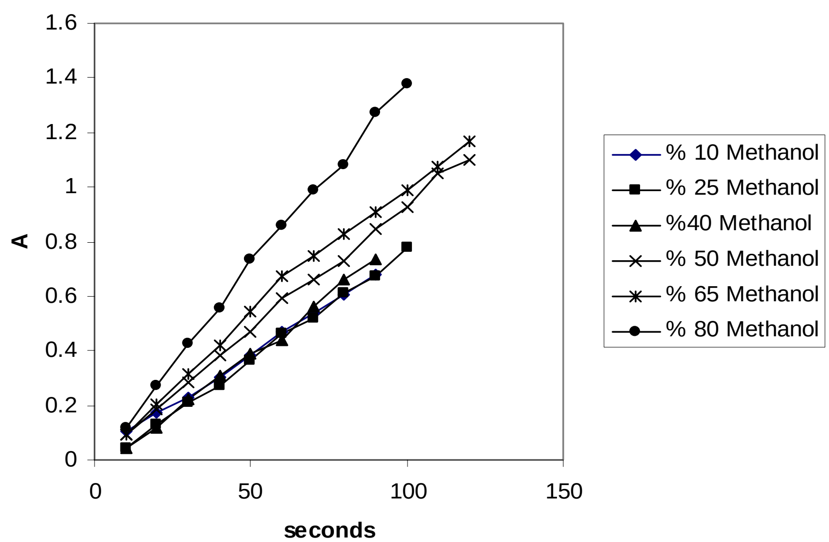

Figure 4.23 Column wicking plots for -150+200 mesh rutile particles with water-methanol mixtures.

Table 4.5 The advancing and receding contact angles of zircon with water-methanol mixtures in the column wicking experiments.

Liquid	θ_A	θ_R	$\theta_A - \theta_R$
Water	69.91	41.19	28.72
10% Methanol	69.49	39.42	30.07
25% Methanol	65.32	39.64	25.68
40% Methanol	66.91	35.04	31.87
50 % Methanol	60.66	32.46	28.2
65% Methanol	52.92	19.09	33.83
80 % Methanol	51.32	20.36	30.96
Methanol	0	0	0

Table 4.6 The advancing and receding contact angles of rutile with water-methanol mixtures in the column wicking experiments.

Liquid	θ_A	θ_R	$\theta_A - \theta_R$
Water	63.55	32.83	30.72
10% Methanol	62.14	23.72	38.42
25% Methanol	61.99	21.47	40.72
40% Methanol	59.10	25.31	33.79
50 % Methanol	56.46	21.29	35.17
65% Methanol	45.95	17.28	28.67
80 % Methanol	34.94	16.36	18.58
Methanol	0	0	0

We can see from the tables that there is a difference of 20° to 40° between the advancing contact angles obtained from column wicking experiments and the receding contact angles obtained from cake dewatering experiments.

Column wicking experiments were also conducted with dodecyl amine and sodium dodecyl sulfate solutions to make a comparison with the cake dewatering experiments, and the results are presented in Figures 4.24-4.30 and Tables 4.7 and 4.8

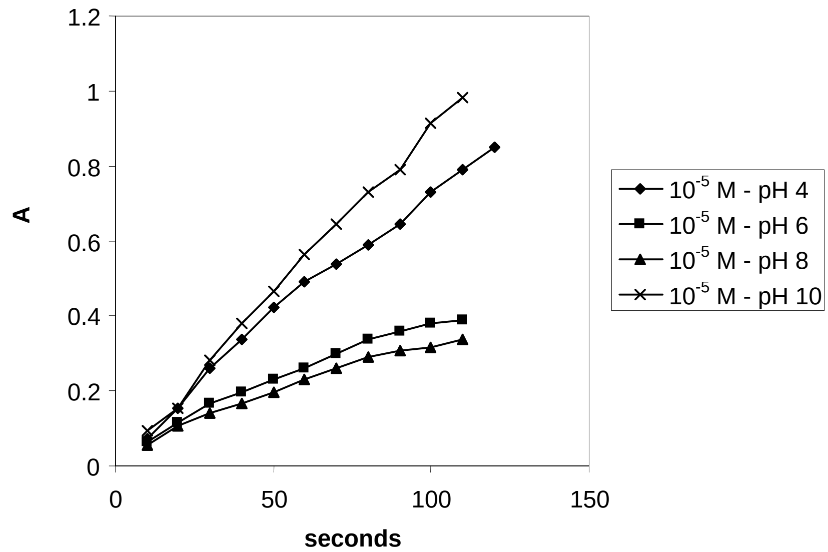

Figure 4.24 Column wicking plots for -150+200 mesh zircon particles with 10^{-5} M dodecyl amine at different pH values.

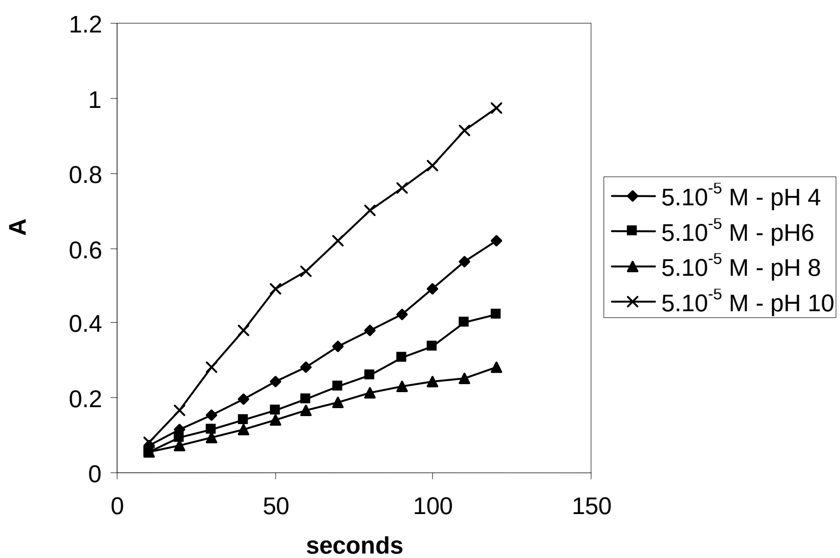

Figure 4.25 Column wicking plots for -150+200 mesh zircon particles with 5.10^{-5} M dodecyl amine at different pH values

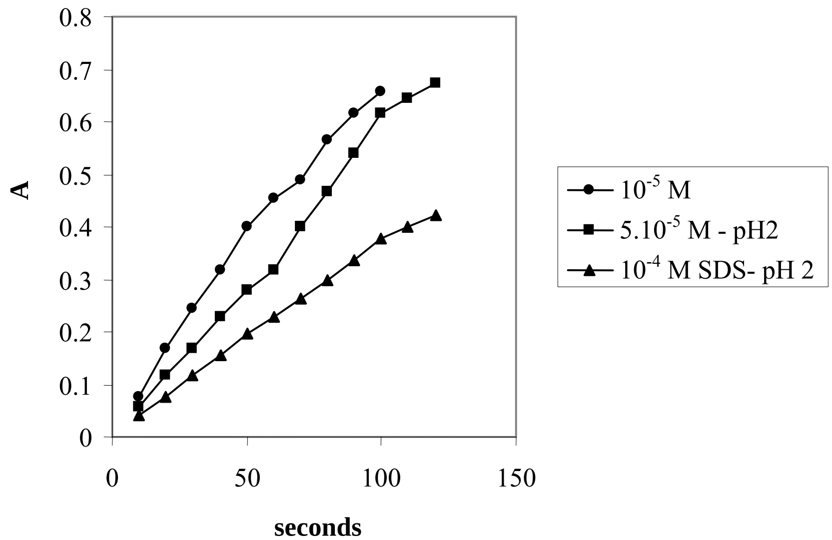

Figure 4.26 Column wicking plots for -150+200 mesh zircon particles with different concentrations of sodium dodecyl sulfate at pH 2.

Table 4.7 The advancing and receding contact angles of zircon from column wicking (θ_A) and cake dewatering experiments (θ_R).

Liquid	pH	θ_A	θ_R	$\theta_A - \theta_R$
10^{-5} M DA	4	72.13	41.3	30.83
	6	80.7	48.7	32
	8	82.07	49.74	32.33
	10	67.85	39.08	28.77
5.10^{-5} M DA	4	79.6	42.48	37.12
	6	82.5	49.83	32.67
	8	84.7	51.31	33.39
	10	69.33	39.98	29.35
10^{-4} M SDS	2	81.06	53.22	27.84
5.10^{-5} M SDS	2	75.49	51.95	23.54
10^{-5} M SDS	2	71.52	49.64	21.88

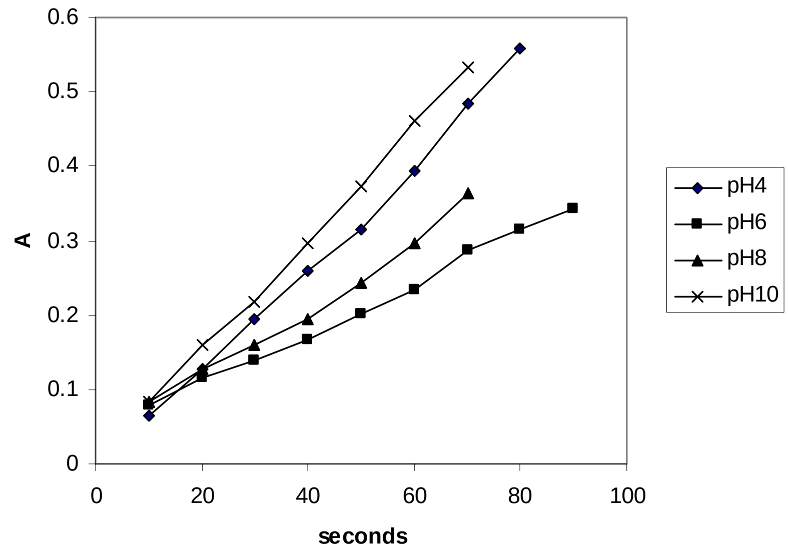

Figure 4.27 Column wicking plots for -150+200 mesh rutile particles with 10^{-5} M dodecyl amine at different pH values.

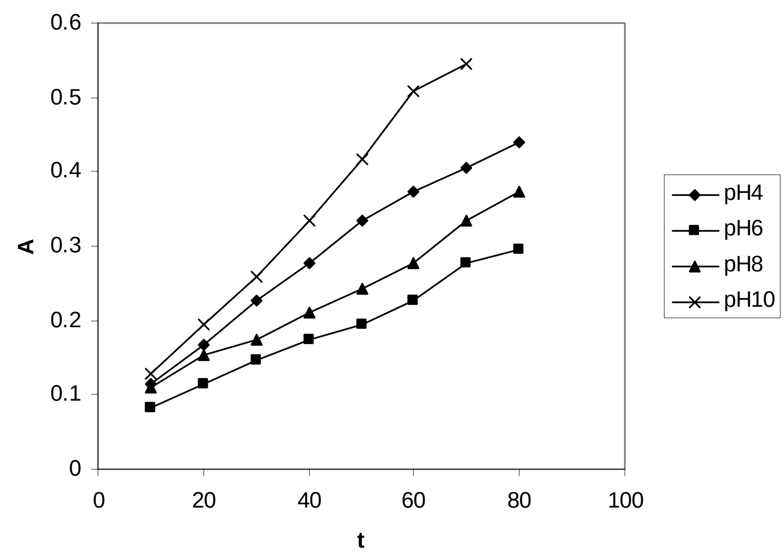

Figure 4.28 Column wicking plots for -150+200 mesh rutile particles with $5x10^{-5}$ M dodecyl amine at different pH values.

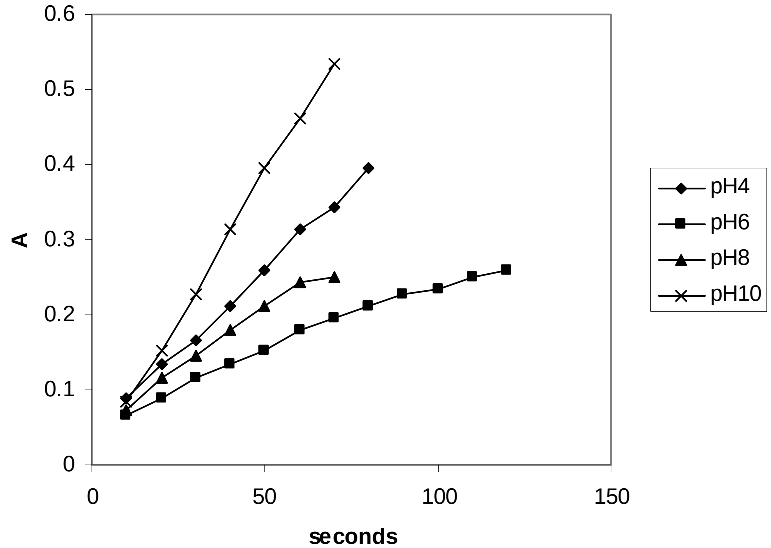

Figure 4.29 Column wicking plots for -150+200 mesh rutile particles with 10^{-4} M dodecyl amine at different pH values.

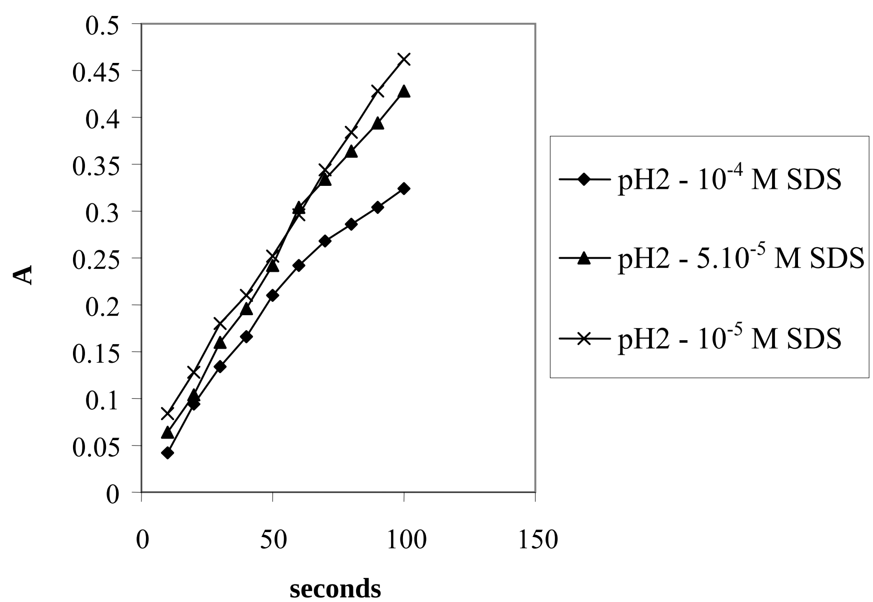

Figure 4.30 Column wicking plots for -150+200 mesh rutile particles with different concentrations of sodium dodecyl sulfate at pH 2.

Table 4.8 The advancing and receding contact angles of rutile from column wicking (θ_A) and cake dewatering experiments (θ_R).

Liquid	pH	θ_A	θ_R	$\theta_A - \theta_R$
10^{-5} M DA	4	65.37	35.31	30.06
	6	78.42	37.22	41.2
	8	73.57	35.66	37.91
	10	63.25	33.19	30.06
5.10^{-5} M DA	4	72.11	35.43	36.68
	6	80.19	38.41	41.78
	8	77.19	35.99	41.2
	10	63.02	32.71	30.31
10^{-4} M SDS	4	74.39	39.04	35.35
	6	83.07	40.91	42.16
	8	79.08	41.71	37.37
	10	63.48	33.79	29.69
10^{-4} M SDS	2	77.97	54.96	23.01
5.10^{-5} M SDS	2	76.84	53.32	23.52
10^{-5} M SDS	2	75.52	40.19	35.33

When the receding and advancing contact angles given in Table 4.7 and Table 4.8 are compared, we may see that there are differences between advancing and receding contact angles. There is an agreement between the results of column wicking and cake dewatering experiments. At pH 8, in all concentrations of dodecyl amine, both receding and advancing contact angles gave a higher degree. In the experiments with sodium dodecyl sulfate, we can see that, at pH 2, the degree of contact angle is getting higher with the increase of collector and also the receding contact angles are parallel to advancing contact angles from the column wicking experiments.

4.3 Microflotation Experiments

Microflotation experiments were performed whether the contact angles obtained from cake dewatering experiments are reliable and correlate well with the flotation behavior of the zircon and rutile particles. Figure 4.31-4.34 present the flotation recoveries obtained at various conditions which were also tested in contact angle measurement experiments.

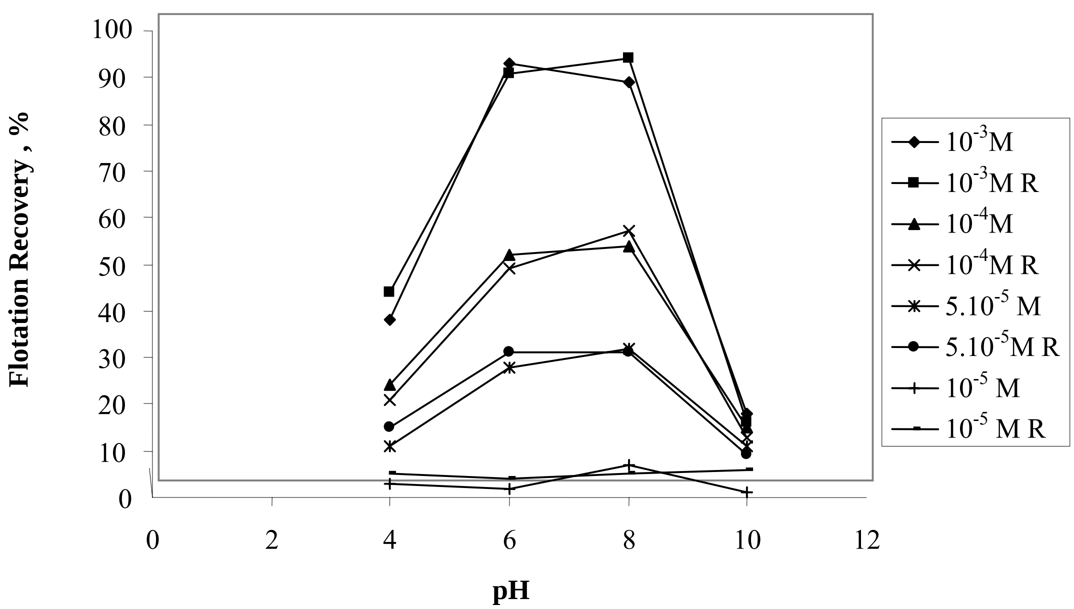

Figure 4.31 Flotation response of -150+200 mesh zircon with dodecyl amine at different pH values. R denotes repeat experiments.

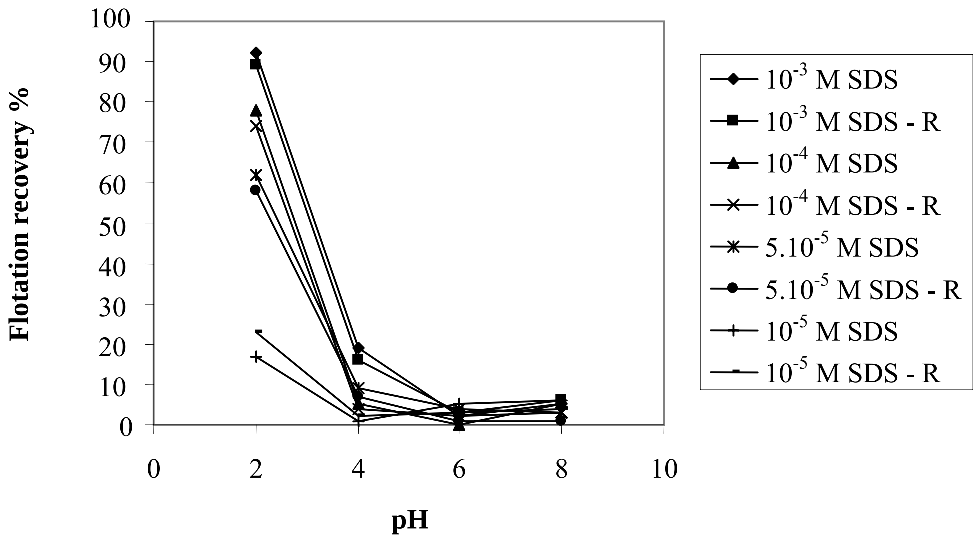

Figure 4.32 Flotation response of -150+200 mesh zircon with sodium dodecyl sulfate at different pH values. R denotes repeat experiments.

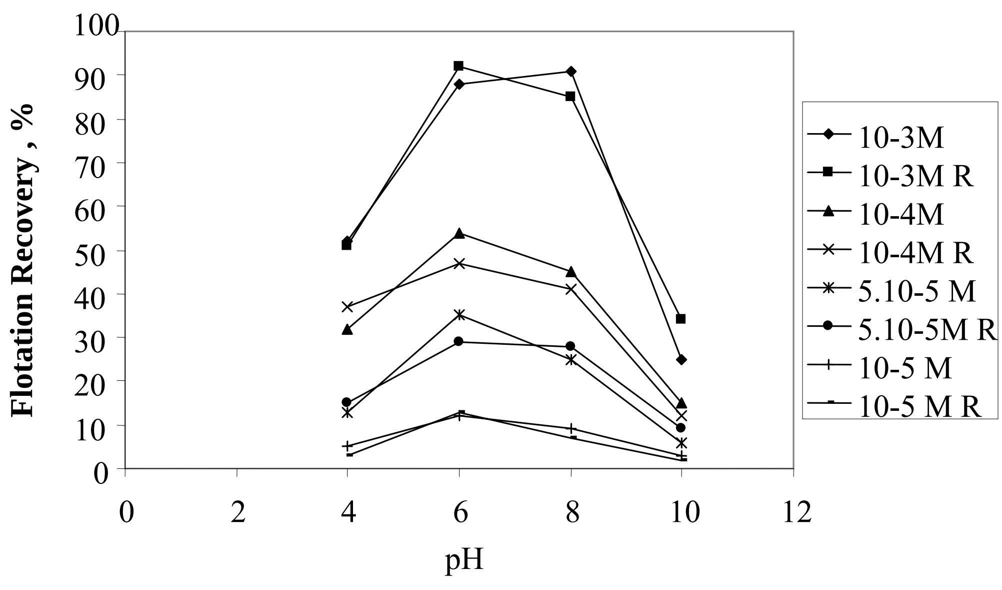

Figure 4.33 Flotation response of -150+200 mesh rutile with dodecyl amine at different pH values. R denotes repeat experiments.

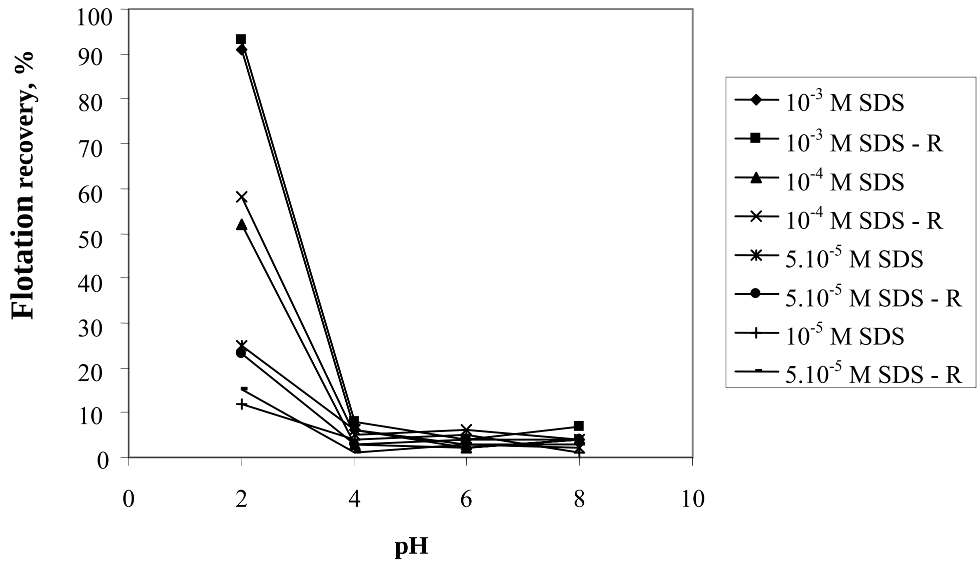

Figure 4.34 Flotation response of -150+200 mesh rutile with sodium dodecyl sulfate at different pH values. R denotes repeat experiments.

It can be seen from the figures that the flotation recovery of minerals are consistent with the contanct angles obtained from the proposed method of measurement in the sense that maximum flotation recovery ranges are in very good agreement with maximum contact angle ranges where we expect highest degrees of hydrophobicity, and, hence, maximum floatability. The only difference between the microflotation tests and capillaric dewatering tests is the amount of collector which adsorbed by the solid, in microflotation 1 gr of solid was used while in dewatering 50 gr of solid was used. This is the reason of high percent of flotation.

These results suggest that, instead of carrying out tedious microflotation tests requiring special experimental set-ups, we may conduct simple and fast filtration experiments to study the wetting characteristics of solid particulates treated with various chemicals. Furthermore, the proposed method of measurement yields the receding contact angles, which represent the true physical event taking place in froth flotation in which air replaces water at already wetted surfaces.

CHAPTER 5

CONCLUSIONS

In this research, the determination of the contact angle by capillaric dewatering of filter cakes was studied on zircon and rutile powders and the findings are compared with column wicking and microflotation experiments. As a result of this study, the following conclusions can be drawn:

- Capillaric dewatering method can be used for determining the receding contact angle of powders. Capillaric dewatering method is an easily applicable technique to determine the contact angles of powders and also for determining the contact angles for flotation applications.

- Comparing column wicking experiments and capillaric dewatering experiments, it is observed that the maximum contact angle range for zircon by using dodecyl amine is from pH 6 to pH 8, and by using sodium dodecyl sulfate it is below pH 3,and comparing the column wicking experiments and capillaric dewatering experiments, it is observed that the maximum contact angle range for rutile by using dodecyl amine is from pH 6 to pH 8, and by using sodium dodecyl sulfate is below 3.

- The difference between advancing and receding contact angles can be higher than 40°.

- Zircon gives a higher contact angle than rutile for the systems studied.

- Highly acidic and highly alkaline conditions are not suitable for flotation of zircon and rutile by using dodecyl amine, as verified by the very low value of the contact angle at these conditions.

REFERENCES

1. Adamson A.W., *Physical Chemistry of Surfaces, 2nd Ed.,* Interscience Publishers, California, 1967

2. Besra L., Sengupta D.K., Roy S.K., *Particle characteristics and their influence on dewatering of kaolin, calcite and quartz suspensions,* International Journal of Mineral Processing, Volume 59, Issue 2, May 2000, Pages 89-112

3. Biliński B., Holysz L., *Some Theoretical and Experimental Limitations in the Determination of Surface Free Energy of Siliceous Solids,* Powder Technology, Volume 102, 1999, Pages 120-126

4. Chibowski E., Carpio R.P., *A Novel Method for Surface Free-Energy Determination of Powdered Solids*, Journal of Colloid and Interface Science, Volume 240, 2001, Pages 473-479

5. Chibowski E., Carpio R.P., *Problems of contact angle and solid surface free energy determination,* Advances in Colloid and Interface Science, Volume 98, 2002, Pages 245-264

6. Condie D.J., Hinkel M., Veal C.J., *Modelling the vacuum filtration of fine coal,* Filtration & Separation, Volume 33, Issue 9, October 1996, Pages 825-834

7. Diggins D., Fokkink L.G.J., Ralston J., *The wetting of angular quartz particles: Capillary pressure and contact angles,* Colloids and Surfaces, Volume 44, 1990, Pages 299-313

8. Douillard J.M., Zajac J., Malandrini H., et al., *Contact angle and film pressure: Study of a talc surface,* Journal of Colloid and Interface Science, Volume 255, November 2002, Pages 341-351

9. Dunstan D., White L.R., *A Capillary Pressure Method for Measurement of Contact Angles in Powders and Porous Media*, Journal of Colloid and Interface Science, Volume 111, May 1986, Pages 60-64

10. Finch J.A., Smith G.W., *Contact Angle and Wetting,* Minerals Sci.Engng, Volume 11, January 1979, Pages 36-63

11. Fowkes F.M, ed., 1964 *Dispersion force contributions to surface and interfacial tensions, Contact angles and heats of immersion,* Advances in Chemistry series, Volume 43, Pages 99ff

12. Good R.J., Mittal K.L., *Contact Angle, Wettability and Adhesion,* Netherlands, 1993

13. Harkins W.D., Feldman, A., 1922, *Spreading of liquids and the spreading coefficient,* Journal of the American Chemical Society, Volume 44, No 12, Pages 2665ff.

14. Heertjes P.M., Kossen N.W.F., *Measuring the contact angles of powder-liquid systems,* Powder Technology, Volume 1, Issue 1, February 1967, Pages 33-42

15. Hoşten, Ç., *Micro-floatability of rutile and zircon with soap and amine type collectors,* Physicochemical Problems of Mineral Processing, Volume 35, 2001, Pages 161-170

16. Hoşten Ç., Sastry K.V.S., *Empirical correlations for the prediction of cake dewatering characteristics,* Minerals Engineering, Volume 2, Issue 1, 1989, Pages 111-119

17. Iveson S.M., Holt S., Biggs S., *Contact angle measurements of iron ore powders*, Colloids and Surfaces, Volume 166, 2000, Pages 203-214

18. Krajewski S.R., Kujawski W., Dijioux F., et al., *Grafting of ZrO_2 powder and ZrO_2 membrane by fluoroalkylsilane,* Colloids and Surfaces A: Physicochemical and Engineering Aspects, Volume 243, Issues 1-3, August 2004, Pages 43-47

19. Muratoğlu R.A., *Floatability and adsorption characteristics of zircon with sodium oleate, Ankara,* Metu, 2000

20. Osipow L.I., *Surface Chemistry, Theory and Industrial Applications*, Reinfold Pub. Corp., New York, 1962

21. Puttock S. J., Fane A.G., Fell C. J. D., et al., *Vacuum filtration and dewatering of alumina trihydrate — The role of cake porosity and interfacial phenomena,* International Journal of Mineral Processing, Volume 17, Issues 3-4, July 1986, Pages 205-224

22. Rondeau X., Affolter C., Kommunjer L., et al., *Experimental determination of capillary forces by crushing strength measurements,* Powder Technology, Volume 130, February 2003, Pages 124-131

23. Siebold A., Nardin M., Schultz J., et al., *Effect of Dynamic Contact Angle on Capillary Rise Phenomena,* Colloids and Surfaces, Volume 161, 2000, Pages 81-87

24. Şan O., Hoşten Ç., *Filtration testing of a ceramic capillary filter produced from a high-silica glaze,* Minerals Engineering, Volume 15, Issue 7, July 2002, Pages 553-556

25. Teixeira P., Azeredo J., Oliveira R., et al., *Interfacial Interactions between Nitrifying Bacteria and Mineral Carriers in Aqueous Media Determined by Contact Angle Measurements and Thin Layer Wicking,* Colloids and Surfaces B: Biointerfaces, Volume 12, 1998, Pages 69-75

26. Wakeman R.J., *Vacuum dewatering and residual saturation of incompressible filter cakes,* International Journal of Mineral Processing, Volume 3, Issue 3, September 1976, Pages 193-206

APPENDIX A

TABLES OF CAPILLARIC DEWATERING EXPERIMENTS

Table A 1. -100+200 mesh quartz experimented with methanol

TEST NO	TEST SOLIDS	TEST LIQUID	SIZE (MESH)	DRY SOLIDS (GRAM)		CAKE POROSITY		
1	Quartz	100% Methanol	-100+200	30		0,53		
Vacuum (inch-Hg)	0,2	0,2	0,6	1	1,5	2	2,5	3
Dewat. Time(min)	0	2	2	2	2	2	2	2
Liquid (Gram)	10,23	10,18	10,09	10,01	9,93	8,71	5,84	4,76
Res Mois %	25,42	25,33	25,16	25,01	24,86	22,50	16,3	13,69
Saturation	1	0,995	0,986	0,978	0,970	0,85	0,570	0,465

Table A.2. -100+200 mesh quartz experimented with water

TEST NO	TEST SOLIDS	TEST LIQUID	SIZE (MESH)	DRY SOLIDS (GRAM)		CAKE POROSITY		
2	Quartz	Water	-100+200	30,02		0,47		
Vacuum (inch-Hg)	1	1	1,5	2	2,5	3	3,5	4
Dewat. Time(min)	0	3	3	3	3	3	3	3
Cake (Gram)	39,91	39,88	39,86	39,7	39,68	38,7	36,2	34
Res Mois %	24,78	24,72	24,68	24,38	24,34	22,36	17	11,7
Saturation	1	0,997	0,994	0,978	0,976	0,87	0,619	0,402

Table A.3. -100+200 mesh quartz experimented with 80% methanol

TEST NO	TEST SOLIDS	TEST LIQUID	SIZE (MESH)	DRY SOLIDS (GRAM)		CAKE POROSITY		
3	Quartz	80% Methanol	-100+200	30		0,47		
Vacuum (inch-Hg)	0,5	0,5	1	1,5	2	2,5	3	3,5
Dewat. Time(min)	0	2	2	2	2	2	2	2
Liquid (Gram)	8,51	8,47	8,42	7,71	5,08	4,41	3,91	3,47
Res Mois %	22,09	22,01	21,91	20,44	14,48	12,8	11,5	10,36
Saturation	1	0,995	0,989	0,905	0,596	0,52	0,46	0,407

Table A.4. -100+200 mesh quartz experimented with 65% methanol

TEST NO	TEST SOLIDS	TEST LIQUID	SIZE (MESH)	DRY SOLIDS (GRAM)		CAKE POROSITY		
4	Quartz	65% Methanol	-100+200	30		0,45		
Vacuum (inch-Hg)	0,5	0,5	1	1,5	2	2,5	3	3,5
Dewat. Time(min)	0	2	2	2	2	2	2	2
Liquid (Gram)	8,06	7,77	7,66	7,02	5,31	4,47	4,02	3,58
Res Mois %	21,17	20,57	20,33	18,96	15,03	13	11,8	10,66
Saturation	1	0,964	0,95	0,87	0,658	0,55	0,5	0,444

Table A.5. -100+200 mesh quartz experimented with 50% methanol

TEST NO	TEST SOLIDS	TEST LIQUID	SIZE (MESH)	DRY SOLIDS (GRAM)		CAKE POROSITY		
5	Quartz	50% Methanol	-100+200	30		0,45		
Vacuum (inch-Hg)	0,5	0,5	1	1,5	2	2,5	3	3,5
Dewat. Time(min)	0	2	2	2	2	2	2	2
Liquid (Gram)	8,32	8,27	8,24	8,21	7,96	6,85	5,08	4,06
Res Mois %	21,71	21,6	21,54	21,48	20,96	18,6	14,5	11,92
Saturation	1	0,993	0,99	0,986	0,956	0,82	0,61	0,487

Table A.6. -100+200 mesh quartz experimented with 40% methanol

TEST NO	TEST SOLIDS	TEST LIQUID	SIZE (MESH)	DRY SOLIDS (GRAM)		CAKE POROSITY		
6	Quartz	40% Methanol	-100+200	30		0,48		
Vacuum (inch-Hg)	0,5	0,5	1	1,5	2	2,5	3	3,5
Dewat. Time(min)	0	2	2	2	2	2	2	2
Liquid (Gram)	9,85	9,82	9,78	9,76	9,06	7,41	5,94	5,37
Res Mois %	24,71	24,66	24,58	24,54	23,19	19,8	16,5	15,18
Saturation	1	0,996	0,992	0,99	0,919	0,75	0,6	0,545

Table A.7. -100+200 mesh quartz experimented with 25% methanol

TEST NO	TEST SOLIDS	TEST LIQUID	SIZE (MESH)	DRY SOLIDS (GRAM)		CAKE POROSITY		
7	Quartz	25% Methanol	-100+200	30		0,48		
Vacuum (inch-Hg)	0,5	0,5	1	1,5	2	2,5	3	3,5
Dewat. Time(min)	0	3	3	3	3	3	3	3
Liquid (Gram)	9,94	9,92	9,84	9,8	9,77	8,8	6,96	5,97
Res Mois %	24,88	24,84	24,69	24,62	24,56	22,7	18,8	16,59
Saturation	1	0,997	0,989	0,985	0,982	0,89	0,7	0,6

Table A.8. -100+200 mesh quartz experimented with 10% methanol

TEST NO	TEST SOLIDS	TEST LIQUID	SIZE (MESH)	DRY SOLIDS (GRAM)		CAKE POROSITY		
8	Quartz	10% Methanol	-100+200	30		0,47		
Vacuum (inch-Hg)	0,5	0,5	1	1,5	2	2,5	3	3,5
Dewat. Time(min)	0	3	3	3	3	3	3	3
Liquid (Gram)	9,98	9,97	9,94	9,92	9,91	9,8	8,01	5,97
Res Mois %	24,96	24,94	24,88	24,84	24,83	24,6	21,1	16,59
Saturation	1	0,998	0,995	0,993	0,992	0,98	0,8	0,598

Table A.9. -100+200 mesh quartz experimented with water

TEST NO	TEST SOLIDS	TEST LIQUID	SIZE MESH		DRY SOLIDS GRAM		CAKE POROSITY	
9	Quartz	Water	-100+200		20		0,463	
Vacuum (inch-Hg)	1	1	1,5	2	2,5	3	3,5	4
Dewat. Time	0	5	5	5	5	5	5	5
Wet Cake Gram	26,8	26,51	26,5	26,48	26,47	25,3	22,9	22,52
Res Mois %	24,64	24,55	24,52	24,47	24,44	20,9	12,8	11,19
Saturation	1	0,99	0,99	0,99	0,98	0,8	0,45	0,38

Table A.10. -200+400 mesh quartz experimented with water

TEST NO	TEST SOLIDS	TEST LIQUID	SIZE MESH		DRY SOLIDS GRAM		CAKE POROSITY	
10	Quartz	Water	-200+400		30		0,551	
Vacuum (inch-Hg)	1	1	1,5	2	2,5	3	3,5	4
Dewat. Time	0	6	6	6	6	6	6	6
Wet Cake Gram	43,96	42,76	42,69	42,67	42,66	42,7	42,6	42,62
Res Mois %	31,75	29,84	29,72	29,69	29,67	29,7	29,6	29,61
Saturation	1	0,91	0,909	0,907	0,906	0,91	0,91	0,904

Table A.11. -100+200 mesh quartz experimented with hexane

TEST NO	TEST SOLID	TEST LIQUID	SIZE MESH		DRY SOLIDS GRAM		CAKE POROSITY	
11	Quartz	Hexane	-100+200		30		0,487	
Vacuum (inch-Hg)	1	1	1,5	2	2,5	3		
Dewat. Time	0	5	5	5	5	5		
Wet Cake Gram	37,13	34,65	33,75	32,69	30,95	30		
Res Mois %	19,2	13,42	11,11	8,23	3,07	0,06		
Saturation	1	0,651	0,526	0,377	0,133	0		

Table A.12. -100+200 mesh quartz experimented with hexane

TEST NO	TEST SOLIDS	TEST LIQUID	SIZE MESH		DRY SOLIDS GRAM		CAKE POROSITY	
12	Quartz	Hexane	-100+200		30		0,479	
Vacuum (inch-Hg)	1	1	1,5	2	2,5	3		
Dewat. Time	0	5	5	5	5	5		
Wet Cake Gram	36,91	34,44	33,64	32,57	30,23	30		
Res Mois %	18,72	12,89	10,82	7,89	0,76	0,03		
Saturation	1	0,643	0,527	0,372	0,033	0		

Table A.13. -200+400 mesh quartz experimented with hexane

TEST NO	TEST SOLIDS	TEST LIQUID	SIZE MESH		DRY SOLIDS GRAM		CAKE POROSITY	
13	Quartz	Hexane	-200+400		30		0,51	
Vacuum (inch-Hg)	0,2	0,2	0,4	0,6	0,8	1	1,2	1,4
Dewat. Time	0	5	5	5	5	5		
Wet Cake Gram	37,88	37,5	37,29	37,08	36,83	36,5	36,2	35,8
Res Mois %	20,8	20	19,55	19,09	18,54	17,9	17,1	16,2
Saturation	1	0,951	0,924	0,897	0,865	0,83	0,78	0,735

Table A.14. -100+200 mesh quartz experimented with water

TEST NO	TEST SOLIDS	TEST LIQUID	SIZE MESH		DRY SOLIDS GRAM		CAKE POROSITY	
14	Quartz	Water	-100+200		30		0,53	
Vacuum (inch-Hg)	0,1		0,2	0,4	0,6	0,8	1	1,2
Dewat. Time	0	2	2	2	2	2	2	2
Liquid Gram	8,61	8,4	8,11	7,83	7,53	7,22	5,87	4,53
Res Mois %	22,2	21,8	21,2	20,69	20	19,4	16,4	13,11
Saturation	1	0,975	0,941	0,909	0,874	0,84	0,68	0,526

Table A.15. -150+200 mesh zircon experimented with water

TEST NO	TEST SOLIDS	TEST LIQUID	SIZE (MESH)	DRY SOLIDS (GRAM)		CAKE POROSITY		
15	Zircon	Water	-150+200	50		0,462		
Vacuum (inch-Hg)	with gravity	0,2	0,5	1	1,5	1,6	1,7	2
Dewat. Time(min)	0	2	2	2	2	2	2	2
Cake (Gram)	59,12	59,09	59,07	59,04	59,03	59	59	55,3
Res Mois %	15,43	15,38	15,35	15,31	15,30	15,30	15,28	9,58
Saturation	1	0,997	0,995	0,991	0,990	0,990	0,989	0,581

Table A.16. -150+200 mesh zircon experimented with methanol

TEST NO	TEST SOLIDS	TEST LIQUID	SIZE (MESH)	DRY SOLIDS (GRAM)		CAKE POROSITY		
16	Zircon	Methanol	-150+200	50		0,47		
Vacuum (inch-Hg)	with gravity	0,2	0,4	0,6	0,7	0,8	1	1,2
Dewat. Time(min)	0	2	2	2	2	2	2	2
Cake (Gram)	57,37	57,31	57,24	57,16	57,15	53,7	53	52,59
Res Mois %	12,85	12,76	12,65	12,53	12,51	6,80	5,57	4,92
Saturation	1,000	0,992	0,982	0,972	0,970	0,495	0,400	0,351

Table A.17. -150+200 mesh zircon experimented with methanol

TEST NO	TEST SOLIDS	TEST LIQUID	SIZE (MESH)	DRY SOLIDS (GRAM)		CAKE POROSITY		
17	Zircon	Methanol	-150+200	50		0,463		
Vacuum (inch-Hg)	with gravity	0,2	0,4	0,6	0,7	0,8	1	1,2
Dewat. Time(min)	0	2	2	2	2	2	2	2
Cake (Gram)	57,29	57,28	57,28	57,21	57,19	55	52,9	51,65
Res Mois %	12,72	12,71	12,71	12,60	12,57	9,06	5,41	3,19
Saturation	1,000	0,999	0,999	0,989	0,986	0,683	0,392	0,226

Table A.18. -150+200 mesh zircon experimented with 10% methanol

TEST NO	TEST SOLIDS	TEST LIQUID	SIZE (MESH)	DRY SOLIDS (GRAM)		CAKE POROSITY		
18	Zircon	Methanol 10%	-150+200	50		0,455		
Vacuum (inch-Hg)	with gravity	0,5	1	1,2	1,4	1,6	1,8	
Dewat. Time(min)	0	2	2	2	2	2	2	
Cake (Gram)	58,72	58,64	58,42	58,4	58,28	55,7	54,3	
Res Mois %	14,85	14,73	14,41	14,38	14,21	10,15	7,83	
Saturation	1,000	0,991	0,966	0,963	0,950	0,648	0,487	

Table A.19. -150+200 mesh zircon experimented with 10% methanol

TEST NO	TEST SOLIDS	TEST LIQUID	SIZE (MESH)	DRY SOLIDS (GRAM)		CAKE POROSITY		
19	Zircon	Methanol 10%	-150+200	50		0,461		
Vacuum (inch-Hg)	with gravity	0,5	1	1,2	1,4	1,6	1,8	
Dewat. Time(min)	0	2	2	2	2	2	2	
Cake (Gram)	58,93	58,92	58,91	58,91	58,91	56,7	54,2	
Res Mois %	15,15	15,14	15,12	15,12	15,12	11,74	7,80	
Saturation	1,000	0,999	0,998	0,998	0,998	0,745	0,474	

Table A.20. -150+200 mesh zircon experimented with 25% methanol

TEST NO	TEST SOLIDS	TEST LIQUID	SIZE (MESH)	DRY SOLIDS (GRAM)		CAKE POROSITY		
20	Zircon	Methanol 25%	-150+200	50		0,461		
Vacuum (inch-Hg)	with gravity	0,5	1	1,1	1,2	1,4	1,6	
Dewat. Time(min)	0	2	2	2	2	2	2	
Cake (Gram)	58,71	58,66	58,63	58,62	56,89	54,8	53,7	
Res Mois %	14,84	14,76	14,72	14,70	12,11	8,78	6,82	
Saturation	1,000	0,994	0,991	0,990	0,791	0,552	0,420	

Table A.21. -150+200 mesh zircon experimented with 25% methanol

TEST NO	TEST SOLIDS	TEST LIQUID	SIZE (MESH)	DRY SOLIDS (GRAM)		CAKE POROSITY		
21	Zircon	Methanol 25%	-150+200	50		0,459		
Vacuum (inch-Hg)	with gravity	0,5	1	1,1	1,2	1,4	1,6	
Dewat. Time(min)	0	2	2	2	2	2	2	
Cake (Gram)	58,65	58,65	58,64	58,62	56,53	55,8	53,3	
Res Mois %	14,75	14,75	14,73	14,70	11,55	10,46	6,12	
Saturation	1,000	1,000	0,999	0,997	0,755	0,675	0,377	

Table A.22. -150+200 mesh zircon experimented with 40% methanol

TEST NO	TEST SOLIDS	TEST LIQUID	SIZE (MESH)	DRY SOLIDS (GRAM)		CAKE POROSITY		
22	Zircon	Methanol 40%	-150+200	50		0,446		
Vacuum (inch-Hg)	with gravity	0,4	0,6	0,8	1	1,2	1,4	
Dewat. Time(min)	0	2	2	2	2	2	2	
Cake (Gram)	57,95	57,77	57,69	57,55	57,41	55,1	54	
Res Mois %	13,72	13,45	13,33	13,12	12,91	9,27	7,32	
Saturation	1,000	0,977	0,967	0,950	0,932	0,643	0,497	

Table A.23. -150+200 mesh zircon experimented with 40% methanol

TEST NO	TEST SOLIDS	TEST LIQUID	SIZE (MESH)	DRY SOLIDS (GRAM)		CAKE POROSITY		
23	Zircon	Methanol 40%	-150+200	50		0,443		
Vacuum (inch-Hg)	with gravity	0,4	0,6	0,8	1	1,2	1,4	
Dewat. Time(min)	0	2	2	2	2	2	2	
Cake (Gram)	57,86	57,85	57,83	57,83	57,82	55,2	52,1	
Res Mois %	13,58	13,57	13,54	13,54	13,52	9,47	4,05	
Saturation	1,000	0,999	0,996	0,996	0,995	0,665	0,268	

Table A.24. -150+200 mesh zircon experimented with 50% methanol

TEST NO	TEST SOLIDS	TEST LIQUID	SIZE (MESH)	DRY SOLIDS (GRAM)		CAKE POROSITY		
24	Zircon	Methanol 50%	-150+200	50		0,439		
Vacuum (inch-Hg)	with gravity	0,5	1	1,2	1,4			
Dewat. Time(min)	0	2	2	2	2			
Cake (Gram)	57,61	57,47	57,4	54,9	54,22			
Res Mois %	13,21	13,00	12,89	8,93	7,78			
Saturation	1,000	0,982	0,972	0,644	0,555			

Table A.25. -150+200 mesh zircon experimented with 50% methanol

TEST NO	TEST SOLIDS	TEST LIQUID	SIZE (MESH)	DRY SOLIDS (GRAM)		CAKE POROSITY		
25	Zircon	Methanol 50%	-150+200	50		0,442		
Vacuum (inch-Hg)	with gravity	0,5	1	1,2	1,4			
Dewat. Time(min)	0	2	2	2	2			
Cake (Gram)	57,68	57,66	57,65	55,23	53,65			
Res Mois %	13,31	13,28	13,27	9,47	6,80			
Saturation	1,000	0,997	0,996	0,681	0,475			

Table A.26. -150+200 mesh zircon experimented with 65% methanol

TEST NO	TEST SOLIDS	TEST LIQUID	SIZE (MESH)	DRY SOLIDS (GRAM)		CAKE POROSITY		
26	Zircon	Methanol 65%	-150+200	50		0,466		
Vacuum (inch-Hg)	with gravity	0,2	0,4	0,6	0,7	0,8	1	
Dewat. Time(min)	0	2	2	2	2	2	2	
Cake (Gram)	57,5	57,42	57,31	57,23	57,21	55,5	54,1	
Res Mois %	13,04	12,92	12,76	12,63	12,60	9,86	7,49	
Saturation	1,000	0,989	0,975	0,964	0,961	0,729	0,540	

Table A.27. -150+200 mesh zircon experimented with 65% methanol

TEST NO	TEST SOLIDS	TEST LIQUID	SIZE (MESH)	DRY SOLIDS (GRAM)		CAKE POROSITY		
27	Zircon	Methanol 65%	-150+200	50		0,441		
Vacuum (inch-Hg)	with gravity	0,4	0,8	1	1,2			
Dewat. Time(min)	0	2	2	2	2			
Cake (Gram)	57,41	57,35	57,3	56,89	54,8			
Res Mois %	12,91	12,82	12,74	12,11	8,76			
Saturation	1,000	0,992	0,985	0,930	0,648			

Table A.28. -150+200 mesh zircon experimented with 80% methanol

TEST NO	TEST SOLIDS	TEST LIQUID	SIZE (MESH)	DRY SOLIDS (GRAM)		CAKE POROSITY		
28	Zircon	Methanol 80%	-150+200	50		0,452		
Vacuum (inch-Hg)	with gravity	0,2	0,4	0,6	0,8	1		
Dewat. Time(min)	0	2	2	2	2	2		
Cake (Gram)	57,44	57,35	57,27	57,21	57,15	54,6		
Res Mois %	12,95	12,82	12,69	12,60	12,51	8,41		
Saturation	1,000	0,988	0,977	0,969	0,961	0,617		

Table A.29. -150+200 mesh zircon experimented with 80% methanol

TEST NO	TEST SOLIDS	TEST LIQUID	SIZE (MESH)	DRY SOLIDS (GRAM)		CAKE POROSITY		
29	Zircon	Methanol 80%	-150+200	50		0,460		
Vacuum (inch-Hg)	with gravity	0,2	0,4	0,6	0,8	1		
Dewat. Time(min)	0	2	2	2	2	2		
Cake (Gram)	57,3	57,22	57,11	57,03	57,02	55,3		
Res Mois %	12,74	12,62	12,45	12,33	12,31	9,52		
Saturation	1,000	0,989	0,974	0,963	0,962	0,721		

Table A.30. -150+200 mesh zircon experimented with 5.10-5 M DA at pH 4

TEST NO	TEST SOLIDS	TEST LIQUID	SIZE (MESH)	DRY SOLIDS (GRAM)		CAKE POROSITY		
30	Zircon	10-5 M D pH 4	-150+200	50		0,485		
Vacuum (inch-Hg)	with gravity	0,2	0,5	1	1,5	2	2,2	
Dewat. Time(min)	0	2	2	2	2	2	2	
Cake (Gram)	60,01	60,01	59,99	59,99	59,98	56,4	55,7	
Res Mois %	33,34	33,34	33,32	33,32	33,31	29,03	28,12	
Saturation	1,000	1,000	0,998	0,998	0,997	0,635	0,564	

Table A.31. -150+200 mesh zircon experimented with 5.10-5 M DA at pH 4

TEST NO	TEST SOLIDS	TEST LIQUID	SIZE (MESH)	DRY SOLIDS (GRAM)		CAKE POROSITY		
31	Zircon	10-5 M D pH 4	-150+200	50		0,483		
Vacuum (inch-Hg)	with gravity	0,2	0,5	1	1,5	2	2,2	
Dewat. Time(min)	0	2	2	2	2	2	2	
Cake (Gram)	59,95	59,85	59,84	59,83	59,83	57,6	56,3	
Res Mois %	33,28	33,17	33,16	33,14	33,14	30,51	28,98	
Saturation	1,000	0,990	0,989	0,988	0,988	0,760	0,635	

Table A.32. -150+200 mesh zircon experimented with 5.10-5 M DA at pH 6

TEST NO	TEST SOLIDS	TEST LIQUID	SIZE (MESH)	DRY SOLIDS (GRAM)		CAKE POROSITY		
32	Zircon	10-5 M D pH 6	-150+200	50		0,451		
Vacuum (inch-Hg)	with gravity	0,2	0,5	1	1,5	2	2,2	
Dewat. Time(min)	0	2	2	2	2	2	2	
Cake (Gram)	58,75	58,75	58,72	58,71	58,7	57,7	57	
Res Mois %	31,91	31,91	31,88	31,87	31,86	30,66	29,76	
Saturation	1,000	1,000	0,997	0,995	0,994	0,879	0,794	

Table A.33. -150+200 mesh zircon experimented with 5.10-5 M DA at pH 6

TEST NO	TEST SOLIDS	TEST LIQUID	SIZE (MESH)	DRY SOLIDS (GRAM)		CAKE POROSITY		
33	Zircon	10-5 M D pH 6	-150+200	50		0,455		
Vacuum (inch-Hg)	with gravity	0,2	0,5	1	1,5	2	2,2	
Dewat. Time(min)	0	2	2	2	2	2	2	
Cake (Gram)	58,87	58,87	58,87	58,85	58,84	57,2	56,6	
Res Mois %	32,05	32,05	32,05	32,03	32,02	30,06	29,27	
Saturation	1,000	1,000	1,000	0,998	0,997	0,811	0,738	

Table A.34. -150+200 mesh zircon experimented with 5.10-5 M DA at pH 8

TEST NO	TEST SOLIDS	TEST LIQUID	SIZE (MESH)	DRY SOLIDS (GRAM)		CAKE POROSITY		
34	Zircon	10-5 M D pH 8	-150+200	50		0,443		
Vacuum (inch-Hg)	with gravity	0,2	0,5	1	1,5	2	2,2	
Dewat. Time(min)	0	2	2	2	2	2	2	
Cake (Gram)	58,47	58,46	58,45	58,43	58,41	57,1	55,7	
Res Mois %	31,59	31,58	31,57	31,54	31,52	29,96	28,12	
Saturation	1,000	0,999	0,998	0,995	0,993	0,839	0,667	

Table A.35. -150+200 mesh zircon experimented with 5.10-5 M DA at pH 10

TEST NO	TEST SOLIDS	TEST LIQUID	SIZE (MESH)	DRY SOLIDS (GRAM)		CAKE POROSITY		
35	Zircon	10-5 M D pH 10	-150+200	50		0,448		
Vacuum (inch-Hg)	with gravity	0,2	0,5	1	1,5	1,8	2	2,2
Dewat. Time(min)	0	2	2	2	2	2	2	2
Cake (Gram)	58,65	58,64	58,65	58,64	58,62	58,6	56,7	55,72
Res Mois %	31,80	31,79	31,80	31,79	31,76	31,75	29,49	28,21
Saturation	1,000	0,999	1,000	0,999	0,997	0,995	0,778	0,661

Table A.36. -150+200 mesh zircon experimented with 5.10-5 M DA at pH 10

TEST NO	TEST SOLIDS	TEST LIQUID	SIZE (MESH)	DRY SOLIDS (GRAM)		CAKE POROSITY		
36	Zircon	10-5 M D pH 10	-150+200	50		0,452		
Vacuum (inch-Hg)	with gravity	0,2	0,5	1	1,5	1,8	2	2,2
Dewat. Time(min)	0	2	2	2	2	2	2	2
Cake (Gram)	58,78	58,77	58,77	58,77	58,77	58,8	57,2	56,83
Res Mois %	31,95	31,94	31,94	31,94	31,94	31,93	30,01	29,61
Saturation	1,000	0,999	0,999	0,999	0,999	0,998	0,814	0,778

Table A.37. -150+200 mesh zircon experimented with 10-5 M DA at pH 4

TEST NO	TEST SOLIDS	TEST LIQUID	SIZE (MESH)	DRY SOLIDS (GRAM)		CAKE POROSITY		
37	Zircon	.0-5 M DA pH 4	-150+200	40		0,489		
Vacuum (inch-Hg)	with gravity	0,2	0,5	1	1,5	2	2,2	
Dewat. Time(min)	0	2	2	2	2	2	2	
Cake (Gram)	48,14	48,12	48,09	48,09	48,06	45,4	43,2	
Res Mois %	16,91	16,87	16,82	16,82	16,77	11,84	7,39	
Saturation	1,000	0,998	0,994	0,994	0,990	0,660	0,392	

Table A.38. -150+200 mesh zircon experimented with 10-5 M DA at pH 4

TEST NO	TEST SOLIDS	TEST LIQUID	SIZE (MESH)	DRY SOLIDS (GRAM)		CAKE POROSITY		
38	Zircon	.0-5 M DA pH 4	-150+200	50		0,476		
Vacuum (inch-Hg)	with gravity	0,2	0,5	1	1,5	2	2,2	
Dewat. Time(min)	0	2	2	2	2	2	2	
Cake (Gram)	59,65	59,64	59,64	59,63	59,62	57,7	56,9	
Res Mois %	32,94	32,93	32,93	32,92	32,91	30,70	29,64	
Saturation	1,000	0,999	0,999	0,998	0,997	0,800	0,710	

Table A.39. -150+200 mesh zircon experimented with 10-5 M DA at pH 6

TEST NO	TEST SOLIDS	TEST LIQUID	SIZE (MESH)	DRY SOLIDS (GRAM)		CAKE POROSITY		
39	Zircon	0-5 M DA pH 6	-150+200	50		0,460		
Vacuum (inch-Hg)	with gravity	0,2	0,5	1	1,5	2	2,2	
Dewat. Time(min)	0	2	2	2	2	2	2	
Cake (Gram)	59,07	59,07	59,06	59,06	57,12	56,1	55,1	
Res Mois %	15,35	15,35	15,34	15,34	12,46	10,89	9,29	
Saturation	1,000	1,000	0,999	0,999	0,785	0,674	0,564	

Table A.40. -150+200 mesh zircon experimented with 10-5 M DA at pH 6

TEST NO	TEST SOLIDS	TEST LIQUID	SIZE (MESH)	DRY SOLIDS (GRAM)		CAKE POROSITY		
40	Zircon	0-5 M DA pH 6	-150+200	50		0,462		
Vacuum (inch-Hg)	with gravity	0,2	0,5	1	1,5			
Dewat. Time(min)	0	2	2	2	2			
Cake (Gram)	59,15	59,15	59,14	59,13	57,52			
Res Mois %	15,47	15,47	15,45	15,44	13,07			
Saturation	1,000	1,000	0,999	0,998	0,822			

Table A.41. -150+200 mesh zircon experimented with 10-5 M DA at pH 8

TEST NO	TEST SOLIDS	TEST LIQUID	SIZE (MESH)	DRY SOLIDS (GRAM)		CAKE POROSITY		
41	Zircon	0-5 M D pH 8	-150+200	50		0,452		
Vacuum (inch-Hg)	with gravity	0,2	0,5	1	1,5	2	2,2	
Dewat. Time(min)	0	2	2	2	2	2	2	
Cake (Gram)	58,76	58,76	58,75	58,73	58,72	56,2	54,3	
Res Mois %	14,91	14,91	14,89	14,86	14,85	10,95	7,89	
Saturation	1,000	1,000	0,999	0,997	0,995	0,702	0,489	

Table A.42. -150+200 mesh zircon experimented with 10-5 M DA at pH 8

TEST NO	TEST SOLIDS	TEST LIQUID	SIZE (MESH)	DRY SOLIDS (GRAM)		CAKE POROSITY		
42	Zircon	0-5 M D pH 8	-150+200	50		0,451		
Vacuum (inch-Hg)	with gravity	0,2	0,5	1	1,5	2		
Dewat. Time(min)	0	2	2	2	2	2		
Cake (Gram)	58,73	58,72	58,72	58,72	58,71	56,5		
Res Mois %	14,86	14,85	14,85	14,85	14,84	11,49		
Saturation	1,000	0,999	0,999	0,999	0,998	0,743		

Table A.43. -150+200 mesh zircon experimented with 10-5 M DA at pH 10

TEST NO	TEST SOLIDS	TEST LIQUID	SIZE (MESH)	DRY SOLIDS (GRAM)		CAKE POROSITY		
43	Zircon	0-5 M D pH 10	-150+200	50		0,448		
Vacuum (inch-Hg)	with gravity	0,2	0,5	1	1,5	1,8	2	
Dewat. Time(min)	0	2	2	2	2	2	2	
Cake (Gram)	58,65	58,64	58,65	58,64	58,62	58,6	56,7	
Res Mois %	14,75	14,73	14,75	14,73	14,70	14,69	11,86	
Saturation	1,000	0,999	1,000	0,999	0,997	0,995	0,778	

Table A.44. -150+200 mesh zircon experimented with 10-5 M DA at pH 10

TEST NO	TEST SOLIDS	TEST LIQUID	SIZE (MESH)	DRY SOLIDS (GRAM)		CAKE POROSITY		
44	Zircon	0-5 M D pH 10	-150+200	50		0,445		
Vacuum (inch-Hg)	with gravity	0,2	0,5	1	1,5	1,8	2	
Dewat. Time(min)	0	2	2	2	2	2	2	
Cake (Gram)	58,54	58,53	58,53	58,53	58,52	58,5	57	
Res Mois %	14,59	14,57	14,57	14,57	14,56	14,54	12,20	
Saturation	1,000	0,999	0,999	0,999	0,998	0,996	0,814	

Table A.45. -150+200 mesh zircon experimented with 10-4 M SDS at pH 2

TEST NO	TEST SOLIDS	TEST LIQUID	SIZE (MESH)	DRY SOLIDS (GRAM)		CAKE POROSITY		
45	Zircon	0-4 M SD pH 2	-150+200	50		0,433		
Vacuum (inch-Hg)	with gravity	0,2	0,5	1	1,5	1,8	2	2,5
Dewat. Time(min)	0	2	2	2	2	2	2	2
Cake (Gram)	58,11	58,11	58,07	58,05	58,05	56,5	55,9	53,43
Res Mois %	13,96	13,96	13,90	13,87	13,87	11,54	10,52	6,42
Saturation	1,000	1,000	0,995	0,993	0,993	0,804	0,725	0,423

Table A.46. -150+200 mesh zircon experimented with 10-4 M SDS at pH 4

TEST NO	TEST SOLIDS	TEST LIQUID	SIZE (MESH)	DRY SOLIDS (GRAM)		CAKE POROSITY		
46	Zircon	0-4 M SD pH 4	-150+200	50		0,454		
Vacuum (inch-Hg)	with gravity	0,2	0,5	1	1,5	1,8	2	2,5
Dewat. Time(min)	0	2	2	2	2	2	2	2
Cake (Gram)	58,85	58,85	58,81	58,8	58,78	58,8	53,9	53,43
Res Mois %	15,04	15,04	14,98	14,97	14,94	14,94	7,20	6,42
Saturation	1,000	1,000	0,995	0,994	0,992	0,992	0,438	0,388

Table A.47. -150+200 mesh zircon experimented with 10-4 M SDS at pH 6

TEST NO	TEST SOLIDS	TEST LIQUID	SIZE (MESH)	DRY SOLIDS (GRAM)		CAKE POROSITY		
47	Zircon	0-4 M SD pH 6	-150+200	50		0,446		
Vacuum (inch-Hg)	with gravity	0,2	0,5	1	1,5	1,8	2	2,5
Dewat. Time(min)	0	2	2	2	2	2	2	2
Cake (Gram)	58,58	58,57	58,57	58,47	58,42	58,4	55,8	53,43
Res Mois %	14,65	14,63	14,63	14,49	14,41	14,37	10,36	6,42
Saturation	1,000	0,999	0,999	0,987	0,981	0,978	0,674	0,400

Table A.48. -150+200 mesh zircon experimented with 10-4 M SDS at pH 8

TEST NO	TEST SOLIDS	TEST LIQUID	SIZE (MESH)	DRY SOLIDS (GRAM)		CAKE POROSITY		
48	Zircon	0-4 M SD pH 8	-150+200	50		0,444		
Vacuum (inch-Hg)	with gravity	0,2	0,5	1	1,5	1,8	2	2,5
Dewat. Time(min)	0	2	2	2	2	2	2	2
Cake (Gram)	58,51	58,51	58,49	58,48	58,45	58,4	56,7	55,5
Res Mois %	14,54	14,54	14,52	14,50	14,46	14,43	11,85	9,91
Saturation	1,000	1,000	0,998	0,996	0,993	0,991	0,790	0,646

Table A.49. -150+200 mesh zircon experimented with 5.10-5 M SDS at pH 2

TEST NO	TEST SOLIDS	TEST LIQUID	SIZE (MESH)	DRY SOLIDS (GRAM)		CAKE POROSITY		
49	Zircon	10-5 M SI pH 2	-150+200	50		0,440		
Vacuum (inch-Hg)	with gravity	0,2	0,5	1	1,5	1,8	2	2,5
Dewat. Time(min)	0	2	2	2	2	2	2	2
Cake (Gram)	58,35	58,34	58,34	58,33	58,31	56,9	56	53,43
Res Mois %	14,31	14,30	14,30	14,28	14,25	12,05	10,68	6,42
Saturation	1,000	0,999	0,999	0,998	0,995	0,820	0,716	0,411

Table A.50. -150+200 mesh zircon experimented with 5.10-5 M SDS at pH 4

TEST NO	TEST SOLIDS	TEST LIQUID	SIZE (MESH)	DRY SOLIDS (GRAM)		CAKE POROSITY		
50	Zircon	10-5 M SI pH 4	-150+200	50		0,448		
Vacuum (inch-Hg)	with gravity	0,2	0,5	1	1,5	1,8	2	2,5
Dewat. Time(min)	0	2	2	2	2	2	2	2
Cake (Gram)	58,65	58,63	58,63	58,62	58,61	58,6	56,8	55,14
Res Mois %	14,75	14,72	14,72	14,70	14,69	14,66	11,99	9,32
Saturation	1,000	0,998	0,998	0,997	0,995	0,993	0,787	0,594

Table A.51. -150+200 mesh zircon experimented with 5.10-5 M SDS at pH 6

TEST NO	TEST SOLIDS	TEST LIQUID	SIZE (MESH)	DRY SOLIDS (GRAM)		CAKE POROSITY		
51	Zircon	10-5 M SI pH 6	-150+200	50		0,462		
Vacuum (inch-Hg)	with gravity	0,2	0,5	1	1,5	1,8	2	2,5
Dewat. Time(min)	0	2	2	2	2	2	2	2
Cake (Gram)	59,15	59,13	59,12	59,12	59,11	59,1	58,2	56,11
Res Mois %	15,47	15,44	15,43	15,43	15,41	15,41	14,02	10,89
Saturation	1,000	0,998	0,997	0,997	0,996	0,996	0,891	0,668

Table A.52. -150+200 mesh zircon experimented with 5.10-5 M SDS at pH 8

TEST NO	TEST SOLIDS	TEST LIQUID	SIZE (MESH)	DRY SOLIDS (GRAM)		CAKE POROSITY		
52	Zircon	10-5 M SI pH 8	-150+200	50		0,457		
Vacuum (inch-Hg)	with gravity	0,2	0,5	1	1,5	1,8	2	
Dewat. Time(min)	0	2	2	2	2	2	2	
Cake (Gram)	58,95	58,92	58,92	58,92	58,91	58,9	57,1	
Res Mois %	15,18	15,14	15,14	15,14	15,12	15,12	12,48	
Saturation	1,000	0,997	0,997	0,997	0,996	0,996	0,797	

Table A.53. -150+200 mesh zircon experimented with 10-5 M SDS at pH 2

TEST NO	TEST SOLIDS	TEST LIQUID	SIZE (MESH)	DRY SOLIDS (GRAM)		CAKE POROSITY		
53	Zircon	0-5 M SD pH 2	-150+200	50		0,452		
Vacuum (inch-Hg)	with gravity	0,2	0,5	1	1,5	2	2,5	
Dewat. Time(min)	0	2	2	2	2	2	2	
Cake (Gram)	58,78	58,77	58,76	58,69	58,68	57	55,8	
Res Mois %	14,94	14,92	14,91	14,81	14,79	12,22	10,31	
Saturation	1,000	0,999	0,998	0,990	0,989	0,793	0,655	

Table A.54. -150+200 mesh zircon experimented with 10-5 M SDS at pH 4

TEST NO	TEST SOLIDS	TEST LIQUID	SIZE (MESH)	DRY SOLIDS (GRAM)		CAKE POROSITY		
54	Zircon	0-5 M SD pH 4	-150+200	50		0,461		
Vacuum (inch-Hg)	with gravity	0,2	0,5	1	1,5	1,8		
Dewat. Time(min)	0	2	2	2	2	2		
Cake (Gram)	59,11	59,10	59,1	59,1	59,09	57,1		
Res Mois %	15,41	15,40	15,40	15,40	15,38	12,46		
Saturation	1,000	0,999	0,999	0,999	0,998	0,782		

Table A.55. -150+200 mesh zircon experimented with 10-5 M SDS at pH 6

TEST NO	TEST SOLIDS	TEST LIQUID	SIZE (MESH)	DRY SOLIDS (GRAM)		CAKE POROSITY		
55	Zircon	0-5 M SD pH 6	-150+200	50		0,459		
Vacuum (inch-Hg)	with gravity	0,2	0,5	1	1,5	1,8	2	
Dewat. Time(min)	0	2	2	2	2	2	2	
Cake (Gram)	59,02	59,01	59,01	59,01	59,01	59	57,2	
Res Mois %	15,28	15,27	15,27	15,27	15,27	15,24	12,62	
Saturation	1,000	0,999	0,999	0,999	0,999	0,997	0,800	

Table A.56. -150+200 mesh zircon experimented with 10-5 M SDS at pH 8

TEST NO	TEST SOLIDS	TEST LIQUID	SIZE (MESH)	DRY SOLIDS (GRAM)		CAKE POROSITY		
56	Zircon	0-5 M SD pH 8	-150+200	50		0,462		
Vacuum (inch-Hg)	with gravity	0,2	0,5	1	1,5	1,8	2	2,5
Dewat. Time(min)	0	2	2	2	2	2	2	2
Cake (Gram)	59,15	59,13	59,12	59,12	59,11	59,1	58,2	56,11
Res Mois %	15,47	15,44	15,43	15,43	15,41	15,41	14,02	10,89
Saturation	1,000	0,998	0,997	0,997	0,996	0,996	0,891	0,668

Table A.57. -150+200 mesh rutile experimented with water

TEST NO	TEST SOLIDS	TEST LIQUID	SIZE (MESH)	DRY SOLIDS (GRAM)		CAKE POROSITY		
57	Rutile	Water	-150+200	50		0,441		
Vacuum (inch-Hg)	with gravity	0,5	1	1,5	2	2,2	2,4	2,6
Dewat. Time(min)	0	2	2	2	2	2	2	2
Cake (Gram)	59,39	59,36	59,35	59,27	59,12	58,8	55,1	54,2
Res Mois %	15,81	15,77	15,75	15,64	15,43	14,89	9,32	7,75
Saturation	1,000	0,997	0,996	0,987	0,971	0,932	0,547	0,447

Table A.58. -150+200 mesh rutile experimented with water

TEST NO	TEST SOLIDS	TEST LIQUID	SIZE (MESH)	DRY SOLIDS (GRAM)		CAKE POROSITY		
58	Rutile	Water	-150+200	50		0,457		
Vacuum (inch-Hg)	with gravity	0,2	0,4	0,6	0,7	0,8	1	1,2
Dewat. Time(min)	0	2	2	2	2	2	2	2
Cake (Gram)	57,94	57,93	57,92	57,91	57,91	55,7	53,7	52,11
Res Mois %	13,70	13,69	13,67	13,66	13,66	10,15	6,80	4,05
Saturation	1,000	0,999	0,997	0,996	0,996	0,712	0,460	0,266

Table A.59. -150+200 mesh rutile experimented with methanol

TEST NO	TEST SOLIDS	TEST LIQUID	SIZE (MESH)	DRY SOLIDS (GRAM)		CAKE POROSITY		
59	Rutile	Methanol	-150+200	50		0,468		
Vacuum (inch-Hg)	with gravity	0,2	0,4	0,6	0,7	0,75	0,8	1
Dewat. Time(min)	0	2	2	2	2	2	2	2
Cake (Gram)	58,31	58,22	58,14	58,03	58,03	58	55,2	54,12
Res Mois %	14,25	14,12	14,00	13,84	13,84	13,81	9,44	7,61
Saturation	1,000	0,989	0,980	0,966	0,966	0,964	0,627	0,496

Table A.60. -150+200 mesh rutile experimented with methanol

TEST NO	TEST SOLIDS	TEST LIQUID	SIZE (MESH)	DRY SOLIDS (GRAM)		CAKE POROSITY		
60	Rutile	Methanol	-150+200	50		0,458		
Vacuum (inch-Hg)	with gravity	0,2	0,4	0,6	0,7	0,75	0,8	1
Dewat. Time(min)	0	2	2	2	2	2	2	2
Cake (Gram)	57,99	57,98	57,92	57,92	57,91	57,9	56,9	55,12
Res Mois %	13,78	13,76	13,67	13,67	13,66	13,66	12,05	9,29
Saturation	1,000	0,999	0,991	0,991	0,990	0,990	0,857	0,641

Table A.61. -150+200 mesh rutile experimented with 10% methanol

TEST NO	TEST SOLIDS	TEST LIQUID	SIZE (MESH)	DRY SOLIDS (GRAM)		CAKE POROSITY		
61	Rutile	Methanol 10%	-150+200	50		0,454		
Vacuum (inch-Hg)	with gravity	0,5	1	1,5	1,8	2	2,2	
Dewat. Time(min)	0	2	2	2	2	2	2	
Cake (Gram)	59,72	59,53	59,51	59,48	59,30	55,9	54,9	
Res Mois %	16,28	16,01	15,98	15,94	15,68	10,47	8,96	
Saturation	1,000	0,980	0,978	0,975	0,957	0,602	0,506	

Table A.62. -150+200 mesh rutile experimented with 10% methanol

TEST NO	TEST SOLIDS	TEST LIQUID	SIZE (MESH)	DRY SOLIDS (GRAM)		CAKE POROSITY		
62	Rutile	Methanol 10%	-150+200	50		0,443		
Vacuum (inch-Hg)	with gravity	0,5	1	1,5	1,8	2	2,2	
Dewat. Time(min)	0	2	2	2	2	2	2	
Cake (Gram)	59,28	59,27	59,27	59,26	59,25	57,2	56,1	
Res Mois %	15,65	15,64	15,64	15,63	15,61	12,63	10,91	
Saturation	1,000	0,999	0,999	0,998	0,997	0,779	0,659	

Table A.63. -150+200 mesh rutile experimented with 25% methanol

TEST NO	TEST SOLIDS	TEST LIQUID	SIZE (MESH)	DRY SOLIDS (GRAM)		CAKE POROSITY		
63	Rutile	Methanol 25%	-150+200	50		0,467		
Vacuum (inch-Hg)	with gravity	0,5	1	1,2	1,4	1,6	1,8	
Dewat. Time(min)	0	2	2	2	2	2	2	
Cake (Gram)	59,99	59,96	59,93	59,91	59,89	57	56,9	
Res Mois %	16,65	16,61	16,57	16,54	16,51	12,34	12,17	
Saturation	1,000	0,997	0,994	0,992	0,990	0,705	0,694	

Table A.64. -150+200 mesh rutile experimented with 25% methanol

TEST NO	TEST SOLIDS	TEST LIQUID	SIZE (MESH)	DRY SOLIDS (GRAM)		CAKE POROSITY		
64	Rutile	Methanol 25%	-150+200	50		0,458		
Vacuum (inch-Hg)	with gravity	0,5	1	1,2	1,4	1,6	1,8	
Dewat. Time(min)	0	2	2	2	2	2	2	
Cake (Gram)	59,64	59,64	59,63	59,62	59,61	58,1	57,4	
Res Mois %	16,16	16,16	16,15	16,14	16,12	13,97	12,82	
Saturation	1,000	1,000	0,999	0,998	0,997	0,842	0,762	

Table A.65. -150+200 mesh rutile experimented with 40% methanol

TEST NO	TEST SOLIDS	TEST LIQUID	SIZE (MESH)	DRY SOLIDS (GRAM)		CAKE POROSITY		
65	Rutile	Methanol 40%	-150+200	50		0,444		
Vacuum (inch-Hg)	with gravity	0,5	1	1,2	1,4	1,6	1,8	
Dewat. Time(min)	0	2	2	2	2	2	2	
Cake (Gram)	58,85	58,81	58,68	58,61	57,23	56,78	55,3	
Res Mois %	15,04	14,98	14,79	14,69	12,63	11,94	9,55	
Saturation	1,000	0,995	0,981	0,973	0,817	0,766	0,597	

Table A.66. -150+200 mesh rutile experimented with 40% methanol

TEST NO	TEST SOLIDS	TEST LIQUID	SIZE (MESH)	DRY SOLIDS (GRAM)		CAKE POROSITY		
66	Rutile	Methanol 40%	-150+200	50		0,449		
Vacuum (inch-Hg)	with gravity	0,5	1	1,2	1,4	1,6		
Dewat. Time(min)	0	2	2	2	2	2		
Cake (Gram)	59,01	59,01	58,98	58,97	57,12	56,12		
Res Mois %	15,27	15,27	15,23	15,21	12,46	10,91		
Saturation	1,000	1,000	0,997	0,996	0,790	0,679		

Table A.67. -150+200 mesh rutile experimented with 50% methanol

TEST NO	TEST SOLIDS	TEST LIQUID	SIZE (MESH)	DRY SOLIDS (GRAM)		CAKE POROSITY		
67	Rutile	Methanol 50%	-150+200	50		0,459		
Vacuum (inch-Hg)	with gravity	0,4	0,6	0,8	1	1,1	1,2	1,4
Dewat. Time(min)	0	2	2	2	2	2	2	2
Cake (Gram)	59,24	59,19	59,13	59,08	59,03	59	57,19	56,24
Res Mois %	15,60	15,53	15,44	15,37	15,30	15,27	12,57	11,10
Saturation	1,000	0,995	0,988	0,983	0,977	0,975	0,778	0,675

Table A.68. -150+200 mesh rutile experimented with 50% methanol

TEST NO	TEST SOLIDS	TEST LIQUID	SIZE (MESH)	DRY SOLIDS (GRAM)		CAKE POROSITY		
68	Rutile	Methanol 50%	-150+200	50		0,466		
Vacuum (inch-Hg)	with gravity	0,4	0,6	0,8	1	1,2	1,4	
Dewat. Time(min)	0	2	2	2	2	2	2	
Cake (Gram)	59,49	59,42	59,38	59,3	59,25	58,33	56,7	
Res Mois %	15,95	15,85	15,80	15,68	15,61	14,28	11,80	
Saturation	1,000	0,993	0,988	0,980	0,975	0,878	0,705	

Table A.69. -150+200 mesh rutile experimented with 65% methanol

TEST NO	TEST SOLIDS	TEST LIQUID	SIZE (MESH)	DRY SOLIDS (GRAM)		CAKE POROSITY		
69	Rutile	Methanol 65%	-150+200	50		0,445		
Vacuum (inch-Hg)	with gravity	0,2	0,4	0,6	0,8	1	1,2	1,4
Dewat. Time(min)	0	2	2	2	2	2	2	2
Cake (Gram)	58,43	58,30	58,2	58,14	58,07	57,99	56,2	55,30
Res Mois %	14,43	14,24	14,09	14,00	13,90	13,78	10,97	9,58
Saturation	1,000	0,985	0,973	0,966	0,957	0,948	0,731	0,629

Table A.70. -150+200 mesh rutile experimented with 65% methanol

TEST NO	TEST SOLIDS	TEST LIQUID	SIZE (MESH)	DRY SOLIDS (GRAM)		CAKE POROSITY		
70	Rutile	Methanol 65%	-150+200	50		0,463		
Vacuum (inch-Hg)	with gravity	0,2	0,4	0,6	0,8	1	1,2	1,4
Dewat. Time(min)	0	2	2	2	2	2	2	2
Cake (Gram)	59,05	58,98	58,91	58,84	58,76	58,71	56,1	55,20
Res Mois %	15,33	15,23	15,12	15,02	14,91	14,84	10,81	9,42
Saturation	1,000	0,992	0,985	0,977	0,968	0,962	0,670	0,575

Table A.71. -150+200 mesh rutile experimented with 80% methanol

TEST NO	TEST SOLIDS	TEST LIQUID	SIZE (MESH)	DRY SOLIDS (GRAM)		CAKE POROSITY		
71	Rutile	Methanol 80%	-150+200	50		0,457		
Vacuum (inch-Hg)	with gravity	0,2	0,4	0,6	0,8	1	1,2	
Dewat. Time(min)	0	2	2	2	2	2	2	
Cake (Gram)	58,50	58,42	58,41	58,14	58,07	55,29	54,5	
Res Mois %	14,53	14,41	14,40	14,00	13,90	9,57	8,29	
Saturation	1,000	0,991	0,989	0,958	0,949	0,622	0,532	

Table A.72. -150+200 mesh rutile experimented with 80% methanol

TEST NO	TEST SOLIDS	TEST LIQUID	SIZE (MESH)	DRY SOLIDS (GRAM)		CAKE POROSITY		
72	Rutile	Methanol 80%	-150+200	50		0,472		
Vacuum (inch-Hg)	with gravity	0,2	0,4	0,6	0,8	1		
Dewat. Time(min)	0	2	2	2	2	2		
Cake (Gram)	59,03	59,02	59,01	58,99	58,97	56,13		
Res Mois %	15,30	15,28	15,27	15,24	15,21	10,92		
Saturation	1,000	0,999	0,998	0,996	0,993	0,679		

Table A.73. -150+200 mesh rutile experimented with 10-4 M DA at pH 4

TEST NO	TEST SOLIDS	TEST LIQUID	SIZE (MESH)	DRY SOLIDS (GRAM)		CAKE POROSITY		
73	Rutile	0-4 M DA pH 4	-150+200	50		0,445		
Vacuum (inch-Hg)	with gravity	0,5	1	1,5	2	2,2	2,4	2,6
Dewat. Time(min)	0	2	2	2	2	2	2	2
Cake (Gram)	59,54	58,46	58,45	58,44	58,42	57,14	56,2	55,76
Res Mois %	24,42	23,02	23,01	23,00	22,97	21,25	19,87	19,30
Saturation	1,000	0,887	0,886	0,885	0,883	0,748	0,646	0,604

Table A.74. -150+200 mesh rutile experimented with 10-4 M DA at pH 4

TEST NO	TEST SOLIDS	TEST LIQUID	SIZE (MESH)	DRY SOLIDS (GRAM)		CAKE POROSITY		
74	Rutile	0-4 M DA pH 4	-150+200	50		0,447		
Vacuum (inch-Hg)	with gravity	0,5	1	1,5	2	2,2	2,4	2,6
Dewat. Time(min)	0	2	2	2	2	2	2	2
Cake (Gram)	59,62	59,61	59,60	59,59	59,58	57,65	56,23	55,76
Res Mois %	24,52	24,51	24,50	24,48	24,47	21,94	19,97	19,30
Saturation	1,000	0,999	0,998	0,997	0,996	0,795	0,648	0,599

Table A.75. -150+200 mesh rutile experimented with 10-4 M DA at pH 6

TEST NO	TEST SOLIDS	TEST LIQUID	SIZE (MESH)	DRY SOLIDS (GRAM)		CAKE POROSITY		
75	Rutile	0-4 M DA pH 6	-150+200	50		0,438		
Vacuum (inch-Hg)	with gravity	0,5	1	1,5	2	2,1	2,2	
Dewat. Time(min)	0	2	2	2	2	2	2	
Cake (Gram)	59,28	58,35	58,35	58,32	58,30	57,32	56,45	
Res Mois %	24,09	22,88	22,88	22,84	22,81	21,49	20,28	
Saturation	1,000	0,900	0,900	0,897	0,894	0,789	0,695	

Table A.76. -150+200 mesh rutile experimented with 10-4 M DA at pH 6

TEST NO	TEST SOLIDS	TEST LIQUID	SIZE (MESH)	DRY SOLIDS (GRAM)		CAKE POROSITY		
76	Rutile	0-4 M DA pH 6	-150+200	50		0,438		
Vacuum (inch-Hg)	with gravity	0,5	1	1,5	2	2,1	2,2	
Dewat. Time(min)	0	2	2	2	2	2	2	
Cake (Gram)	59,28	58,35	58,35	58,32	58,30	57,32	56,45	
Res Mois %	24,09	22,88	22,88	22,84	22,81	21,49	20,28	
Saturation	1,000	0,900	0,900	0,897	0,894	0,789	0,695	

Table A.77. -150+200 mesh rutile experimented with 10-4 M DA at pH 8

TEST NO	TEST SOLIDS	TEST LIQUID	SIZE (MESH)	DRY SOLIDS (GRAM)		CAKE POROSITY		
77	Rutile	10-4 M DA pH 8	-150+200	50		0,435		
Vacuum (inch-Hg)	with gravity	0,5	1	1,5	2	2,1	2,2	
Dewat. Time(min)	0	2	2	2	2	2	2	
Cake (Gram)	59,17	59,16	59,14	59,13	59,12	57,16	55,25	
Res Mois %	23,95	23,94	23,91	23,90	23,88	21,27	18,55	
Saturation	1,000	0,999	0,997	0,996	0,995	0,781	0,573	

Table A.78. -150+200 mesh rutile experimented with 10-4 M DA at pH 8

TEST NO	TEST SOLIDS	TEST LIQUID	SIZE (MESH)	DRY SOLIDS (GRAM)		CAKE POROSITY		
78	Rutile	10-4 M DA pH 8	-150+200	50		0,430		
Vacuum (inch-Hg)	with gravity	0,5	1	1,5	2	2,1	2,2	
Dewat. Time(min)	0	2	2	2	2	2	2	
Cake (Gram)	58,99	58,99	58,98	58,98	58,98	57,36	55,12	
Res Mois %	23,72	23,72	23,70	23,70	23,70	21,55	18,36	
Saturation	1,000	1,000	0,999	0,999	0,999	0,819	0,570	

Table A.79. -150+200 mesh rutile experimented with 10-4 M DA at pH 10

TEST NO	TEST SOLIDS	TEST LIQUID	SIZE (MESH)	DRY SOLIDS (GRAM)		CAKE POROSITY		
79	Rutile	10-4 M DA pH 10	-150+200	50		0,438		
Vacuum (inch-Hg)	with gravity	0,5	1	1,5	2	2,2	2,4	
Dewat. Time(min)	0	2	2	2	2	2	2	
Cake (Gram)	59,28	59,28	59,28	59,27	59,23	59,21	56,1	
Res Mois %	24,09	24,09	24,09	24,08	24,02	24,00	19,83	
Saturation	1,000	1,000	1,000	0,999	0,995	0,992	0,661	

Table A.80. -150+200 mesh rutile experimented with 10-4 M DA at pH 10

TEST NO	TEST SOLIDS	TEST LIQUID	SIZE (MESH)	DRY SOLIDS (GRAM)		CAKE POROSITY		
80	Rutile	10-4 M DA pH 10	-150+200	50		0,435		
Vacuum (inch-Hg)	with gravity	0,5	1	1,5	2	2,2	2,4	
Dewat. Time(min)	0	2	2	2	2	2	2	
Cake (Gram)	59,15	59,13	59,13	59,10	59,09	59,04	57,1	
Res Mois %	23,92	23,90	23,90	23,86	23,84	23,78	21,22	
Saturation	1,000	0,998	0,998	0,995	0,993	0,988	0,778	

Table A.81. -150+200 mesh rutile experimented with 5.10-5 M DA at pH 4

TEST NO	TEST SOLIDS	TEST LIQUID	SIZE (MESH)	DRY SOLIDS (GRAM)		CAKE POROSITY		
81	Rutile	10-5 M D pH 4	-150+200	50		0,433		
Vacuum (inch-Hg)	with gravity	0,5	1	1,5	2	2,2	2,4	
Dewat. Time(min)	0	2	2	2	2	2	2	
Cake (Gram)	59,10	59,08	59,08	59,07	59,06	59,01	57,7	
Res Mois %	23,86	23,83	23,83	23,82	23,81	23,74	21,94	
Saturation	1,000	0,998	0,998	0,997	0,996	0,990	0,841	

Table A.82. -150+200 mesh rutile experimented with 5.10-5 M DA at pH 4

TEST NO	TEST SOLIDS	TEST LIQUID	SIZE (MESH)	DRY SOLIDS (GRAM)		CAKE POROSITY		
82	Rutile	10-5 M D pH 4	-150+200	50		0,438		
Vacuum (inch-Hg)	with gravity	0,5	1	1,5	2	2,2	2,4	
Dewat. Time(min)	0	2	2	2	2	2	2	
Cake (Gram)	59,26	59,25	59,21	59,19	59,18	59,17	58	
Res Mois %	24,06	24,05	24,00	23,97	23,96	23,95	22,43	
Saturation	1,000	0,999	0,995	0,992	0,991	0,990	0,865	

Table A.83. -150+200 mesh rutile experimented with 5.10-5 M DA at pH 6

TEST NO	TEST SOLIDS	TEST LIQUID	SIZE (MESH)	DRY SOLIDS (GRAM)		CAKE POROSITY		
83	Rutile	10-5 M D pH 6	-150+200	50		0,447		
Vacuum (inch-Hg)	with gravity	0,5	1	1,5	2	2,2	2,4	
Dewat. Time(min)	0	2	2	2	2	2	2	
Cake (Gram)	59,63	59,58	59,57	59,57	59,55	58,55	57,1	
Res Mois %	24,53	24,47	24,46	24,46	24,43	23,14	21,20	
Saturation	1,000	0,995	0,994	0,994	0,992	0,888	0,738	

Table A.84. -150+200 mesh rutile experimented with 5.10-5 M DA at pH 6

TEST NO	TEST SOLIDS	TEST LIQUID	SIZE (MESH)	DRY SOLIDS (GRAM)		CAKE POROSITY		
84	Rutile	10-5 M D pH 6	-150+200	50		0,449		
Vacuum (inch-Hg)	with gravity	0,5	1	1,5	2	2,2		
Dewat. Time(min)	0	2	2	2	2	2		
Cake (Gram)	59,69	59,68	59,67	59,67	59,64	57,99		
Res Mois %	24,61	24,60	24,59	24,59	24,55	22,40		
Saturation	1,000	0,999	0,998	0,998	0,995	0,825		

Table A.85. -150+200 mesh rutile experimented with 5.10-5 M DA at pH 8

TEST NO	TEST SOLIDS	TEST LIQUID	SIZE (MESH)	Y SOLIDS (GRAM)		CAKE POROSITY		
85	Rutile	10-5 M D pH 8	-150+200	50		0,444		
Vacuum (inch-Hg)	with gravity	0,5	1	1,5	2	2,2	2,4	
Dewat. Time(min)	0	2	2	2	2	2	2	
Cake (Gram)	59,51	59,51	59,48	59,47	59,45	57,38	56,2	
Res Mois %	24,38	24,38	24,34	24,33	24,31	21,58	19,97	
Saturation	1,000	1,000	0,997	0,996	0,994	0,776	0,655	

Table A.86. -150+200 mesh rutile experimented with 5.10-5 M DA at pH 8

TEST NO	TEST SOLIDS	TEST LIQUID	SIZE (MESH)	Y SOLIDS (GRAM)		CAKE POROSITY		
86	Rutile	10-5 M D pH 8	-150+200	50		0,443		
Vacuum (inch-Hg)	with gravity	0,5	1	1,5	2	2,2	2,4	
Dewat. Time(min)	0	2	2	2	2	2	2	
Cake (Gram)	59,45	59,43	59,42	59,42	59,42	56,25	55,1	
Res Mois %	24,31	24,28	24,27	24,27	24,27	20,00	18,36	
Saturation	1,000	0,998	0,997	0,997	0,997	0,661	0,542	

Table A.87. -150+200 mesh rutile experimented with 5.10-5 M DA at pH 10

TEST NO	TEST SOLIDS	TEST LIQUID	SIZE (MESH)	DRY SOLIDS (GRAM)		CAKE POROSITY		
87	Rutile	10-5 M D pH 10	-150+200	50		0,441		
Vacuum (inch-Hg)	with gravity	0,5	1	1,5	2	2,2	2,4	
Dewat. Time(min)	0	2	2	2	2	2	2	
Cake (Gram)	59,40	59,38	59,32	59,31	59,29	59,29	57,1	
Res Mois %	24,24	24,22	24,14	24,13	24,10	24,10	21,16	
Saturation	1,000	0,998	0,991	0,990	0,988	0,988	0,753	

Table A.88. -150+200 mesh rutile experimented with 10-5 M DA at pH 4

TEST NO	TEST SOLIDS	TEST LIQUID	SIZE (MESH)	DRY SOLIDS (GRAM)		CAKE POROSITY		
88	Rutile	.0-5 M DA pH 4	-150+200	50		0,434		
Vacuum (inch-Hg)	with gravity	0,5	1	1,5	2	2,2	2,4	
Dewat. Time(min)	0	2	2	2	2	2	2	
Cake (Gram)	59,11	59,01	59,01	59,01	58,97	59	57,8	
Res Mois %	15,41	15,27	15,27	15,27	15,21	15,21	13,48	
Saturation	1,000	0,989	0,989	0,989	0,985	0,985	0,855	

Table A.89. -150+200 mesh rutile experimented with 10-5 M DA at pH 4

TEST NO	TEST SOLIDS	TEST LIQUID	SIZE (MESH)	DRY SOLIDS (GRAM)		CAKE POROSITY		
89	Rutile	0-5 M DA pH 4	-150+200	50		0,430		
Vacuum (inch-Hg)	with gravity	0,5	1	1,5	2	2,2	2,4	
Dewat. Time(min)	0	2	2	2	2	2	2	
Cake (Gram)	58,99	58,97	58,96	58,95	58,95	58,9	57,7	
Res Mois %	15,24	15,21	15,20	15,18	15,18	15,12	13,27	
Saturation	1,000	0,998	0,997	0,996	0,996	0,991	0,851	

Table A.90. -150+200 mesh rutile experimented with 10-5 M DA at pH 6

TEST NO	TEST SOLIDS	TEST LIQUID	SIZE (MESH)	DRY SOLIDS (GRAM)		CAKE POROSITY		
90	Rutile	0-5 M DA pH 6	-150+200	50		0,428		
Vacuum (inch-Hg)	with gravity	0,5	1	1,5	2	2,2	2,4	
Dewat. Time(min)	0	2	2	2	2	2	2	
Cake (Gram)	58,89	58,87	58,86	58,86	58,84	58,8	56,4	
Res Mois %	15,10	15,07	15,05	15,05	15,02	15,02	11,38	
Saturation	1,000	0,998	0,997	0,997	0,994	0,994	0,722	

Table A.91. -150+200 mesh rutile experimented with 10-5 M DA at pH 6

TEST NO	TEST SOLIDS	TEST LIQUID	SIZE (MESH)	DRY SOLIDS (GRAM)		CAKE POROSITY		
91	Rutile	10-5 M DA pH 6	-150+200	50		0,431		
Vacuum (inch-Hg)	with gravity	0,5	1	1,5	2	2,2	2,4	
Dewat. Time(min)	0	2	2	2	2	2	2	
Cake (Gram)	59,03	59,03	59,02	59,01	58,88	58,9	57,7	
Res Mois %	15,30	15,30	15,28	15,27	15,08	15,07	13,33	
Saturation	1,000	1,000	0,999	0,998	0,983	0,982	0,852	

Table A.92. -150+200 mesh rutile experimented with 10-5 M DA at pH 8

TEST NO	TEST SOLIDS	TEST LIQUID	SIZE (MESH)	DRY SOLIDS (GRAM)		CAKE POROSITY		
92	Rutile	10-5 M DA pH 8	-150+200	50		0,432		
Vacuum (inch-Hg)	with gravity	0,5	1	1,5	2	2,2	2,4	
Dewat. Time(min)	0	2	2	2	2	2	2	
Cake (Gram)	59,07	59,06	59	58,98	58,97	58,9	57	
Res Mois %	15,35	15,34	15,25	15,23	15,21	15,05	12,22	
Saturation	1,000	0,999	0,992	0,990	0,989	0,977	0,767	

Table A.93. -150+200 mesh rutile experimented with 10-5 M DA at pH 8

TEST NO	TEST SOLIDS	TEST LIQUID	SIZE (MESH)	DRY SOLIDS (GRAM)		CAKE POROSITY		
93	Rutile	0-5 M DA pH 8	-150+200	50		0,435		
Vacuum (inch-Hg)	with gravity	0,5	1	1,5	2	2,2	2,4	
Dewat. Time(min)	0	2	2	2	2	2	2	
Cake (Gram)	59,16	59,15	59,12	59,12	59,11	59,1	57,9	
Res Mois %	15,48	15,47	15,43	15,43	15,41	15,37	13,57	
Saturation	1,000	0,999	0,996	0,996	0,995	0,991	0,857	

Table A.94. -150+200 mesh rutile experimented with 10-5 M DA at pH 10

TEST NO	TEST SOLIDS	TEST LIQUID	SIZE (MESH)	DRY SOLIDS (GRAM)		CAKE POROSITY		
94	Rutile	0-5 M DA pH 10	-150+200	50		0,440		
Vacuum (inch-Hg)	with gravity	0,5	1	1,5	2	2,2	2,4	
Dewat. Time(min)	0	2	2	2	2	2	2	
Cake (Gram)	59,35	59,33	59,32	59,32	59,3	59,3	57,4	
Res Mois %	15,75	15,73	15,71	15,71	15,68	15,64	12,92	
Saturation	1,000	0,998	0,997	0,997	0,995	0,991	0,794	

Table A.95. -150+200 mesh rutile experimented with 10-5 M DA at pH 10

TEST NO	TEST SOLIDS	TEST LIQUID	SIZE (MESH)	DRY SOLIDS (GRAM)		CAKE POROSITY		
95	Rutile	0-5 M DA pH 10	-150+200	50		0,442		
Vacuum (inch-Hg)	with gravity	0,5	1	1,5	2	2,2	2,4	
Dewat. Time(min)	0	2	2	2	2	2	2	
Cake (Gram)	59,44	59,41	59,41	59,39	59,38	59,4	58,1	
Res Mois %	15,88	15,84	15,84	15,81	15,80	15,78	13,97	
Saturation	1,000	0,997	0,997	0,995	0,994	0,993	0,860	

Table A.96. -150+200 mesh rutile experimented with 10-4 M SDS at pH 2

TEST NO	TEST SOLIDS	TEST LIQUID	SIZE (MESH)	DRY SOLIDS (GRAM)		CAKE POROSITY		
96	Rutile	0-5 M SD pH 2	-150+200	50		0,428		
Vacuum (inch-Hg)	with gravity	0,5	1	1,5	2	2,2		
Dewat. Time(min)	0	2	2	2	2	2		
Cake (Gram)	58,89	58,85	58,85	58,86	57,16	56,1		
Res Mois %	15,10	15,04	15,04	15,05	12,53	10,92		
Saturation	1,000	0,996	0,996	0,997	0,805	0,690		

Table A.97. -150+200 mesh rutile experimented with 10-4 M SDS at pH 4

TEST NO	TEST SOLIDS	TEST LIQUID	SIZE (MESH)	DRY SOLIDS (GRAM)		CAKE POROSITY		
97	Rutile	0-4 M SD pH 4	-150+200	50		0,439		
Vacuum (inch-Hg)	with gravity	0,5	1	1,5	2	2,2	2,4	
Dewat. Time(min)	0	2	2	2	2	2	2	
Cake (Gram)	59,32	59,31	59,28	59,26	59,26	59,3	57,3	
Res Mois %	15,71	15,70	15,65	15,63	15,63	15,61	12,68	
Saturation	1,000	0,999	0,996	0,994	0,994	0,992	0,779	

Table A.98. -150+200 mesh rutile experimented with 10-4 M SDS at pH 6

TEST NO	TEST SOLIDS	TEST LIQUID	SIZE (MESH)	DRY SOLIDS (GRAM)		CAKE POROSITY		
98	Rutile	0-4 M SD pH 6	-150+200	50		0,443		
Vacuum (inch-Hg)	with gravity	0,5	1	1,5	2	2,2	2,4	
Dewat. Time(min)	0	2	2	2	2	2	2	
Cake (Gram)	59,46	59,43	59,41	59,41	59,41	59,4	57,2	
Res Mois %	15,91	15,87	15,84	15,84	15,84	15,80	12,51	
Saturation	1,000	0,997	0,995	0,995	0,995	0,992	0,756	

Table A.99. -150+200 mesh rutile experimented with 10-4 M SDS at pH 8

TEST NO	TEST SOLIDS	TEST LIQUID	SIZE (MESH)	DRY SOLIDS (GRAM)		CAKE POROSITY		
99	Rutile	0-4 M SD pH 8	-150+200	50		0,434		
Vacuum (inch-Hg)	with gravity	0,5	1	1,5	2	2,2	2,4	
Dewat. Time(min)	0	2	2	2	2	2	2	
Cake (Gram)	59,12	59,11	59,11	59,11	59,08	59,1	57,6	
Res Mois %	15,43	15,41	15,41	15,41	15,37	15,37	13,22	
Saturation	1,000	0,999	0,999	0,999	0,996	0,996	0,836	

Table A.100. -150+200 mesh rutile experimented with 5.10-5 M SDS at pH 2

TEST NO	TEST SOLIDS	TEST LIQUID	SIZE (MESH)	DRY SOLIDS (GRAM)		CAKE POROSITY		
100	Rutile	10-5 M SI pH 2	-150+200	50		0,441		
Vacuum (inch-Hg)	with gravity	0,5	1	1,5	2	2,2	2,4	
Dewat. Time(min)	0	2	2	2	2	2	2	
Cake (Gram)	59,38	59,37	59,37	59,36	58,16	57,2	56,2	
Res Mois %	15,80	15,78	15,78	15,77	14,03	12,51	11,00	
Saturation	1,000	0,999	0,999	0,998	0,870	0,762	0,659	

Table A.101. -150+200 mesh rutile experimented with 5.10-5 M SDS at pH 4

TEST NO	TEST SOLIDS	TEST LIQUID	SIZE (MESH)	DRY SOLIDS (GRAM)		CAKE POROSITY		
101	Rutile	10-5 M SI pH 4	-150+200	50		0,457		
Vacuum (inch-Hg)	with gravity	0,5	1	1,5	2	2,2	2,4	
Dewat. Time(min)	0	2	2	2	2	2	2	
Cake (Gram)	60,01	59,99	59,97	59,93	59,92	59,9	58,7	
Res Mois %	16,68	16,65	16,62	16,57	16,56	16,56	14,86	
Saturation	1,000	0,998	0,996	0,992	0,991	0,991	0,872	

Table A.102. -150+200 mesh rutile experimented with 5.10-5 M SDS at pH 6

TEST NO	TEST SOLIDS	TEST LIQUID	SIZE (MESH)	DRY SOLIDS (GRAM)		CAKE POROSITY		
102	Rutile	10-5 M SI pH 6	-150+200	50		0,454		
Vacuum (inch-Hg)	with gravity	0,5	1	1,5	2	2,2	2,4	
Dewat. Time(min)	0	2	2	2	2	2	2	
Cake (Gram)	59,88	59,85	59,83	59,83	59,82	59,8	57,5	
Res Mois %	16,50	16,46	16,43	16,43	16,42	16,40	13,07	
Saturation	1,000	0,997	0,995	0,995	0,994	0,993	0,761	

Table A.103. -150+200 mesh rutile experimented with 5.10-5 M SDS at pH 8

TEST NO	TEST SOLIDS	TEST LIQUID	SIZE (MESH)	DRY SOLIDS (GRAM)		CAKE POROSITY		
103	Rutile	10-5 M SI pH 8	-150+200	50		0,450		
Vacuum (inch-Hg)	with gravity	0,5	1	1,5	2	2,2	2,4	
Dewat. Time(min)	0	2	2	2	2	2	2	
Cake (Gram)	59,73	59,72	59,72	59,71	59,69	59,7	58	
Res Mois %	16,29	16,28	16,28	16,26	16,23	16,22	13,78	
Saturation	1,000	0,999	0,999	0,998	0,996	0,995	0,821	

Table A.104. -150+200 mesh rutile experimented with 10-5 M SDS at pH 2

TEST NO	TEST SOLIDS	TEST LIQUID	SIZE (MESH)	DRY SOLIDS (GRAM)		CAKE POROSITY		
104	Rutile	0-5 M SD pH 2	-150+200	50		0,437		
Vacuum (inch-Hg)	with gravity	0,5	1	1,5	2	2,2	2,4	
Dewat. Time(min)	0	2	2	2	2	2	2	
Cake (Gram)	59,25	59,25	59,24	59,23	59,23	57,7	55,7	
Res Mois %	15,61	15,61	15,60	15,58	15,58	13,33	10,27	
Saturation	1,000	1,000	0,999	0,998	0,998	0,831	0,618	

Table A.105. -150+200 mesh rutile experimented with 10-5 M SDS at pH 4

TEST NO	TEST SOLIDS	TEST LIQUID	SIZE (MESH)	DRY SOLIDS (GRAM)		CAKE POROSITY		
105	Rutile	0-5 M SD pH 4	-150+200	50		0,436		
Vacuum (inch-Hg)	with gravity	0,5	1	1,5	2	2,2	2,4	
Dewat. Time(min)	0	2	2	2	2	2	2	
Cake (Gram)	59,19	59,18	59,17	59,12	59,11	59,1	57,2	
Res Mois %	15,53	15,51	15,50	15,43	15,41	15,41	12,56	
Saturation	1,000	0,999	0,998	0,992	0,991	0,991	0,781	

Table A.106. -150+200 mesh rutile experimented with 10-5 M SDS at pH 6

TEST NO	TEST SOLIDS	TEST LIQUID	SIZE (MESH)	DRY SOLIDS (GRAM)		CAKE POROSITY		
106	Rutile	0-5 M SD pH 6	-150+200	50		0,438		
Vacuum (inch-Hg)	with gravity	0,5	1	1,5	2	2,2	2,4	
Dewat. Time(min)	0	2	2	2	2	2	2	
Cake (Gram)	59,28	59,24	59,24	59,23	59,22	59,2	58,2	
Res Mois %	15,65	15,60	15,60	15,58	15,57	15,55	14,03	
Saturation	1,000	0,996	0,996	0,995	0,994	0,992	0,879	

Table A.107. -150+200 mesh rutile experimented with 10-5 M SDS at pH 8

TEST NO	TEST SOLIDS	TEST LIQUID	SIZE (MESH)	DRY SOLIDS (GRAM)		CAKE POROSITY		
107	Rutile	0-5 M SD pH 8	-150+200	50		0,444		
Vacuum (inch-Hg)	with gravity	0,5	1	1,5	2	2,2	2,4	
Dewat. Time(min)	0	2	2	2	2	2	2	
Cake (Gram)	59,52	59,47	59,46	59,45	59,42	59,4	57,9	
Res Mois %	15,99	15,92	15,91	15,90	15,85	15,84	13,70	
Saturation	1,000	0,995	0,994	0,993	0,989	0,988	0,834	

APPENDIX B

TABLES OF COLUMN WICKING EXPERIMENTS

Table B.1. -150+200 mesh zircon experimented with water

TEST NO : 109	
seconds	cm
10	1,8
20	2,6
30	3,4
40	3,9
50	4,4
60	4,6
70	4,9
80	5,4
90	5,6
100	5,8
110	6

TEST NO : 110	
seconds	cm
10	1,8
20	2,6
30	3,2
40	3,6
50	3,9
60	4,1
70	4,4
80	4,6
90	4,8
100	5
110	5,2
120	5,4

Table B.2. -150+200 mesh zircon experimented with methanol

TEST NO : 111	
seconds	cm
10	2
20	3,1
30	3,9
40	4,6
50	5,1
60	5,6
70	6,1
80	6,5
90	6,8
100	7,2
110	7,4
120	7,7
130	8,1
140	8,2
150	8,5
160	8,7
170	8,8

TEST NO : 112	
seconds	cm
10	2
20	3
30	3,6
40	4,2
50	4,7
60	5,1
70	5,6
80	5,8
90	6,2
100	6,6
110	6,8
120	7,2
130	7,4
140	7,8
150	8

Table B.3. -150+200 mesh zircon experimented with hexane

TEST NO : 113	
seconds	cm
10	0
20	0
30	0
40	0
50	0
60	0
70	0
80	0
90	0
100	0
110	0
120	0

Table B.4. -150+200 mesh zircon experimented with formamide

TEST NO : 114	
seconds	cm
10	1,1
20	1,8
30	2,2
40	2,6
50	2,8
60	3,2
70	3,4
80	3,6
90	3,8
100	4

TEST NO : 115	
seconds	cm
10	1,1
20	1,8
30	2,4
40	2,8
50	3
60	3,2
70	3,6
80	3,7
90	3,8
100	4

Table B.5. -150+200 mesh zircon experimented with 10% methanol

TEST NO : 116	
seconds	cm
10	1,4
20	2,2
30	2,7
40	3,2
50	3,6
60	4
70	4,2
80	4,4
90	4,6
100	4,9
110	5,2

TEST NO : 117	
seconds	cm
10	1,4
20	2,1
30	2,7
40	3,2
50	3,6
60	3,9
70	4,2
80	4,3
90	4,6
100	4,8

Table B.6. -150+200 mesh zircon experimented with 25% methanol

TEST NO : 118	
seconds	cm
10	1,4
20	2,3
30	2,7
40	3,1
50	3,5
60	3,8
70	4
80	4,2
90	4,4

TEST NO : 119	
seconds	cm
10	1,5
20	2,3
30	2,7
40	3
50	3,3
60	3,7
70	4
80	4,3
90	4,5

Table B.7. -150+200 mesh zircon experimented with 40% methanol

TEST NO : 120	
seconds	cm
10	1,5
20	2,2
30	2,6
40	3,1
50	3,6
60	3,9
70	4,2
80	4,3
90	4,6
100	5

TEST NO : 121	
t	cm
10	1,6
20	2,3
30	2,7
40	3,2
50	3,7
60	4,1
70	4,4
80	4,7
90	5
100	5,3

Table B.8. -150+200 mesh zircon experimented with 50% methanol

TEST NO : 122	
seconds	cm
10	1,4
20	2
30	2,6
40	3
50	3,4
60	3,7
70	4
80	4,4
90	4,6
100	4,8
110	5

TEST NO : 123	
seconds	cm
10	1,5
20	2,1
30	2,6
40	3
50	3,4
60	3,6
70	4
80	4,3
90	4,6
100	4,9
110	5,1

Table B.9. -150+200 mesh zircon experimented with 65% methanol

TEST NO : 124	
seconds	cm
10	1,4
20	2,2
30	2,8
40	3,4
50	3,8
60	4,2
70	4,6
80	4,9
90	5,1
100	5,4
110	5,6
120	5,8

TEST NO : 125	
seconds	cm
10	1,5
20	2,3
30	2,8
40	3,5
50	3,9
60	4,2
70	4,5
80	4,8
90	5,2
100	5,5
110	5,8
120	6,1

Table B.10. -150+200 mesh zircon experimented with 80% methanol

TEST NO : 126	
seconds	cm
10	1,6
20	2,2
30	2,8
40	3,2
50	3,6
60	4,2
70	4,4
80	4,9
90	5,2
100	5,5
110	5,8

TEST NO : 127	
seconds	cm
10	1,5
20	2,3
30	2,8
40	3,2
50	3,6
60	4
70	4,3
80	4,6
90	4,9
100	5,3
110	5,6

Table B.11. -150+200 mesh zircon experimented with 5.10-5 M DA at pH 4

TEST NO : 128	
seconds	cm
10	1,6
20	2
30	2,3
40	2,6
50	2,9
60	3,1
70	3,4
80	3,6
90	3,8
100	4,1
110	4,4
120	4,6

TEST NO : 129	
seconds	cm
10	1,5
20	2,1
30	2,3
40	2,7
50	3
60	3,2
70	3,4
80	3,6
90	3,8
100	4
110	4,1
120	4,3

Table B.12. -150+200 mesh zircon experimented with 5.10-5 M DA at pH 6

TEST NO : 130	
seconds	cm
10	1,4
20	1,8
30	2
40	2,2
50	2,4
60	2,6
70	2,8
80	3
90	3,25
100	3,4
110	3,7
120	3,8

TEST NO : 131	
seconds	cm
10	1,4
20	1,7
30	2
40	2,3
50	2,5
60	2,7
70	2,9
80	3,1
90	3,3
100	3,4
110	3,6
120	3,9

Table B.13. -150+200 mesh zircon experimented with 5.10-5 M DA at pH 8

TEST NO : 132	
seconds	cm
10	1,4
20	1,6
30	1,8
40	2
50	2,2
60	2,4
70	2,55
80	2,7
90	2,8
100	2,9
110	2,95
120	3,1

TEST NO : 133	
seconds	cm
10	1,3
20	1,5
30	1,7
40	1,9
50	2,1
60	2,3
70	2,5
80	2,6
90	2,7
100	3
110	3,2
120	3,3

Table B.14. -150+200 mesh zircon experimented with 5.10-5 M DA at pH 10

TEST NO : 134	
seconds	cm
10	1,65
20	2,4
30	3,1
40	3,6
50	4,1
60	4,3
70	4,6
80	4,9
90	5,1
100	5,3
110	5,6
120	5,78

TEST NO : 135	
seconds	cm
10	1,6
20	2,4
30	3,1
40	3,5
50	3,8
60	4,2
70	4,6
80	5
90	5,3
100	5,5
110	5,8
120	6

Table B.15. -150+200 mesh zircon experimented with 10-5 M DA at pH 4

TEST NO : 136	
seconds	cm
10	1,6
20	2,3
30	3
40	3,4
50	3,8
60	4,1
70	4,3
80	4,5
90	4,7
100	5
110	5,2
120	5,4

TEST NO : 137	
seconds	cm
10	1,6
20	2,2
30	2,6
40	3,1
50	3,6
60	4
70	4,4
80	4,8
90	5,1
100	5,4
110	5,5
120	5,7

Table B.16. -150+200 mesh zircon experimented with 10-5 M DA at pH 6

TEST NO : 138	
seconds	cm
10	1,5
20	2
30	2,4
40	2,6
50	2,8
60	3
70	3,2
80	3,4
90	3,5
100	3,6
110	3,65

TEST NO : 139	
seconds	cm
10	1,5
20	2
30	2,4
40	2,6
50	2,9
60	3,1
70	3,3
80	3,5
90	3,7
100	4
110	4,1

Table B.17. -150+200 mesh zircon experimented with 10-5 M DA at pH 8

TEST NO : 140	
seconds	cm
10	1,4
20	1,9
30	2,2
40	2,4
50	2,6
60	2,8
70	3
80	3,15
90	3,25
100	3,3
110	3,4

TEST NO : 141	
seconds	cm
10	1,5
20	1,9
30	2,2
40	2,4
50	2,7
60	2,9
70	3,1
80	3,2
90	3,3
100	3,4
110	3,5

Table B.18. -150+200 mesh zircon experimented with 10-5 M DA at pH 10

TEST NO : 142	
seconds	cm
10	1,8
20	2,3
30	3,1
40	3,6
50	4
60	4,4
70	4,7
80	5
90	5,2
100	5,6
110	5,8

TEST NO : 143	
seconds	cm
10	1,7
20	2,2
30	3
40	3,5
50	3,9
60	4,4
70	4,6
80	4,8
90	5
100	5,3

Table B.19. -150+200 mesh zircon experimented with 10-5 M SDS at pH 2

TEST NO 144	
seconds	cm
10	1,6
20	2,4
30	2,9
40	3,3
50	3,7
60	3,95
70	4,1
80	4,4
90	4,6
100	4,75

TEST NO : 145	
seconds	cm
10	1,5
20	2,3
30	3
40	3,2
50	3,5
60	3,8
70	4,2
80	4,5
90	4,6
100	4,8

Table B.20. -150+200 mesh zircon experimented with 5.10-5 M SDS at pH 2

TEST NO : 146	
seconds	cm
10	1,4
20	2
30	2,4
40	2,8
50	3,1
60	3,3
70	3,7
80	4
90	4,3
100	4,6
110	4,7
120	4,8

TEST NO : 147	
seconds	cm
10	1,4
20	2
30	2,4
40	2,7
50	2,9
60	3,2
70	3,6
80	3,9
90	4,2
100	4,4
110	4,7
120	5

Table B.21. -150+200 mesh zircon experimented with 10-4 M SDS at pH 2

TEST NO 148	
seconds	cm
10	1,2
20	1,6
30	2
40	2,3
50	2,6
60	2,8
70	3
80	3,2
90	3,4
100	3,6
110	3,7
120	3,8

TEST NO : 149	
seconds	cm
10	1,3
20	1,7
30	2
40	2,3
50	2,6
60	2,9
70	3,1
80	3,3
90	3,5
100	3,7
110	3,8
120	3,9

Table B.22. -150+200 mesh rutile experimented with water

TEST NO : 150	
seconds	cm
10	1,6
20	2,4
30	3
40	3,6
50	3,9
60	4,2
70	4,6
80	4,8
90	5
100	5,2
110	5,5
120	5,6
130	5,8
140	6
150	6,1
160	6,4
170	6,6

TEST NO : 151	
seconds	cm
10	1,6
20	2,4
30	3
40	3,4
50	3,8
60	4,2
70	4,6
80	4,8
90	5
100	5,4
110	5,5
120	5,6
130	5,9
140	6
150	6,2
160	6,4
170	6,6

Table B.23. -150+200 mesh rutile experimented with methanol

TEST NO : 153	
seconds	cm
10	1,7
20	2,6
30	3,2
40	3,8
50	4,2
60	4,7
70	5
80	5,4
90	5,8
100	6,1
110	6,4
120	6,6
130	6,9
140	7,1
150	7,3
160	7,5
170	7,7
180	7,9
190	8,1
200	8,3
210	8,4

TEST NO : 154	
seconds	cm
10	1,6
20	2,4
30	3,1
40	3,7
50	4,1
60	4,5
70	4,9
80	5,3
90	5,7
100	5,8
110	6,2
120	6,5
130	6,7
140	7
150	7,2
160	7,4
170	7,6
180	7,8
190	8

Table B.24. -150+200 mesh rutile experimented with 10% methanol

TEST NO : 155	
seconds	cm
10	1,4
20	1,8
30	2,1
40	2,4
50	2,7
60	3
70	3,2
80	3,4
90	3,6

TEST NO : 156	
seconds	cm
10	1,5
20	1,8
30	2,2
40	2,5
50	2,8
60	3
70	3,3
80	3,5
90	3,6

Table B.25. -150+200 mesh rutile experimented with 25% methanol

TEST NO : 157	
seconds	cm
10	1
20	1,8
30	2,3
40	2,6
50	3
60	3,4
70	3,6
80	3,9
90	4,1
100	4,4

TEST NO : 158	
seconds	cm
10	1,3
20	1,9
30	2,4
40	2,7
50	3,1
60	3,4
70	3,7
80	4
90	4,2
100	4,4

Table B.26. -150+200 mesh rutile experimented with 40% methanol

TEST NO : 159	
seconds	cm
10	1
20	1,6
30	2,2
40	2,6
50	2,9
60	3,1
70	3,5
80	3,8
90	4

TEST NO : 160	
seconds	cm
10	1,2
20	1,7
30	2,2
40	2,6
50	3
60	3,3
70	3,6
80	3,8
90	4,1

Table B.27. -150+200 mesh rutile experimented with 50% methanol

TEST NO : 161	
seconds	cm
10	1,4
20	2
30	2,5
40	2,9
50	3,2
60	3,6
70	3,8
80	4
90	4,3
100	4,5
110	4,8
120	4,9

TEST NO : 162	
seconds	cm
10	1,4
20	2
30	2,5
40	3
50	3,3
60	3,6
70	4
80	4,3
90	4,6
100	4,9
110	5,1
120	5,3

Table B.28. -150+200 mesh rutile experimented with 65% methanol

TEST NO : 163	
seconds	cm
10	1,4
20	2,1
30	2,6
40	3
50	3,4
60	3,8
70	4
80	4,2
90	4,4
100	4,6
110	4,8
120	5

TEST NO : 164	
seconds	cm
10	1,4
20	2,1
30	2,7
40	3
50	3,3
60	3,7
70	4
80	4,3
90	4,5
100	4,7

Table B.29. -150+200 mesh rutile experimented with 80% methanol

TEST NO : 165	
seconds	cm
10	1,5
20	2,3
30	2,9
40	3,3
50	3,8
60	4,1
70	4,4
80	4,6
90	5
100	5,2

TEST NO : 166	
seconds	cm
10	1,4
20	2,2
30	2,9
40	3,3
50	3,8
60	4,1
70	4,3
80	4,7
90	4,9
100	5

Table B.30. -150+200 mesh rutile experimented with 10-4 M DA at pH 4

TEST NO : 167	
seconds	cm
10	1,75
20	2,15
30	2,4
40	2,7
50	3
60	3,3
70	3,45
80	3,7

TEST NO : 168	
t	cm
10	1,7
20	2,2
30	2,6
40	2,9
50	3,1
60	3,5
70	3,7
80	3,9

Table B.31. -150+200 mesh rutile experimented with 10-4 M DA at pH 6

TEST NO : 169	
seconds	cm
10	1,5
20	1,75
30	2
40	2,15
50	2,3
60	2,5
70	2,6
80	2,7
90	2,8
100	2,85
110	2,95
120	3

TEST NO : 170	
t	cm
10	1,4
20	1,8
30	2,2
40	2,5
50	2,8
60	3,1
70	3,4
80	3,6
90	3,8

Table B.32. -150+200 mesh rutile experimented with 10-4 M DA at pH 8

TEST NO : 171	
seconds	cm
10	1,6
20	2
30	2,25
40	2,5
50	2,7
60	2,9
70	2,95

TEST NO : 172	
seconds	cm
10	1,6
20	2
30	2,3
40	2,6
50	2,8
60	3
70	3,2

Table B.33. -150+200 mesh rutile experimented with 10-4 M DA at pH 10

TEST NO : 172	
seconds	cm
10	1,7
20	2,3
30	2,8
40	3,3
50	3,7
60	4
70	4,3

TEST NO : 173	
seconds	cm
10	1,6
20	2,3
30	2,9
40	3,2
50	3,5
60	3,8
70	4

Table B.34. -150+200 mesh rutile experimented with 5.10-5 M DA at pH 4

TEST NO : 174	
seconds	cm
10	2
20	2,4
30	2,8
40	3,1
50	3,4
60	3,6
70	3,75
80	3,9
90	3,9
100	4,05

Table B.35. -150+200 mesh rutile experimented with 5.10-5 M DA at pH 6

TEST NO : 175	
t	cm
10	1,7
20	2
30	2,25
40	2,45
50	2,6
60	2,8
70	3,1
80	3,2

Table B.36. -150+200 mesh rutile experimented with 5.10-5 M DA at pH 8

TEST NO : 176	
seconds	cm
10	1,95
20	2,3
30	2,45
40	2,7
50	2,9
60	3,1
70	3,4
80	3,6

Table B.37. -150+200 mesh rutile experimented with 5.10-5 M DA at pH 10

TEST NO : 177	
seconds	cm
10	2,1
20	2,6
30	3
40	3,4
50	3,8
60	4,2
70	4,35

Table B.38. -150+200 mesh rutile experimented with 10-5 M DA at pH 4

TEST NO : 178	
seconds	cm
10	1,5
20	2,1
30	2,6
40	3
50	3,3
60	3,7
70	4,1
80	4,4

Table B.39. -150+200 mesh rutile experimented with 10-5 M DA at pH 6

TEST NO : 179	
seconds	cm
10	1,65
20	2
30	2,2
40	2,4
50	2,65
60	2,85
70	3,15
80	3,3
90	3,45

Table B.40. -150+200 mesh rutile experimented with 10-5 M DA at pH 8

TEST NO : 180	
seconds	cm
10	1,7
20	2,1
30	2,35
40	2,6
50	2,9
60	3,2
70	3,55

Table B.41. -150+200 mesh rutile experimented with 10-5 M DA at pH 10

TEST NO : 181	
seconds	cm
10	1,7
20	2,35
30	2,75
40	3,2
50	3,6
60	4
70	4,3

APPENDIX C

TABLES OF MICROFLOTATION EXPERIMENTS

Table C.1. -150+200 mesh zircon experimented with water

recovery, %	tailing, %
91	9
93	7
91	9
90	1
92	8

Table C.2. -150+200 mesh zircon experimented with 10-3 M DA at different pH values

pH 4		pH 6	
recovery, %	tailing, %	recovery, %	tailing, %
38	62	93	7
44	56	91	9
pH 8		**pH 10**	
recovery, %	**tailing, %**	**recovery, %**	**tailing, %**
89	11	18	82
94	6	16	84

Table C.3. -150+200 mesh zircon experimented with 10-4 M DA at different pH values

pH 4		pH 6	
recovery, %	tailing, %	recovery, %	tailing, %
24	76	52	48
21	79	49	51
pH 8		**pH 10**	
recovery, %	**tailing, %**	**recovery, %**	**tailing, %**
54	46	15	85
57	43	13	87

Table C.4. -150+200 mesh zircon experimented with 5.10-5 M DA at different pH values

pH 4		**pH 6**	
recovery, %	**tailing, %**	**recovery, %**	**tailing, %**
11	89	28	72
15	85	31	69
pH 8		**pH 10**	
recovery, %	**tailing, %**	**recovery, %**	**tailing, %**
32	68	11	89
31	69	9	91

Table C.5. -150+200 mesh zircon experimented with 10-5 M DA at different pH values

pH 4		**pH 6**	
recovery, %	**tailing, %**	**recovery, %**	**tailing, %**
3	97	9	91
5	95	4	96
pH 8		**pH 10**	
recovery, %	**tailing, %**	**recovery, %**	**tailing, %**
7	93	1	99
5	95	6	94

Table C.6. -150+200 mesh zircon experimented with 10-3 M SDS at different pH values

pH 2		**pH 4**	
recovery, %	**tailing, %**	**recovery, %**	**tailing, %**
92	8	19	81
89	11	16	84
pH 6		**pH 8**	
recovery, %	**tailing, %**	**recovery, %**	**tailing, %**
2	98	5	95
3	97	6	94

Table C.7. -150+200 mesh zircon experimented with 10-4 M SDS at different pH values

pH 2		**pH 4**	
recovery, %	**tailing, %**	**recovery, %**	**tailing, %**
78	22	5	95
74	26	4	96
pH 6		**pH 8**	
recovery, %	**tailing, %**	**recovery, %**	**tailing, %**
0	100	5	95
2	98	3	97

Table C.8. -150+200 mesh zircon experimented with 5.10-5 M SDS at different pH values

pH 2		**pH 4**	
recovery, %	**tailing, %**	**recovery, %**	**tailing, %**
62	38	9	91
58	42	7	93
pH 6		**pH 8**	
recovery, %	**tailing, %**	**recovery, %**	**tailing, %**
4	96	0,03	0,97
1	99	0	1

Table C.9. -150+200 mesh zircon experimented with 10-5 M SDS at different pH values

pH 2		**pH 4**	
recovery, %	**tailing, %**	**recovery, %**	**tailing, %**
17	83	1	99
23	77	2	98
pH 6		**pH 8**	
recovery, %	**tailing, %**	**recovery, %**	**tailing, %**
5	95	6	94
3	97	4	96

Table C.10. -150+200 mesh rutile experimented with 10-3 M DA at different pH values

pH 4		**pH 6**	
recovery, %	**tailing, %**	**recovery, %**	**tailing, %**
45	55	88	12
42	58	92	8
pH 8		**pH 10**	
recovery, %	**tailing, %**	**recovery, %**	**tailing, %**
91	9	25	75
85	15	34	66

Table C.11. -150+200 mesh rutile experimented with 10-4 M DA at different pH values

pH 4		**pH 6**	
recovery, %	**tailing, %**	**recovery, %**	**tailing, %**
18	82	54	46
22	78	47	53
pH 8		**pH 10**	
recovery, %	**tailing, %**	**recovery, %**	**tailing, %**
45	55	15	85
41	59	12	88

Table C.12. -150+200 mesh rutile experimented with 5.10-5 M DA at different pH values

pH 4		**pH 6**	
recovery, %	**tailing, %**	**recovery, %**	**tailing, %**
13	87	35	65
15	85	29	71
pH 8		**pH 10**	
recovery, %	**tailing, %**	**recovery, %**	**tailing, %**
25	75	6	94
28	72	9	91

Table C.13. -150+200 mesh rutile experimented with 10-5 M DA at different pH values

pH 4		**pH 6**	
recovery, %	**tailing, %**	**recovery, %**	**tailing, %**
5	95	12	88
3	97	13	87
pH 8		**pH 10**	
recovery, %	**tailing, %**	**recovery, %**	**tailing, %**
9	91	3	97
7	93	2	98

Table C.14. -150+200 mesh rutile experimented with 10-3 M SDS at different pH values

pH 2		**pH 4**	
recovery, %	**tailing, %**	**recovery, %**	**tailing, %**
91	9	6	94
93	7	8	92
pH 6		**pH 8**	
recovery, %	**tailing, %**	**recovery, %**	**tailing, %**
2	98	4	96
4	96	7	93

Table C.15. -150+200 mesh rutile experimented with 10-4 M SDS at different pH values

pH 2		**pH 4**	
recovery, %	**tailing, %**	**recovery, %**	**tailing, %**
88	12	3	97
92	8	5	95
pH 6		**pH 8**	
recovery, %	**tailing, %**	**recovery, %**	**tailing, %**
2	98	4	96
6	94	4	96

Table C.16. -150+200 mesh rutile experimented with 5.10-5 M SDS at different pH values

pH 2		**pH 4**	
recovery, %	**tailing, %**	**recovery, %**	**tailing, %**
25	75	6	94
23	77	3	97
pH 6		**pH 8**	
recovery, %	**tailing, %**	**recovery, %**	**tailing, %**
3	97	2	98
4	96	4	96

Table C.17. -150+200 mesh rutile experimented with 10-5 M SDS at different pH values

pH 2		**pH 4**	
recovery, %	**tailing, %**	**recovery, %**	**tailing, %**
12	88	4	96
15	85	1	99
pH 6		**pH 8**	
recovery, %	**tailing, %**	**recovery, %**	**tailing, %**
5	95	1	99
3	97	3	97

APPENDIX D

TABLES OF CONTACT ANGLES OBTAINED FROM CAPILLARIC DEWATERING EXPERIMENTS WITH REPEAT TESTS

Table D.1.The reproducibilty of -150+200 mesh zircon experimented with 10% methanol

Experiment 1	Experiment 2
39.42	37.69

Table D.2.The reproducibilty of -150+200 mesh zircon experimented with 25% methanol

Experiment 1	Experiment 2
39.64	40.09

Table D.3.The reproducibilty of -150+200 mesh zircon experimented with 40% methanol

Experiment 1	Experiment 2
35.04	35.90

Table D.4.The reproducibilty of -150+200 mesh zircon experimented with 50% methanol

Experiment 1	Experiment 2
32.46	31.51

Table D.5.The reproducibilty of -150+200 mesh zircon experimented with 65% methanol

Experiment 1	Experiment 2
19.09	15.74

Table D.6.The reproducibilty of -150+200 mesh zircon experimented with 80% methanol

Experiment 1	Experiment 2
20.36	14.36

Table D.7.The reproducibilty of -150+200 mesh zircon experimented with 5.10-5 M DA at pH 4

Experiment 1	Experiment 2
42.37	42.79

Table D.8.The reproducibilty of -150+200 mesh zircon experimented with 5.10-5 M DA at pH 6

Experiment 1	Experiment 2
49.83	49.08

Table D.9.The reproducibilty of -150+200 mesh zircon experimented with 5.10-5 M DA at pH 8

Experiment 1	Experiment 2
51.41	50.39

Table D.10.The reproducibilty of -150+200 mesh zircon experimented with 5.10-5 M DA at pH 10

Experiment 1	Experiment 2
40.31	40.42

Table D.11.The reproducibilty of -150+200 mesh zircon experimented with 10-5 M DA at pH 4

Experiment 1	Experiment 2
44.56	47.56

Table D.12.The reproducibilty of -150+200 mesh zircon experimented with 10-5 M DA at pH 6

Experiment 1	Experiment 2
48.70	48.31

Table D.13.The reproducibilty of -150+200 mesh zircon experimented with 10-5 M DA at pH 8

Experiment 1	Experiment 2
49.64	49.83

Table D.14.The reproducibilty of -150+200 mesh zircon experimented with 10-5 M DA at pH 10

Experiment 1	Experiment 2
40.09	40.97

Table D.15.The reproducibilty of -150+200 mesh rutile experimented with water

Experiment 1	Experiment 2
32.83	32.95

Table D.16.The reproducibilty of -150+200 mesh rutile experimented with 10% methanol

Experiment 1	Experiment 2
23.72	28.81

Table D.17.The reproducibilty of -150+200 mesh rutile experimented with 25% methanol

Experiment 1	Experiment 2
21.47	26.23

Table D.18.The reproducibilty of -150+200 mesh rutile experimented with 40% methanol

Experiment 1	Experiment 2
25.31	22.71

Table D.19.The reproducibilty of -150+200 mesh rutile experimented with 50% methanol

Experiment 1	Experiment 2
21.29	16.82

Table D.20.The reproducibilty of -150+200 mesh rutile experimented with 65% methanol

Experiment 1	Experiment 2
22.88	17.28

Table D.21.The reproducibilty of -150+200 mesh rutile experimented with10-4 M DA at pH 4

Experiment 1	Experiment 2
39.04	38.41

Table D.22.The reproducibilty of -150+200 mesh rutile experimented with10-4 M DA at pH 6

Experiment 1	Experiment 2
40.90	40.88

Table D.23.The reproducibilty of -150+200 mesh rutile experimented with10-4 M DA at pH 8

Experiment 1	Experiment 2
41.71	42.98

Table D.24.The reproducibilty of -150+200 mesh rutile experimented with10-4 M DA at pH 10

Experiment 1	Experiment 2
33.79	34.85

Table D.25.The reproducibilty of -150+200 mesh rutile experimented with 5.10-5 M DA at pH 4

Experiment 1	Experiment 2
35.43	33.79

Table D.26.The reproducibilty of -150+200 mesh rutile experimented with 5.10-5 M DA at pH 6

Experiment 1	Experiment 2
38.41	37.87

Table D.27.The reproducibilty of -150+200 mesh rutile experimented with 5.10-5 M DA at pH 8

Experiment 1	Experiment 2
39.25	39.57